

# Investigation of Creases

How the crease is affected by displaced crease plates

*David Alberius & Fredrik Gerstner*

---

*Maskinkonstruktion • Institutionen för designvetenskaper • LTH • 2011*

Maskinkonstruktion, Institutionen för designvetenskaper LTH  
Lunds Universitet  
Box 118  
221 00 LUND

ISRN LUTMDN/TMKT 10/5408 SE

Tryckt av Media-Tryck, Lund





## **Preface**

This master thesis is the final step to obtain Master of Science in Mechanical Engineering degree. It has been done in collaboration with Tetra Pak in Lund and the Mechanical Design department of Design Sciences at the University of Lund.

First of all we would like to thank Magnus Dahl who is the originator of the project; our supervisor at Tetra Pak, Henrik Skanse and our supervisor at University of Lund, Giorgos Nikoleris for all their support and help during this project. We would also like to thank Mikael Nygårds and Mattias Månsson for help with the simulation model and Johan Tryding, Emma Lörd and Mikael Andersson for all the information they have been giving us. Finally we would like to thank Johan Nilsson for all his help with MODDE.

Lund, December 2010  
David Alberius and Fredrik Gerstner



## Abstract

One of the main concepts that made Tetra Pak a world leading company in producing packages for liquids, is the idea of folding paperboards. To get a good and precise fold it is necessary to crease the paper before the folding process takes part. By using creasing, the package can get more precise, stronger folds and can be produced at high speed. The creasing tool consists of a male plate and a female plate. The male plate presses the paperboard into the female plate to weaken the paper in the desired area. Since the creasing process consists of a male die pressing the paperboard into a female die, the position of the male die affects the crease properties. To get the ultimate result, the male die should be positioned exactly in the middle of the female die.

The purpose of this master thesis is in general to determine how a displacement of the dies affects the actual crease. Since cracks are fatal for the creasing procedure it is necessary to investigate how the displacement influences the ease of crack initiation and if it is possible to somehow prevent it. This subject has hardly been explored. Due to the lack of information about displaced creasing tools, it is not possible to scale down the problem by using already known facts. Instead, several studies and tests had to be undertaken where many parameters were observed.

The different tests involved an experimental part and a simulation part. The experimental part is divided into three different parts. The main part is when making straight creases by using a flat bed creasing machine. MODDE has been used to obtain information about which factors may be significant. MODDE is software that employs Design of Experiments. The second part of the laboratory tests also comprised use of a flat bed creasing machine, but with a tool consisting of a bottom pattern of a straight crease. The third and last experimental part was in Tetra Pak's pilot plant, where analyses of the process in full scale were done.

The simulation part was done in ABAQUS/CAE. The simulation is important since it is of particular interest to compare simulations with the real tests that were made. The simulation makes it easy to get graphs that can be compared between the different experimental parts.

From the experimental tests on the straight creases the significant factors were picked out and insignificant factors were discarded from interest.

In the second experimental part on the bottom crease pattern, tests on both MD (machine direction) and CD (cross direction) were made, and the goal was to crease as close to the crack limit as possible and with different displacements.

The same thought was when creasing in the pilot plant i.e. as close to the crack limit as possible. From these different tests, results were plotted and information could be read out.

It is determined that it is possible to crease different depths depending on what type of paperboard is used. The crease depth is also affected by the displacement of the die since it is not possible to crease as deep with a displaced die as with a centered one.

The distortion does completely change with displaced dies. Two curves were plotted to see when the displacement is significant and when it is insignificant, one curve for

the thick paperboard and one for the thin paperboard. Curves were also plotted to make it easy for the operator to use the RCSp (see page 39) to foresee if there will be cracks in the paperboard or not.

**Keywords:** Distortion, uncentering, displacement, creasing, RCS



## Sammanfattning

Detta examensarbete har gjorts i samarbete med Tetra Pak i Lund och Maskinkonstruktion vid Lunds Tekniska Högskola. Examensarbetet utgör den avslutande delen av civilingenjörsutbildningen i maskinteknik med inriktning mot produktutveckling vid LTH. Examensarbetet har som fokus att inrikta sig på hur ocentrerade verktyg kan påverka resultatet vid bigning. Arbetet kommer att behandla bland annat experimentella undersökningar i laboratorium, digitala simuleringar, hållfasthetsanalyser baserat på FEM samt en körning i Tetra Paks testmaskin.

År 1943 startade arbetet med att framställa en förpackning som görs av minimal mängd material men som fortfarande ger maximal hygien. Slutresultatet för detta blev en tetraedriskt formad förpackning. Detta projektet var starten för företaget Tetra Pak. Tetra Pak grundades av Ruben Rausing och Erik Wallenberg som ett dotterbolag till Åkerlund & Rausing och man placerade företag i Lund, Sverige. Under kommande årtionden växte företaget till ett internationellt företag som tillverkade fyllningsmaskiner över hela världen.

För att en förpackning ska bli en bra och hållbar måste den vikas på ett bra sätt. Detta erhålls genom att deformationer initieras som ett mönster. Dessa deformationer görs med hjälp av han- och honplattor som är monterade på stora valsar. Kartongen pressas mellan valsarna och blir därmed deformerat. Denna process kallas för bigning.

I detta examensarbete har fokus varit på hur ocentrerade han- och honverktyg påverkar bigens egenskaper. Eftersom det absolut inte får finnas sprickor i kartongen är det nödvändigt att göra en undersökning för att ta reda på hur ocentrerade bigplattor påverkar bigprocessen. Ocentreringen kan uppkomma av flera anledningar, såsom termisk påverkan, slitage av plattor och felinställda plattor vid start. Dessa områden har tidigare undersökts väldigt lite. Eftersom inte så mycket information kunde erhållas från tidigare studier, finns det ingen möjlighet att skala ner problemet. De två högsta prioriteringarna är:

- Hur påverkas och ändras RCS-värdet utifrån ocentrerade verktyg, bigdjup och banspänning?
- Ett kriterium för acceptabla bigar i kartongen då man mäter RCSp-värden (se sidan 39) i produktionen.

I den experimentella delen är antal experiment definierade av antalet parametrar. Dessa olika parametrar kan kombineras med varandra och på så sätt utgör ett antal experiment. För att få en hanterbar mängd experiment måste vissa avgränsningar göras. Den första experimentella delen gjordes på raka bigar. Detta är bigar som enbart biger i cross direction, dvs. tvärs över kartongens fibrer. Följande restriktioner gjordes:

- Två olika typer av kartongleverantörer, en enskiktskartong A och en flerskiktskartong B

- Två olika böjstyvheter på kartong
- Tre olika banspänningar
- Tre olika ocentreringar

Den andra experimentella delen är på bottenplattan. Denna gången är utrustningen en begränsning och restriktioner gjordes enligt följande:

- Två olika typer av kartongleverantörer, en enskiktsparkong A och en flerskiktsparkong B
- Två olika böjstyvheter på kartong
- En typ av banspänning
- Tre olika ocentreringar

Den tredje experimentella delen är i Tetra Pak's testanläggning. Där tester görs i verklig skala. Följande restriktioner gjordes:

- En typ av papperstillverkare, flerskiktsparkong, B
- Två olika böjstyvheter på kartongen.
- En typ av banspänning
- Tre olika ocentreringar

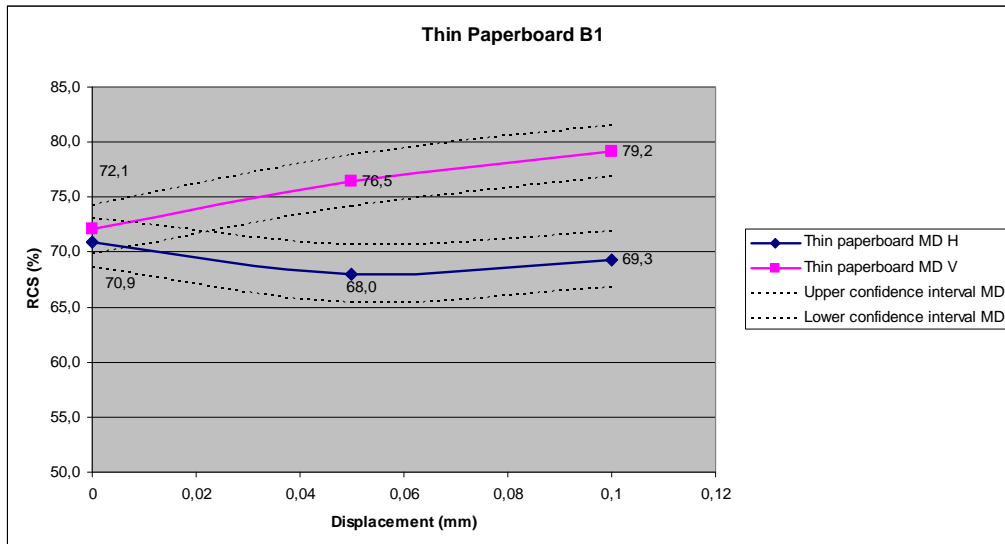
Hela arbetet delas in i tre större delar där första delen innehåller det som tidigare är beskrivet, de experimentella delarna i Tetra Pak's laboratorium. För att kunna välja antalet tester och vilka olika kombinationer av parametrar som ska utföras, används ett program som heter MODDE, som bygger på Design of Experiments (DOE). Andra delen är att utföra datorsimuleringar på de raka bigarna i programmet ABAQUS. Tredje delen är att göra prover i Tetra Pak's testanläggning.

Den första delen som innehåller experiment med raka bigverktyg gav information om vilka faktorer som påverkar responsen som vi är ute efter. Från detta experiment kan vi på så sätt sortera ut de signifikanta faktorerna från de insignifikanta. Detta leder till att färre tester behöver utföras. Liknande tester gjordes, fast med ett bottenverktyg för att undersöka hur bigarna påverkas då verktyget är ocentrerat i två riktningar istället.

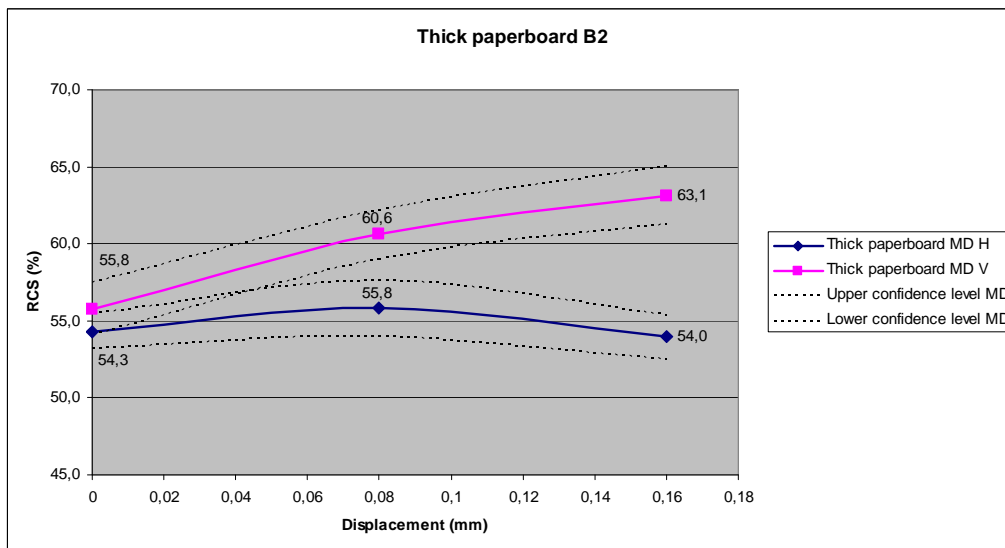
I den andra delen gjordes datorsimuleringar i ABAQUS. Enbart inställningar för raka bigar utfördes. ABAQUS användes för att undersöka vad som händer i kartongen då en ocentrering uppstår.

Den tredje och sista delen utfördes i Tetra Pak's testanläggning. Med hjälp av resultat från de tidigare experimenten kunde en testplan generas för en effektiv körning i verklig skala. Tillsammans med det inbyggda mätverktyget RCSp kunde ett kriterium för när sprickor bildas vid en viss ocentrering räknas ut. Detta kriterium tar även hänsyn till bigens höjd som kan orsakas av bigdjup samt slitage på bigverktyget.

Utifrån de olika tester som genomförts så kunde resultat plockas fram. Experimentet på de raka bigarna genererade bland annat i två grafer där det kan utläsas när ocentreringen påverkar RCS-värdena signifikant (*figur 1 och 2*).

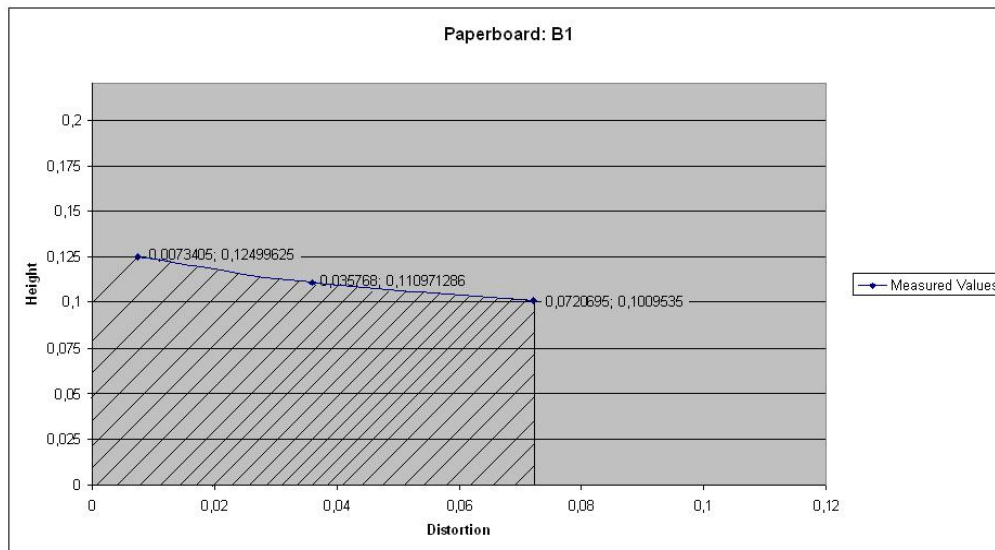


Figur 1. Visar signifikantintervallet för RCS mot ocentrering

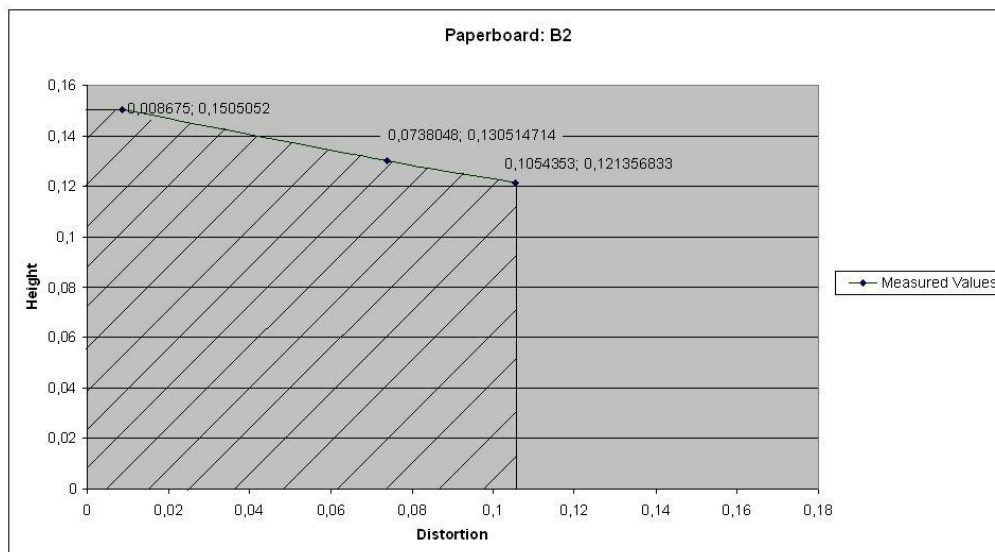


Figur 2. Visar signifikantintervallet för RCS mot ocentrering

På nästa sida visas de två figurer som beskriver när sprickor uppkommer (*figur 3 och 4*). Befinner sig mätningen utanför det skuggade området så är risken väldigt stor att sprickor uppkommer i kartongen då den viks.



Figur 3. Sprickgräns för kartong B1



Figur 4. Sprickgräns för kartong B2

Slutsatser som kunde dras från de erhållna resultaten är följande:

- Det är bekräftat att det kan bigas olika djupt beroende på vilken kartongtillverkare materialet kommer från, samt att det inte är möjligt att biga lika djupt då en ocentrering finns
- Bigdjup samt ocentrering är de två faktorer som påverkar sprickbildning mest
- Distortionen följer ocentreringen av verktyg mycket väl

- När ocentrerad bigning sker så erhålls två olika RCS-värden. Den sida med lägst värde löper störst risk för sprickbildning
- RCS-värdet för en enskiktsparkong är alltid lägre än för en flerskiktsparkong
- Sprickor uppkommer lättast på den sida som har lägst RCS-värde
- Maximal böjkraft uppträder oftast efter  $30^\circ$  för de tunna kartongerna



## Table of contents

1. Introduction.....	1
2 Objective.....	3
3. Method.....	5
3.1 Work procedure.....	5
3.2 Design of Experiments - DOE.....	7
4. Theory.....	13
4.1 Explanation of expressions.....	13
Why creasing?.....	13
How does creasing work?.....	13
What is displacement?.....	13
What is crease depth?.....	14
What is RCS?.....	14
What is web tension?.....	14
What is crease force?.....	14
What is bending force?.....	14
What is crack angle?.....	15
What is distortion?.....	15
4.2 Paperboard.....	15
4.3 Finite Element Method.....	17
4.3.1 Equations of motion.....	18
4.3.2 Weak formulation.....	19
4.3.3 Nonlinear Finite Element Method.....	20
4.3.4 Newton Raphson scheme.....	22
5. Experimental work.....	25
5.1 Experimental tools, parameters and procedure.....	25
5.1.1 Laboratory creasing tool.....	25
5.1.2 Creasability tester.....	27
5.1.3 Creasability procedure.....	29
5.1.4 Topography.....	29
5.1.5 Topography procedure.....	30
5.2 First experimental part: straight creases.....	31
5.2.1 Parameters.....	31
5.2.2 Laboratory creasing procedure.....	31
5.2.3 Creasability procedure.....	33
5.3 Second experimental part: bottom crease pattern.....	33
5.3.1 Parameters.....	33
5.3.2 Laboratory creasing procedure.....	34
5.3.3 Creasability procedure.....	35
5.4 Third experimental part: Pilot plant.....	35
5.4.1 Parameters.....	36
5.4.2 Creasing procedure.....	36
5.4.3 Creasability procedure.....	37
6 Computer simulations.....	39
6.1 ABAQUS.....	39
6.2 Model.....	39

6.3 Boundary conditions .....	40
6.4 Mesh.....	40
6.5 Procedure .....	41
7 Results.....	43
7.1 Experimental part.....	43
7.1.1 Straight creases .....	43
7.1.2 Bottom crease pattern.....	46
Pilot plant.....	47
7.2 Simulations .....	48
7.2.1 Simulation vs. experiments .....	49
7.2.2 Plastic deformations.....	49
8 Discussion.....	51
8.1 Topography .....	51
8.2 MTS .....	52
8.3 RCS.....	52
8.4 Tuning.....	53
8.5 Pilot plant.....	54
8.6 Computer simulations .....	57
9 Conclusion .....	59
10 Recommendations and further investigations .....	61
11 References.....	63
List of Appendices .....	65



## 1. Introduction

In 1943, development began creating a package for milk that required a minimum of material while still providing maximum hygiene. The end result was the tetra-hedron-shaped package. This project also led to the founding of Tetra Pak in the early 1950's. Ruben Rausing and Erik Wallenberg established Tetra Pak in Lund, Sweden, as a subsidiary of Åkerlund & Rausing. Over the next decades the company grew to an international company with filling machines all over the world. In 1993 the company took the name Tetra Laval Group and today, 2010, this group consists of four industrial groups, Tetra Pak, Tetra Laval Food, Alfa Laval and Alfa Laval Agri. Today Tetra Pak provides their customers with nine different shapes of packages, also called families. Each family consists of several sizes to cover the range of uses. Tetra Pak provides complete processing and packaging systems to their customers. Even though Tetra Pak has a wide range of package products for example, juice, tea drink, soy drink, tomato products and wine, the main package product is still for dairy products [13].

One of the main properties that made Tetra Pak a world leading company in producing packages for liquids, is the idea of folding paperboards.

To get a good and precise fold it is necessary to crease the paper before the folding process begins. By using creasing, the packages get more precise, they get stronger folds and are able to be produced at high speed.

When creasing the paperboards a crease pattern is used (*Figure 1.1*).

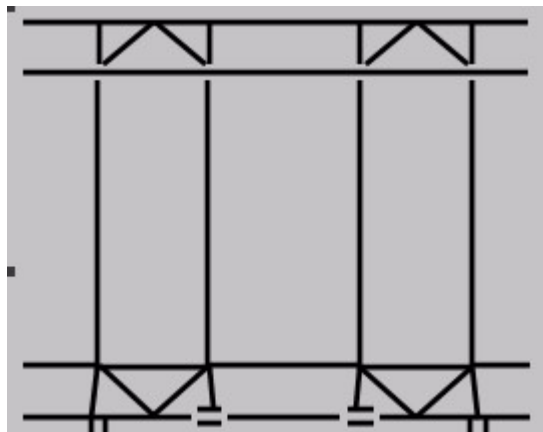


*Figure 1.1* The creasing pattern

The creasing tool consists of a male plate and a female plate. The male plate presses against the décor side of the paperboard into the female plate to weaken the paper in the desired area [3]. This type of creasing is called outside creasing, and is the most common technique used by Tetra Pak (*Figure 1.2*).

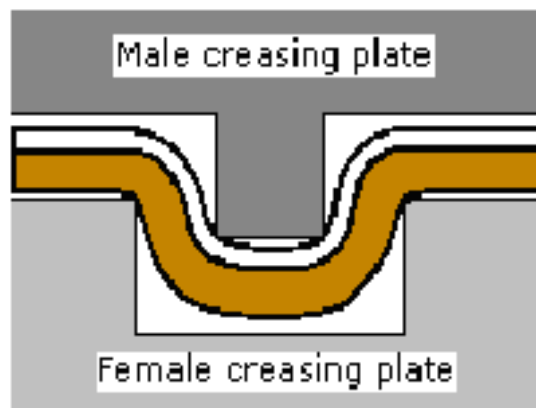


*Figure 1.2* Illustration of outside creasing

Since the creasing process consists of a male die pressing the paperboard into a female die, the position of the male die affects the crease properties. To get the ultimate result, the male die should be positioned exactly in the middle of the female die. The opposite would be that the male die is close to one of the female die's edges, which will end up with a cut in the paper instead of creasing it.

Problems with off-centered creases are well known but no deeper studies have been conducted. By knowing the breaking point set by the displacement and crease depth, the problem of cracks in the board can be avoided. This saves time and money in production.

When the creasing plates are mounted, the technician checks how the female die is mounted relative to the male die by creasing a plastic film. The film is observed by the technicians well trained eye under a magnifying glass for any visible displacements. If any displacements are found, the creasing plates have to be adjusted. This is an iterative procedure.

If a perfectly centered crease is used, it will have the same bending properties on both sides of the crease. If one of the dies is displaced a little bit, the crease will have different bending properties depending on which side that is observed. This behavior also increases the initiation of cracks. Since cracks are fatal, it is important to know how much the dies can be off-centered before there is any risk of getting cracks.

## 2 Objective

The purpose of this master thesis is in mainly to determine how a displacement of the dies affects the actual crease. Since cracks are fatal for the creasing procedure it is necessary to investigate how the displacement influences the ease of crack initiation and if it is possible to somehow prevent it.

This subject has hardly been explored. Due to the lack of information about displaced creasing tools, it is not possible to scale down the problem by using already known facts. Instead, several studies and tests have to be done where many parameters are observed. The data from the tests provides information about how the parameters change during the displaced creasing. The two highest priorities are:

- How does the ability to get a low RCS-value change due to displacement of the dies, crease depth and web tension?
- Acceptance criteria when looking for warped creases by measuring distortion in the in line RCSp system.

### 2.1 Focus and delimitations

The manufacturing of packaging material consists of three steps:

- Printing/creasing
- Lamination
- Slitting

This master thesis was focused to only analyze the first step Printing/creasing.

In the experimental part, the number of experiments is defined by the number of parameters. These different parameters can be combined with each other which lead to an increasing number of experiments. To get a manageable number of test combinations and parameters, some delimitation must be made.

The first experimental part concerns straight creases. The restrictions were as following:

- Two different types of paperboard suppliers, one single layer A, and one multi layer B
- Two different thickness of paperboard
- Three different web tensions
- Three different displacements

The second experimental part concerns the bottom plate. This time the test equipment was a limitation and confines the restrictions to following:

- Two different types of paperboard suppliers, one single layer A, and one multi layer, B
- Two different thickness of the paperboard
- One web tension

- Three different displacements

The third experimental part is in Tetra Pak's test facility. The restrictions were the following:

- One type of paperboard supplier, with multi layer, B
- Two different thickness of paperboard
- One web tensions
- Three different displacements

In the computer simulations, the restrictions were made as following:

- One type of paperboard supplier, with multi layer, B
- One thickness of paperboard
- Three different web tensions
- Three different displacements

### 3. Method

This chapter is divided in two major parts. The first part presents what types of experiments were done in the laboratory and the second part concerns the establishment of a work plan for the tests.

#### 3.1 Work procedure

The work procedure was based on the “focus and delimitations” and the “objective” chapter mentioned earlier. The first step was to collect information, not only about displaced creases, but everything from the structure of the paperboard to the creasing procedure. This part was crucial since it is necessary to have good insight into the subject to be able to know how to confront it. The gathering of information involved lectures [17], books, old research reports and internet sites. In order to perform, do the desired tests and simulations it was necessary to learn how the computer programs (Matlab, MODDE and ABAQUS) work. This was mostly done by means of the tutorials and help functions built into the programs and lectures [16]. After the gathering of information was done, the experimental work was divided into three main parts. The reason why the experimental part was divided into three smaller parts was due to each of the parts having a specific goal, which was subsequently combined to get a valid result.

1. The first part of the experiment was done in Tetra Pak’s creasing laboratory. The tests made in this laboratory are in a controlled environment compared to the pilot plant which is described in part three. By using the computer program MODDE (described in next chapter) a specific work plan was established. The plan indicated in what order the tests need to be performed, and which parameters needed to be changed from one test to another. The reason why the tests follow a specific plan was because by doing so the computer program could use statistic analyses from the received test results. Furthermore, the results from the statistic analysis gave information about how the parameters affected the result. The goal of this part was to obtain an idea of how the result changed with the parameters. This could off course be achieved without the computer program, but another important aspect was the ability to easily observe which factors that were not significant and could thus be removed as factors for the coming tests. This method was only used on the tests with straight creases, even though tests with bottom crease patterns were done in this laboratory as well. The bottom crease patterns was used to observe how deep it was possible to crease without initializing any cracks and to confirm differences in creasing with a displacement in both machine direction (MD) and cross direction (CD)(*figure 3.1*) The DD creases are not analyzed since it is considered waste of time. The DD creases are the hypotenuse of the MD and CD creases and it is thereby known that if a displacement in MD or/and CD is initialized, the DD crease’s displacement will also change. In addition the

female die has wider groove to compensate displacements in MD and CD.

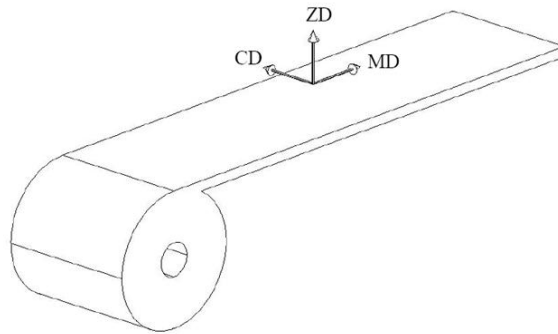


**Figure 3.1** Illustration of the different directions of the paperboard

2. The second part contained computer simulations in the FEM-analysis program ABAQUS. The computer simulations were made to verify if it was possible to predict the creasing results with simulations. This was relevant since it was cheaper and required less time to simulate procedures than doing them physically. The results from the simulation were both compared with part two and three in this working procedure. The use of simulation tools in industries is rapidly increasing due to companies' realization that is inexpensive and in many cases gives pedagogical illustrations that were easy to understand and good in presentational use.
3. The third part was done in Tetra Pak's pilot plant which is the actual creasing machine used in production. Due to this machine is involved in a lot of research work it was only possible to do a few numbers of tests. Therefore it was necessary to plan this procedure with help from step two, to get valid tests. To get maximum information it was decided to perform the deepest creasing with each displacement setting. This characterizes the worst case scenario in the real production setup, which was the goal for the test.

Creases from all the experimental parts were folded in an L&W creasability tester. This was mainly to get the RCS value, but even other results like energy, crack angle, bending force, etc. Since the test samples were creased with a displacement of the dies, it was important to fold the samples exactly the same way. The reason was, if the dies were not centered the crease will be weaker at one side and stronger at the other side. Therefore, each test consists of two different RCS-values, which were important to keep them separate.

All of the creases were also observed under an optical 3D measuring program called MikroCAD by GFM. This device measures the shape of the crease. It was desirable to know this in order to be able to confirm if it changes together with the displacement of the dies.

### **3.2 Design of Experiments - DOE**

Design of experiments, DOE, mainly consists of three different parts – Screening, Optimization and Robustness testing. These were used to ensure that the selected experiment's results contained a maximum amount of relevant information. Because the model was an approximation, it was important to know that the study was a simplification of reality and will never be 100% perfect. Even though it was not perfect, it can still be very useful.

#### **Screening**

By using screening it was possible to get a good picture of how the different parameters affected the response value. The whole idea with screening was to reduce the numbers of required experiments, while still considering all the parameters.

#### **Optimization**

This method was used when parameters affected the end result, and an optimum solution was desired. By doing a lot of tests and changing the parameters, different results were obtained. By using the optimization method it was possible to go backwards i.e. use the results to get optimal values for the parameters. After all the tests were done it was possible to come up with a result that was believed to be the optimum result. By doing so, a couple of solutions of how the parameters were to be set in order to achieve the desired result were obtained.

#### **Robustness testing**

The robustness testing was used to determine how sensitive a response was to small changes in the factor settings, i.e. how devastating were the consequences of having a “bad day” on the production line or if the customers do not use the product as indicated in the instructions?

Regardless of which of the various methods above was used, the problem formulation was of high importance. This was because it was necessary for all involved parties to have a hundred percent understanding in the intentions underlying the experimental investigation. There were several things to discuss and agree about, and it was necessary to consider the six following steps:

1. The experimental objective – This part defined what kind of investigation was required to obtain the desired goal. To do so, one should reflect over why the experiment was done, what the purpose and desired result was? Screening was used in this master thesis, since the interest was to find out how the factors affected the response. The Pareto principle, named after the famous economist Vilfredo Pareto, states that 80% of the effects on the responses are caused by 20% of the investigated factors, and applies well to this stage.

2. Definition of factors – This step is about how the system or the process was affected due to changes in the parameter levels. One way of categorize factors may be to divide them into *controllable* and *uncontrollable* factors. The controllable factors are the easiest to handle and investigate. The experimenter is usually alerted when such factors change. Uncontrollable factors are hard to regulate, but they may have an impact on the result. Another way of dividing the factors is into quantitative or qualitative. A quantitative factor is a factor that may change according to a continuous scale and a qualitative factor is a categorical variable, which can only assume certain discrete values.
3. Specification of responses – In this step it was important to select responses that were relevant according to the problem formulation. It is often important to have many responses to be able to describe the properties of a product or the performance characteristics of a process. The responses can be quantitative or qualitative. A quantitative response is a metric with a distinct value, and a qualitative response describes how well the response is perceived on a scale, i.e. 1-5 where 1 is worthless and 5 is excellent. Quantitative responses are easier to handle than qualitative, since interpretation of regression models is rendered easier.
4. Selection of model – This step was about selecting an appropriate regression model of the integral part of the problem formulation. There are three main types of polynomial models:

Linear  $y = \beta_0 + \beta_1x_1 + \beta_2x_2 + \dots + \varepsilon$

Interaction  $y = \beta_0 + \beta_1x_1 + \beta_2x_2 + \beta_{12}x_1x_2 + \dots + \varepsilon$

Quadratic  $y = \beta_0 + \beta_1x_1 + \beta_2x_2 + \beta_{11}x_1^2 + \beta_{22}x_2^2 + \beta_{12}x_1x_2 + \dots + \varepsilon$

The quadratic model is the most complex and requires the most experiments. The linear model is thus the least complex and requires the fewest experiments of the three alternatives. The choice of which model to be used is not completely free. When the experimental objective was selected in the first step of the problem formulation, a part of the choice has already been made. If optimization had been selected, only a quadratic model would do. If screening had been selected both a linear and an interaction model would be appropriate. The interaction model is recommended if the number of experiments required is practical. However, in this master thesis the linear model was used due to a high number of factors which made it appropriate.

5. Generation of design – This was the next step of the problem formulation, comprising the generation of an appropriate experimental design. It is of high importance that a random experimental design is not chosen, and then hope for it to work for a given problem. The MODDE software considers the number of factors, their levels and nature (quantitative, qualitative,...), and



the selected experimental objective, and propose a recommended design, which will suit the given problem. It is possible to override the proposed design, but this choice should only be made by an experienced MODDE user. In this master thesis changes were actually made from the suggested design. This because MODDE suggested three center-points and the laboratory tests required four center-points, two for each paperboard. This was done in collaboration with a professional MODDE user [15].

6. Creation of worksheet – The worksheet was in principle very similar to the table containing the selected experimental design. The big difference was that the worksheet displays in which order the experiments should be performed, and the setup of the parameters.

When the results from the tests were obtained and put into MODDE, the program created bar charts that showed the analysis in different ways. One of the charts is called a histogram plot. It is used to study the distributional shape of a response variable. If the histogram is not approximately normally distributed like the figure bellow, it could indicate that one measurement is not like the other. It is not recommended to perform a regression analysis to a response with this appearance. The problem can in most cases be solved by different kinds of mathematical transformations.

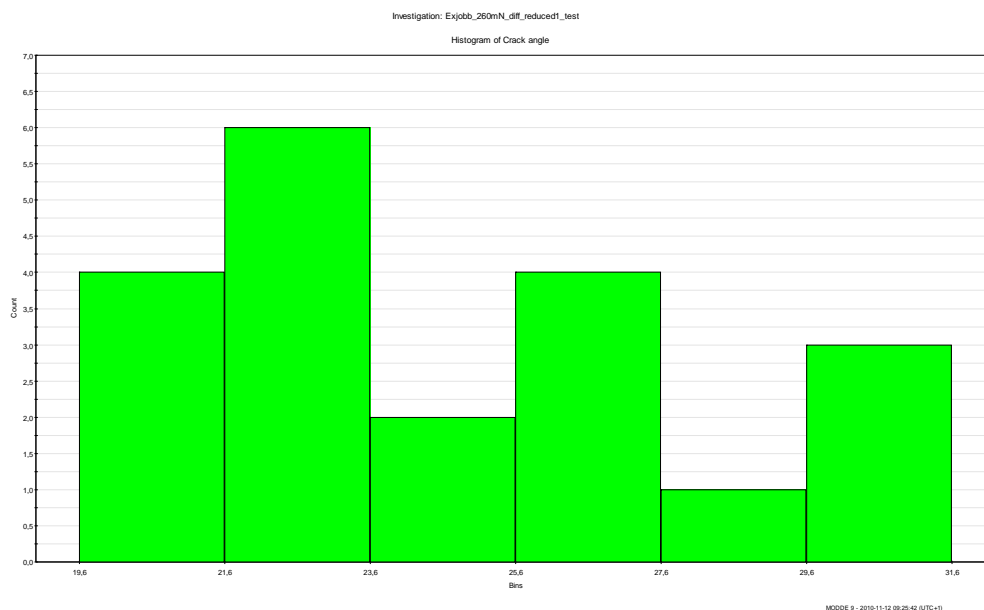


*Figure 3.2 Example of a histogram plot*

Furthermore, a summary of fit model can be established. The bars in this plot tell the user how reliable the results are and how well they can be predicted. The green bar  $R^2$  is a parameter that is called the goodness of fit, and is a measure of how well the regression model can be made to fit the raw data.  $R^2$  can vary between 0 and 1, where

## Method

1 indicates a perfect model and 0 no model at all. The blue bar Q2 is called goodness of prediction. It tells the user the predictive power of the model. This is a more realistic and useful performance indicator than R2 as it reflects how good the predictions of new experiments are. As R2, Q2 has an upper bound of 1, but its lower limit is minus infinity. Generally, both R2 and Q2 should be high, but preferably not more divergent than 0.2-0.3. A larger difference points toward an inappropriate model. A Q2 value greater than 0.5 is considered as a good model and a Q2 value greater than 0.9 is regarded as excellent.

The yellow and third bar in the summary of fit plot is called model validity. This bar reflects whether the model is appropriate in a general sense, i.e. if the correct model was chosen for the problem. A higher value is a more valid model, and a value above 0.25 suggests a valid model. The last bar, which is the turquoise one, is called the reproducibility diagnostic tool. The higher this numerical value is, the smaller the replicate error is in relation to the variability seen across the entire design. If this value is lower than 0.5, pure errors exist and poor control of the experimental procedure is obtained [7].

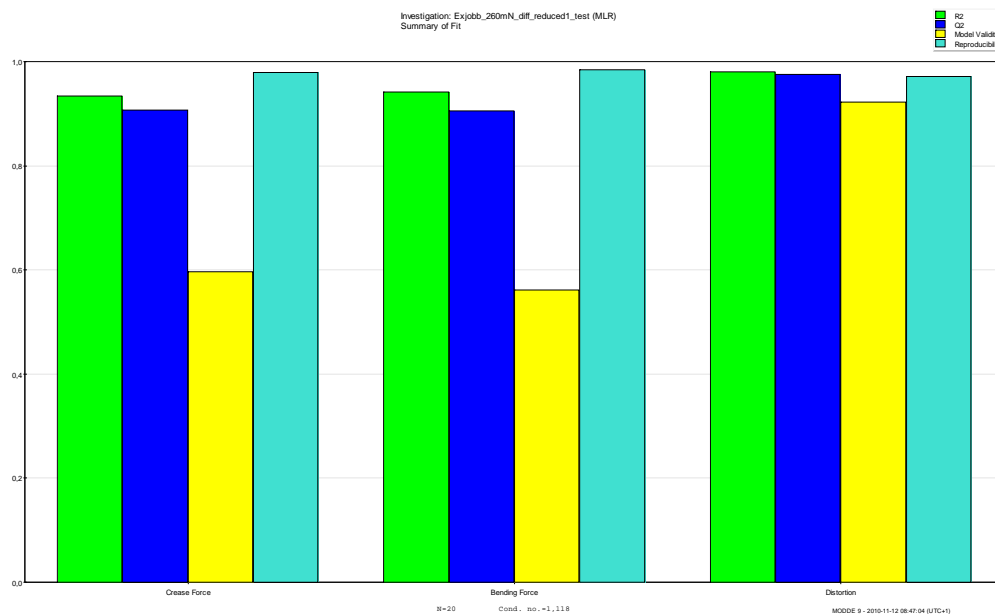


**Figure 3.3** Example of a summary plot

To detect interactions between different factors and responses, a Regression coefficient plot is used. The green bars indicate the real effects of the factor on each response. As can be seen in *figure 3.4*, the factor Depth has the strongest impact on the response. The fact that the Web-bar is negative tells that the response is working in the opposite direction to the factors, i.e. if a high crack angle is desired, the web tension has to be low. The uncertainty of the coefficients is given by the confidence intervals and the size of those depends on the amount of noise. When the confidence intervals reach both the positive and negative side, it tells the user that this factor is not significant, i.e. it does not affect the response.

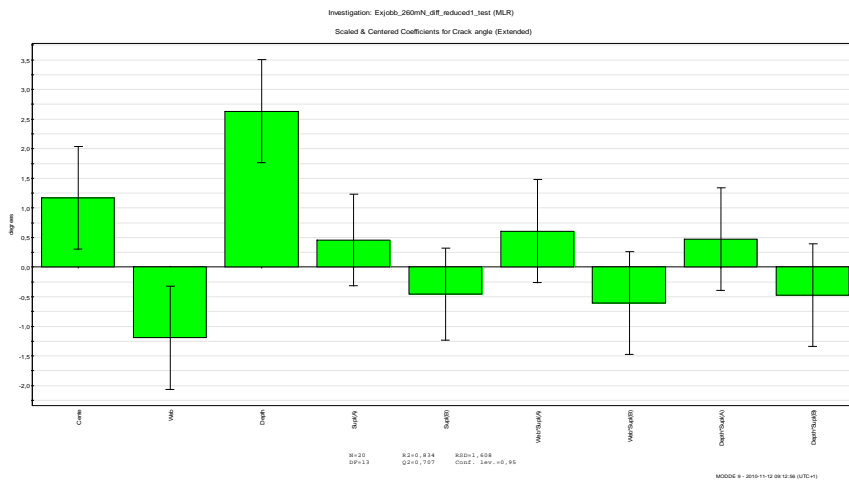


Figure 3.4 Example of regression coefficient plot



## 4. Theory

To be able to make any conclusions about the results that are achieved, some theory is needed. This chapter contains information about expressions, paperboard and finite element method.

### 4.1 Explanation of expressions

To be able to understand this master thesis more easily, some terms are described below.

#### Why creasing?

The reason why the creasing process is important, is because it makes permanent deformations in the paperboard and thus weakens it. The weakening makes it easier to fold the paperboard and it also determines where the paperboard should be folded. This results in a fancy and dense package with good edges, high durability and strength.

#### How does creasing work?

The male and female dies are mounted on big cylinders. The paperboard is placed between the cylinders, and when they rotate, the male die presses the paperboard in to the female die. When the paperboard has passed the cylinders a pattern can easily be seen in the paper. The patterns are the creases where permanent deformation and delamination has been initialized.

#### What is displacement?

The displacement is measured from the center line of the male die to the edges on the female die (*figure 3.1*). The displacement is calculated by measuring the difference between the right and the left side and divides it by two.

It is very difficult to mount the dies without having any displacement at all. It takes hours and sometimes days for a technician to calibrate the dies in the correct position. The easiest way to be sure that the dies are centered is by creasing a plastic film and then checks the marks in the film with a magnifying glass. The magnifying glass is a handy tool to be able to see if the left and the right side of the male die have equal widths. The *figure 3.1* shows dies with no displacement and dies with displacement.

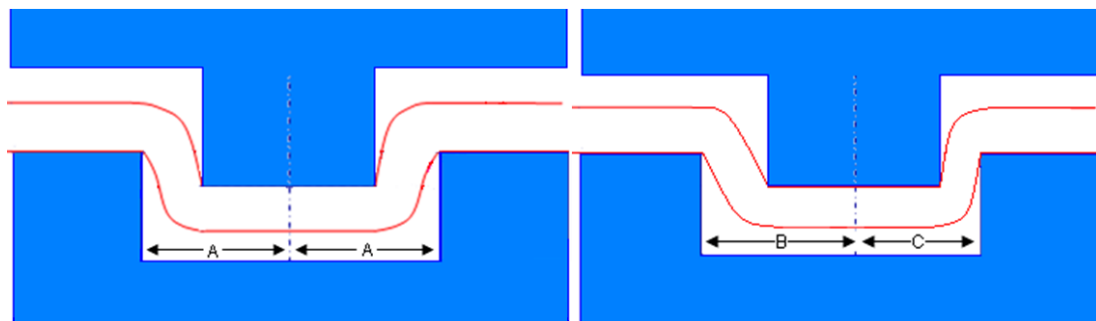


**Figure 4.1** Male and female die centered (left), male and female die with a displacement (right)

### What is crease depth?

Crease depth is set to be the distance the male die enters the female die (*figure 3.2*). The crease depth can be set to a certain distance when the creasing plates are new, but changes with wear of the creasing plates.

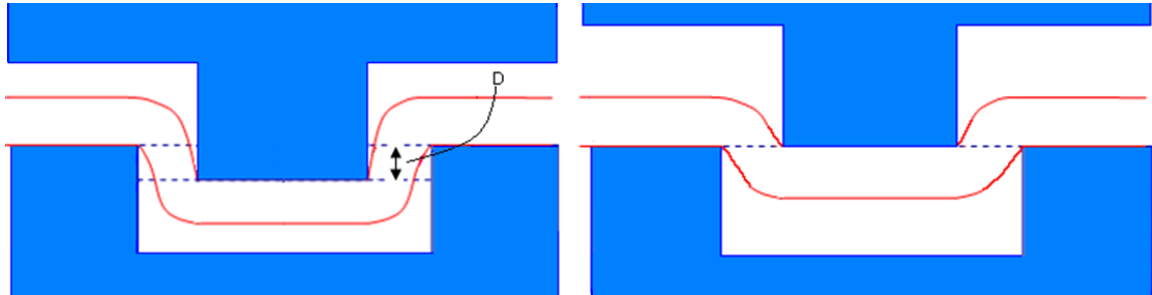


*Figure 4.2* Crease depth *D* have been made (left), just before the male die enters the female die, ground zero (right)

### What is RCS?

A very often used key unit is the RCS-value. The RCS-value is the relation between the maximum bending force at or below 30 degrees of the creased sample divided by the maximum bending force at or below 30 degrees of the uncreased sample. It is desirable with a low RCS-value.

$$RCS = \frac{\text{Bending force creased sample}}{\text{Bending force uncreased sample}}$$

### What is web tension?

When the paperboard arrives at the production line, it is rolled up on big cylinders. Each of the cylinders contains 6000 meters of paperboard. The big roll is placed in one end of the production line and then steered thru the creasing line and then rolled up to a new cylinder in the end. To prevent any problems with paperboard jam in the line, it is necessary to stretch the paper a bit. The tension that appears due to the stretch of the paperboard is called web tension.

### What is crease force?

The crease force is a measure of how much force is needed to apply the male die to get a desired crease depth.

### What is bending force?

Bending force is the required force needed to fold a creased or uncreased paperboard.

### What is crack angle?

When measuring the RCS-value in an L&W folding machine, it is possible to get a graph of how the bending force changes with the bending angle. The point where maximum force is required is called the crack angle.

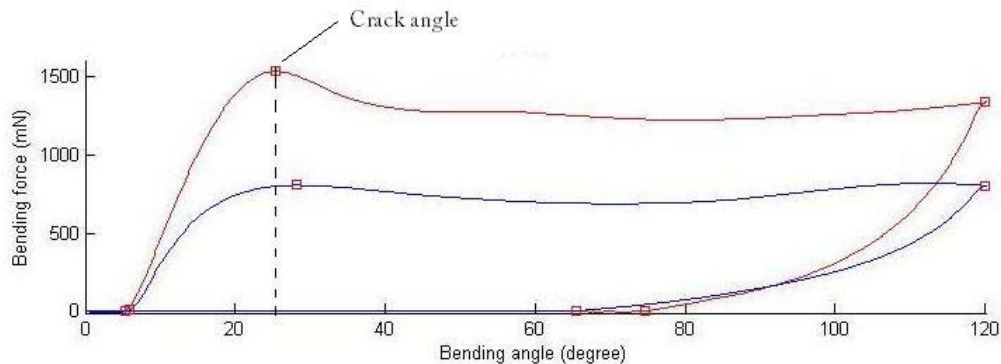


Figure 4.3 Shows the crack angle in a RCS-curve

### What is distortion?

When looking at the crease's topography, one or several graphs show the surface of the crease. Distortion is a measure of how the maximum height of the crease is placed relative to the center of the crease. The distortion is calculated by measuring the horizontal distance from the 20 percent and 80 percent of the highest point to the left and right side of the crease ( $x$  and  $y$  in figure 3.4), and then subtract the right distance from the left distance. The distortion can be a positive- or a negative value. The difference is only that a positive value refers to the crease is bigger on the left side and a negative value refers to that the right side is bigger.

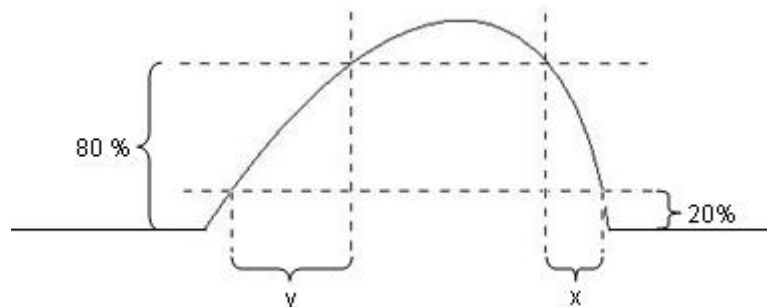


Figure 4.4 Shows how the distortion is calculated

## 4.2 Paperboard

The basic principles of paperboard production are the same today as it was a few thousand years ago, when it was first discovered. Just as before, the process begins with a very dilute mixture of fibers and water. Most of the water is removed by

draining and drying and the finished paper sheet consist of a dense network of cellulose fibers.

The step from paper to paperboard is not big. There are two different types of paperboard: single layer and multilayer. For quality reasons, paperboard is usually built up in several layers. These multi-layer materials are widely used for graphic products and for different packaging purposes.

Since the mid-1800s, the cellulose fibers are mainly derived from wood. Cellulose fibers are extracted either in a chemical or mechanical way. The fibers in a log are arranged longitudinally in the log. Fiber length varies by species but generally the length is greater than the width.

The wood fiber's chemical composition is dependent on which process that is used. Initially the wood fibers consist of cellulose, hemi cellulose and lignin. The percentage distribution depends on the species of tree.

Depending on which properties that are desired in the paperboard, three different fiber orientation processes are used:

1. Mechanical
2. Chemical mechanical
3. Chemical

These processes use different kinds of techniques and equipment, which give three different types of pulp: mechanical pulp, recycled pulp and chemical pulp. In many occasions bleach is used to make the fibers look better. However, it is not only the kind of fibers and pulps that matter in what kind of properties the paperboard will have. The coating and how the structure of the fibers is set up do also have an impact on the paperboard's properties.

By forming several layers of pulp in wet condition, the making of paperboard combines the advantageous properties of different types of pulp in one single paperboard. Even though it is the same pulp in each layer, every layer is treated and shaped separately. A multi layer structure provides benefits in particular creasing and folding.



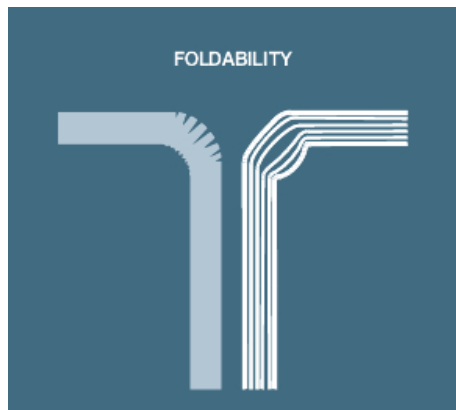


*Figure 4.5 The difference between one layered paperboard and multi-layer paperboard [12]*

The coating contains white pigment, usually based on clay or calcium carbonate. The coating is added on the top of the paperboard. It can consist of one, two or even three layers on top of each other. The coating process improves the whiteness, smoothness and shine to the paperboard, which improve printing properties [12].

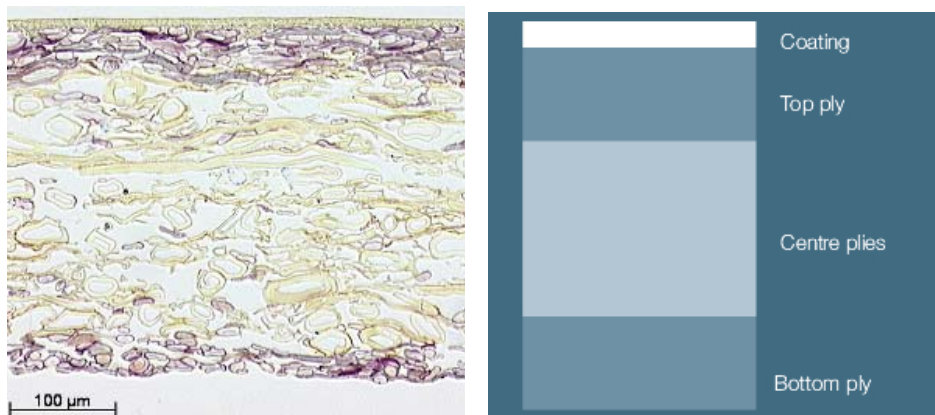


*Figure 4.6 Cross section of multi layer board (left), Cross section of paperboard (right) [12]*

### 4.3 Finite Element Method

In engineering mechanics all the physical phenomena encountered are modeled by using differential equations. Usually these kinds of problems are too complicated to be solved by classical methods. To be able to solve these problems in a numerical approach the finite element method can be used.

The problem can be described by either one or several equations that are assumed to be held over a certain region. This region can be one-, two-, or three-dimensional depending on the problem. Instead of trying to find approximations that hold over the

entire region, the region is divided into smaller, so called finite elements. Even if the problem is nonlinear, it is a good approximation to say that each element behaves linearly. This is the approach that will be used over the entire region. The collection of all these parts over the region is called the finite element mesh.

When the type of approximation which is to be applied over each element is selected, the behavior of each element can be determined. As the behavior for each element is determined, all the elements can be assembled together to form the entire region which will obtain an approximate solution for the behavior of the entire body.

In what is commonly referred as the FEM-equation the relationship between forces and displacements can be described as:

$$Ka = f$$

where  $K$  is the global stiffness matrix of the structure,  $a$  is a column matrix which contains the displacements of the nodal points and  $f$  is a column vector which contains the external forces applied at the nodal points. The global stiffness matrix is structured by every element's stiffness matrix. The structure of element matrix can be illustrated by looking at the simplest elastic element, the bar element. A bar element can by definition only obtain tensile- and compressive forces (torsion is disregarded in this example) [9]. A bar element can be assumed to consist of two nodal points and one bar with the length  $L$  between the two points. In a two dimensional case, each of the nodal points have two degrees of freedom which is illustrated by  $x_1, x_2, y_1$  and  $y_2$  in figure 3.4.

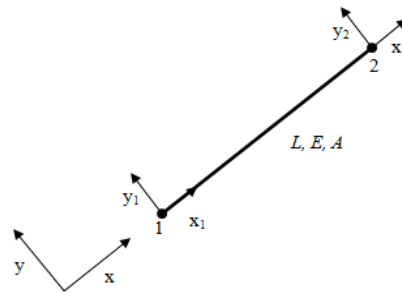


Figure 4.7 Two dimensional bar element

### 4.3.1 Equations of motion

An arbitrary part of a body has a volume  $V$ , and an outer surface  $S$  with an outer normal unit vector  $n$ . The force that is acting on the arbitrary body is given by the traction vector  $t_i$  and the body force  $b_i$  per unit volume in the region  $V$ . Displacement of the acceleration vector  $\ddot{u}_i$  denoted by  $u$ , is where a point denotes the time derivatives. Newton's second law says that:

$$\int_S t_i dS + \int_V b_i dV = \int_V \rho \ddot{u}_i dV \quad (1)$$

where  $\rho$  is the mass density. To reformulate Eq. (1), we recall the *divergence theorem of Gauss*, which says that for an arbitrary vector  $\mathbf{q}$ , the following relation holds:

$$\int_V \text{div} \mathbf{q} dV = \int_S \mathbf{q}^T \mathbf{n} dS \quad (2)$$

And we have per definition:

$$\text{div} \mathbf{q} = \frac{\partial q_1}{\partial x_1} + \frac{\partial q_2}{\partial x_2} + \frac{\partial q_3}{\partial x_3} = q_{i,i}; \quad \mathbf{q}^T \mathbf{n} = q_i n_i$$

Therefore, the divergence theorem can be written as:

$$\int_V q_{i,i} dV = \int_S q_i n_i dS \quad (3)$$

If  $q_i$  is chosen as the quantity  $c_{ii}$ , a relation analogous with Eq. (3) is obtained. Likewise, similar relations can be obtained by choosing  $q_i$  as  $c_{2i}$  and so on. By collecting all these results, we can obtain for an arbitrary quantity  $c_{ij}$  that generalizes to:

$$\int_V c_{i,j} dV = \int_S q_{i,j} n_j dS$$

By using:

$$t_i = \sigma_{ij} n_j \text{ or } t = \sigma \mathbf{n} \quad (4)$$

we can now reformulate (1) by means of (3) to obtain:

$$\int_V (\sigma_{ij,j} + b_i - \rho \ddot{u}_i) dV = 0 \quad (5)$$

Since Eq. (4) holds for arbitrary regions  $V$  of the body, we can conclude that:

$$\sigma_{ij,j} + b_i = \rho \ddot{u}_i \quad (6)$$

These equations are the *equations of motion* for the body.

### 4.3.2 Weak formulation

From the equation of motion we shall now derive the so-called *weak formulation*. We multiply Eq. (5) by an arbitrary vector  $v_i$  - the *weight vector* - and integrate over the volume to obtain:

$$\int_V v_i (\sigma_{ij,j} + b_i - \rho \ddot{u}_i) dV = 0$$

This equation can be written as:

$$\int_V [(\sigma_{ij} v_i)_{,j} - \sigma_{ij} v_{i,j}] dV + \int_V (v_i b_i - \rho v_i \ddot{u}_i) dV = 0 \quad (7)$$

Divergence theorem (3) and (4) gives us:

$$\int_V (\sigma_{ij} v_i)_{,j} dV = \int_S \sigma_{ij} v_i n_j dS = \int_S v_i t_i dS$$

This expression used in (7) gives us:

$$\int_V \rho v_i \ddot{u}_i dV + \int_V v_{i,j} \sigma_{ij} dV = \int_S v_i t_i dS + \int_V v_i b_i dV \quad (8)$$

Introducing a symmetric tensor:

$$\varepsilon_{ij}^v = \frac{1}{2}(v_{i,j} + v_{j,i}) \quad (9)$$

That gives the weak form:

$$\int_V \rho v_i \ddot{u}_i dV + \int_V \varepsilon_{ij}^v \sigma_{ij} dV = \int_S v_i t_i dS + \int_V v_i b_i dV \quad (10)$$

### 4.3.3 Nonlinear Finite Element Method

Since paperboard is a non-linear anisotropic material, we are forced to make use of the nonlinear finite element method to solve the problem. How the equations are formulated in the finite element method is shown below. They are based on the weak form from Eq. (10)

The variables are here defined in matrix form:

$$\varepsilon = \begin{bmatrix} \varepsilon_{xx} \\ \varepsilon_{yy} \\ \varepsilon_{zz} \\ 2\varepsilon_{xy} \\ 2\varepsilon_{xz} \\ 2\varepsilon_{yz} \end{bmatrix}; \quad \sigma = \begin{bmatrix} \sigma_{xx} \\ \sigma_{yy} \\ \sigma_{zz} \\ \sigma_{xy} \\ \sigma_{xz} \\ \sigma_{yz} \end{bmatrix}; \quad \ddot{u} = \begin{bmatrix} \ddot{u}_x \\ \ddot{u}_y \\ \ddot{u}_z \end{bmatrix}; \quad v = \begin{bmatrix} v_x \\ v_y \\ v_z \end{bmatrix}; \quad t = \begin{bmatrix} t_x \\ t_y \\ t_z \end{bmatrix}; \quad b = \begin{bmatrix} b_x \\ b_y \\ b_z \end{bmatrix}$$

Green-Lagrange's strain can be written as:

$$E = \begin{bmatrix} \frac{\partial u_x}{\partial x} \\ \frac{\partial u_y}{\partial y} \\ \frac{\partial u_z}{\partial z} \\ \frac{\partial u_x}{\partial y} + \frac{\partial u_y}{\partial x} \\ \frac{\partial u_x}{\partial z} + \frac{\partial u_z}{\partial x} \\ \frac{\partial u_y}{\partial z} + \frac{\partial u_z}{\partial y} \end{bmatrix} + \frac{1}{2} \begin{bmatrix} \left(\frac{\partial u_x}{\partial x}\right)^2 + \left(\frac{\partial u_y}{\partial x}\right)^2 + \left(\frac{\partial u_z}{\partial x}\right)^2 \\ \left(\frac{\partial u_x}{\partial y}\right)^2 + \left(\frac{\partial u_y}{\partial y}\right)^2 + \left(\frac{\partial u_z}{\partial y}\right)^2 \\ \left(\frac{\partial u_x}{\partial z}\right)^2 + \left(\frac{\partial u_y}{\partial z}\right)^2 + \left(\frac{\partial u_z}{\partial z}\right)^2 \\ 2\left(\frac{\partial u_x}{\partial x} \frac{\partial u_x}{\partial y} + \frac{\partial u_y}{\partial y} \frac{\partial u_y}{\partial x} + \frac{\partial u_z}{\partial x} \frac{\partial u_z}{\partial y}\right) \\ 2\left(\frac{\partial u_x}{\partial z} \frac{\partial u_x}{\partial y} + \frac{\partial u_y}{\partial y} \frac{\partial u_y}{\partial z} + \frac{\partial u_z}{\partial z} \frac{\partial u_z}{\partial y}\right) \\ 2\left(\frac{\partial u_x}{\partial x} \frac{\partial u_x}{\partial z} + \frac{\partial u_y}{\partial z} \frac{\partial u_y}{\partial x} + \frac{\partial u_z}{\partial x} \frac{\partial u_z}{\partial z}\right) \end{bmatrix}$$

or shorter as:

$$E = \nabla_i u + \frac{1}{2} A(u) \nabla_u u$$

The weak form can now be rewritten as:

$$\int_V \rho v^T \ddot{u}_i dV + \int_V (\varepsilon^v)^T \sigma dV = \int_S v^T t dS + \int_V v^T b dV \quad (11)$$

The boundary conditions of the body can be expressed as:

$$\mathbf{u} = \text{is given along } S_u$$

$$\mathbf{t} = \text{is given along } S_t$$

The displacement vector  $\mathbf{u}$  is prescribed along the boundary surface  $S_u$  and the traction vector  $\mathbf{t}$  is prescribed along the boundary surface  $S_t$ .

According to the finite element method the displacement vector  $\mathbf{u}$  can be approximated by:

$$\mathbf{u} = N\mathbf{a} \quad (12)$$

where  $N$  contains the global shape features and  $\mathbf{a}$  the body displacements. The shape function only depends on position while the displacement vector  $\mathbf{u}$  depends on both position and time:

$$\mathbf{u} = \mathbf{u}(x_i, t); N = N(x_i); \mathbf{a} = \mathbf{a}(t) \quad (13)$$

This gives the acceleration:

$$\ddot{\mathbf{u}} = N\ddot{\mathbf{a}} \quad (14)$$

The strain can then be expressed as:

$$\varepsilon = B\mathbf{a}; B = B(x_i) \quad (15)$$

where  $B$  is given by the derivate of  $N$ . According to the Galerkin method the weight vector  $\mathbf{v}$  can be applied as:

$$\mathbf{v} = N\mathbf{c} \quad (16)$$

Column matrix  $\mathbf{c}$  is arbitrary, since  $\mathbf{v}$  is arbitrary and the global shape function is determined by us. (12) gives us the information that  $\mathbf{c}$  does not depend on position. From (16) the quantity  $\varepsilon^v$  can be determined on the similar way as (15) i.e.

$$\varepsilon^v = B\mathbf{c} \quad (17)$$

By using (16) and (17) in the weak form (11) of equations of motion gives:

$$\mathbf{c}^T \left[ \left( \int_V \rho N^T N dV \right) \ddot{\mathbf{a}} + \int_V B^T \sigma dV - \int_S N^T t dS - \int_V N^T b dV \right] = 0$$

Since this equation holds for arbitrary  $\mathbf{c}$ -matrices, it can be written as:

$$M\ddot{a} + \int_V B^T \sigma dV = f \quad (17)$$

where  $M$  is the mass matrix and can be defined as:

$$M = \int_V \rho N^T N dV$$

and  $f$  is defined as the external forces:

$$f = \int_S N^T t dS + \int_V N^T b dV$$

Eq.(17) is derived entirely from the equations of motion without any information on the particular constitutive relation and (17) therefore holds for any constitutive relation. When the acceleration  $\ddot{a}$  are zero the equations of motion (17) are reduced to the equilibrium equations:

$$\psi(a) = 0 \quad (18)$$

where

$$\psi = \int_V B^T \sigma dV - f \quad (19)$$

These equations form the base in the Newton-Raphson method.

#### 4.3.4 Newton Raphson scheme

The fundamental idea of the Newton-Raphson approach is to linearize the nonlinear function about a given point. This is done by guessing the start value  $x^0$ , at the corresponding point on the curve  $f(x)$ . The tangent is determined and this tangent is extrapolated to obtain the next estimate  $x^1$  for the solution. This procedure is then repeated so that the tangent point at B (see *figure 3.5*) provides the next estimate  $x^2$  and so on.

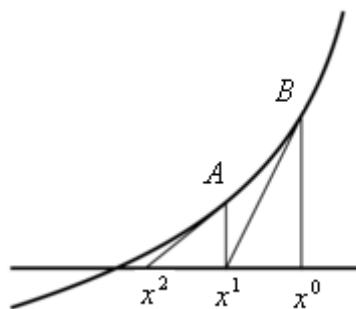


*Figure 4.8* Newton-Raphson strategy for a one-dimensional problem

Assuming that the approximation  $a^{i-1}$  to the true solution  $\mathbf{a}$  have been determined, a Taylor expansion of  $\psi$  about  $a^{i-1}$  yields:

$$\psi(a^i) = \psi(a^{i-1}) + \left( \frac{\partial \psi}{\partial a} \right)^{i-1} (a^i - a^{i-1}) \quad (21)$$

This expression represents the tangent to the curve at point  $a^{i-1}$ . Similar to the one-dimensional case above it requires that  $\psi(a^i) = 0$  and it then follows from eq. (21) that

$$0 = \psi(a^{i-1}) + \left( \frac{\partial \psi}{\partial a} \right)^{i-1} (a^i - a^{i-1}) \quad (22)$$

To continue, the derivate  $\frac{\partial \psi}{\partial a}$  has to be identified. Since the external load is fixed, (19) gives.

$$\frac{\partial \psi}{\partial a} = \int_{\mathbf{v}} \mathbf{B}^T \frac{d\sigma}{da} dV \quad (23)$$

With help from the constitutive relation  $\dot{\sigma} = D_t \dot{\varepsilon}$  and the variable is now  $\mathbf{a}$ , it can now be obtained.

$$\frac{d\sigma}{da} = D_t B \quad (24)$$

Inserting eq. (23) into eq. (24) yields

$$\frac{\partial \psi}{\partial a} = K_t \text{ where } K_t = \int_{\mathbf{v}} \mathbf{B}^T D_t B dV \quad (25)$$

$K_t$  is the tangential stiffness matrix of the body.

Eq. (22) now takes the form

$$(K_t)_n (a^i - a^{i-1}) = -\psi(a^{i-1}) \quad (26)$$

When using Newton-Raphson it is important to start in a state where equilibrium is fulfilled and all stresses, strains, displacement and loadings are known. The goal is to find the equivalent stresses, strains and displacement when the external loadings are changed to  $f_{n+1}$ . To obtain the starting condition, we know the out of balance forces

$\psi(a^{i-1})$

$$\psi(a^{i-1}) = \int_{\mathbf{v}} \mathbf{B}^T S^{i-1} dV - f_{n+1} \quad (27)$$

and then take the most recent known values as starting point.

$$a^0 = a_n; \quad S^0 = S_n; \quad (K_t)^0 = (K_t)_n \quad (28)$$

For the first iteration  $i=1$ , we find

$$(K_t)_n (a^1 - a_n) = f_{n+1} - \int_V B^T \sigma_n dV \quad (29)$$

The element software will stop the iterations of the out of balance forces  $\psi(a^{i-1})$  at a certain value specified in the software since the balance forces will not reach exactly zero. When the value of  $\psi(a^{i-1})$  is this small one can accept the solution  $a^{i-1}$ .

$$a_{n+1} = a^{i-1}; \quad \varepsilon_{n+1} = \varepsilon^{i-1}; \quad S_{n+1} = S^{i-1} \quad (30)$$

Every Newton-Raphson iterations is costly, since the  $K_t$ - matrix needs to be established in every step. This results in the modified Newton-Raphson method being often used instead. In this method the  $K_t$ - matrix is only recalculated once in every load step. The equations above are used in ABAQUS but in an updated Lagrange formulation. This updated formulation simplifies the equation system if the reference configuration is updated continuously in every iteration this so as to become equal to the current configuration [10].



## 5. Experimental work

The experimental work is divided into three different parts. The main part is when making straight creases by using a flat bed creasing machine with a straight creasing tool. These results are later compared to the simulations made in ABAQUS to obtain important information about the paper's behavior. The second part of the laboratory tests also consists of a flat bed creasing machine but with a bottom patterned tool instead of a straight tool. The results from the patterned crease are then compared to the straight crease to obtain differences in the creasing behavior. The third and last experimental part is in Tetra Pak's pilot plant, where analyses of the process in full scale are done.

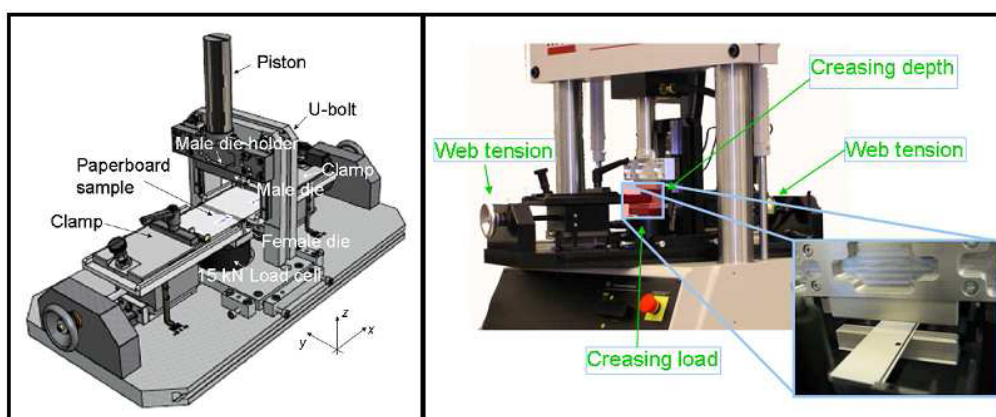


Figure 5.1 Laboratory creasing tool (MTS)

### 5.1 Experimental tools, parameters and procedure

Different kinds of tools are used to create and measure several properties and values. The different tools are described in the following subchapters.

#### 5.1.1 Laboratory creasing tool

To be able to do the tests, a hydraulic pull tester called MTS 858 Table Top System was used. Since it is hydraulic powered it was possible to run tests at high speed with good precision. The male die is mounted to a holder that is restricted to only move in the z-direction by rails that are mounted on a U-bolt. Along with the rails, an extensometer is mounted on the U-bolt. The extensometer makes it possible to measure and adjust the crease depth with an accuracy of a thousand of a millimeter. The female die is mounted on a load cell that can measure forces up to 15 kN (creasing force). Since this master thesis is analyzing the affects of displacement of the male/female tool, it was necessary to tune one of the dies a very short distance to obtain a controlled displacement. To be able to do this, four screws are mounted in the bottom of the U-bolt which allow moving the male creasing tool in the x-direction (MD), y-direction (CD) and rotating it around the z-axis [1].

The figure below is a schematic drawing of the creasing tool in the  $xz$ -plane during creasing of the paperboard. The male die has a ruler that sticks out from the base. This ruler has different widths depending on what type of paperboard that is to be creased. The female die has a groove where the paperboard is pressed down by the rule during creasing.

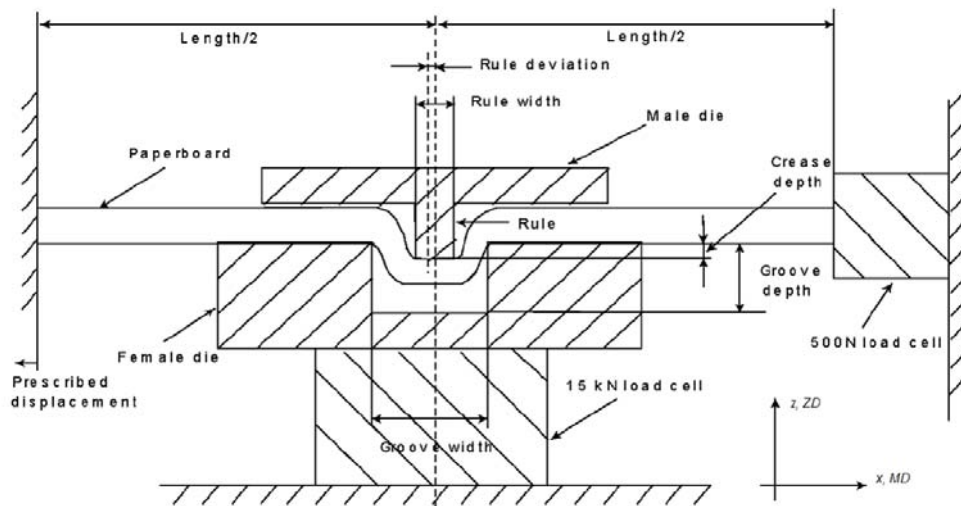


*Figure 5.2 A principle sketch of the creasing tool*

To be able to perform an experiment that is as close to a real procedure as possible it was necessary to apply web tension to the paperboard. Web tension is the tensile force that appears in the paperboards MD ( $x$ -direction) when the paperboard is stretched. By fastening both ends of the paperboard in to adjustable clamps and adding a precise load cell, it was possible to adjust the web tension as desired.

As stated above, the MTS-machine makes it possible to control the web tension, creasing depth and the creasing speed. In addition, it is possible to monitor the web tension, creasing depth and creasing load as a function of time. By using Matlab the crease force can be plotted as a function of crease depth. By doing so the following parameters are established:

- Maximum force
- Energy; area below the curve
- Remaining deformation of the crease with applied web tension

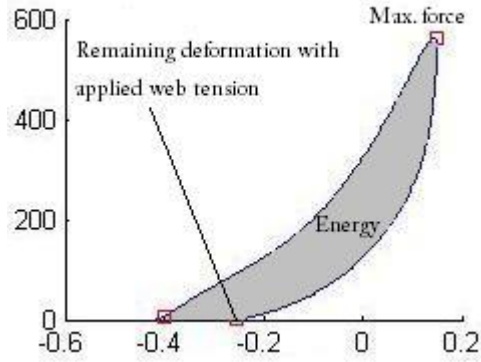


Figure 5.3 Creasing parameters

### 5.1.2 Creasability tester

To get the folding forces a Lorentzen & Wettre creasability tester (L&W) was used. By fastening the samples in a clamp on the L&W and then letting the machine rotate the sample from 0 to 120 degrees, the bending force could then be measured by the load cell.

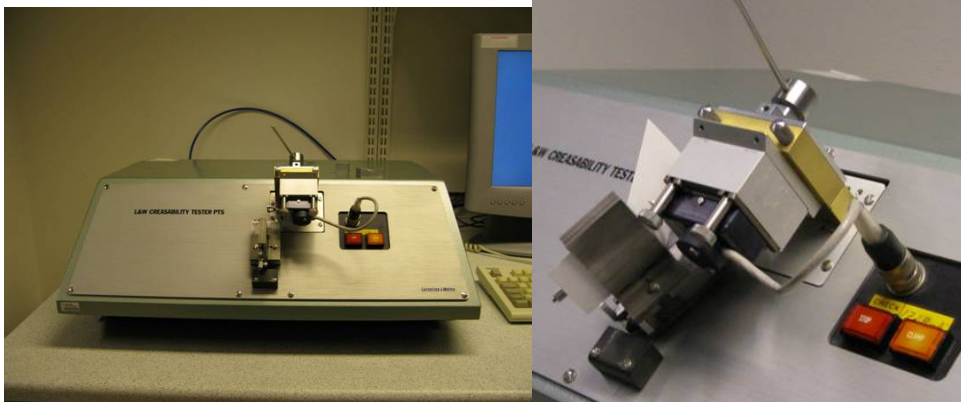


Figure 5.4 L&W Creasability tester

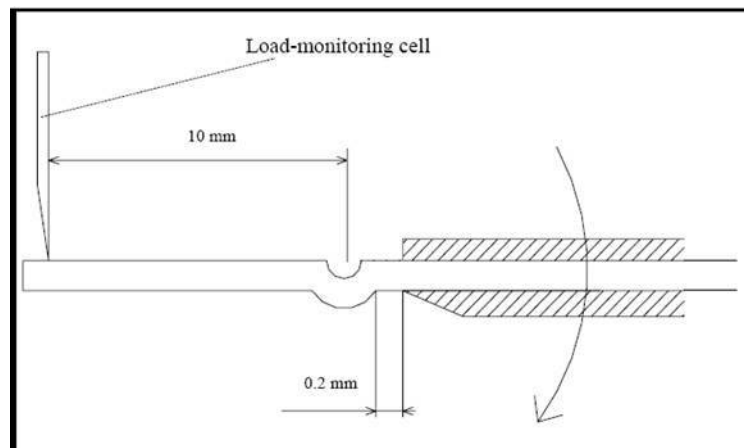


Figure 5.5 Principle sketch of the L&W creasability tester

Both the creased and uncreased paperboards are folded in the machine to achieve the two necessary parameters to calculate the RCS-value. By using Matlab the relation between the bending force and the bending angle can be plotted.

The following parameters were established:

- Maximum force at or below 30 degrees of the creased sample
- Energy (the area under the curve of the creased sample)
- Initial inclination of the creased sample (same as initial stiffness of the crease)
- Final angle after released bending force of the creased sample
- Relative Crease Strength – RCS

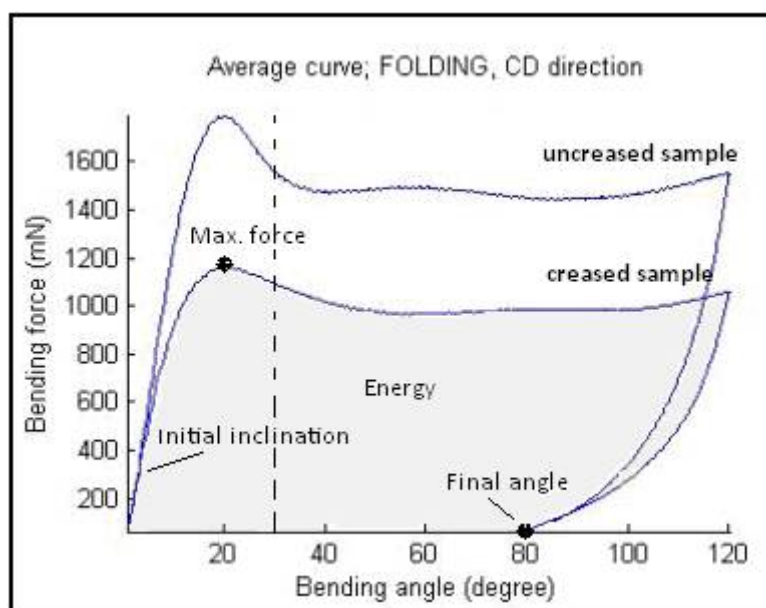


Figure 5.6 Folding parameters

### **5.1.3 Creasability procedure**

The creased samples were tested in the creasability machine by inserting the creased sample between the fastening clamps and let the machine bend the sample 120 degrees. The sensor cell in the creasability tester is able to measure bending forces up to 5000 mN. For each of the creasing setups, ten creasability tests were done. When there is a displacement in the creasing procedure the paperboard will be more compressed on one side than the other side. This result in the RCS-value will be different depending on what side is measured. Therefore it is important to measure the RCS-value on both sides. Five of the samples with the creasing displacement downwards and the other five with the creasing displacement upwards were measured.

### **5.1.4 Topography**

To be able to study the surface of the paperboard an optical 3D measuring system called MikroCAD, manufactured by GFM were used. This tool is a computer assisted optical surface measuring system and is used to measure 2D and 3D profiles, as well as roughness of small and microscopic objects. The optical method used for measuring is the digital stripe projection technique, based on digital micro mirror projectors by Texas Instruments. Stripes with sinusoidal intensity of brightness are projected onto the surface of the measuring object and their projection (the stripes changed by the height profile of the measuring object) is recorded with a defined triangulation angle by a CCD camera. The topography of the measuring object is calculated from the stripes position and the grey value of all registered individual image points. Depending on the concrete measurement task different stripe projection procedures can be used.

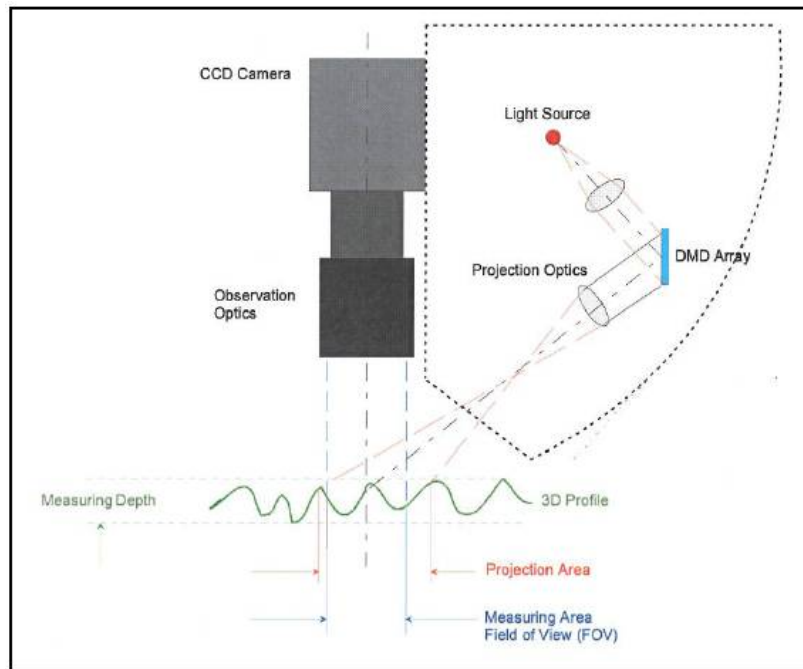


Figure 5.7 Principle sketch of optical 3D sensor

### 5.1.5 Topography procedure

Each sample was fastened to a vacuum holder to keep the sample from moving under the scanning device. The focus and the light source were adjusted until the result was satisfying. Due to the measurement's sensitivity to light it is very important to make sure that no other light from the surroundings reaches the instrument. After the sample has been scanned it is possible to collect a lot of information from it. By doing 30 parallel lines across the crease, it was possible to get a graph of the variation of the heights for each line. This makes it possible to analyze how the crease changes.

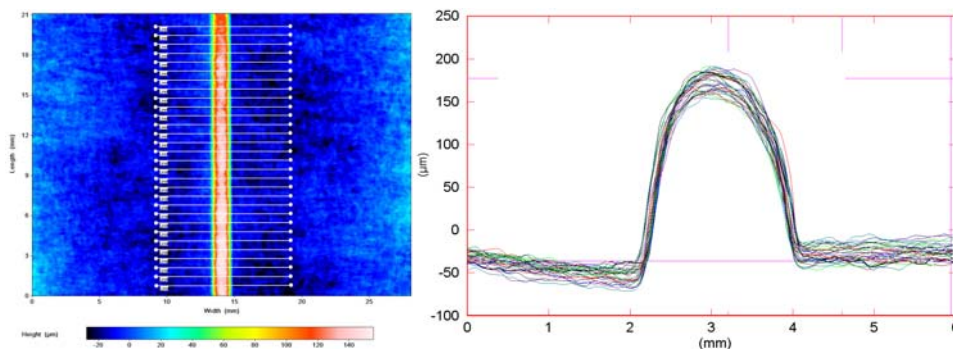
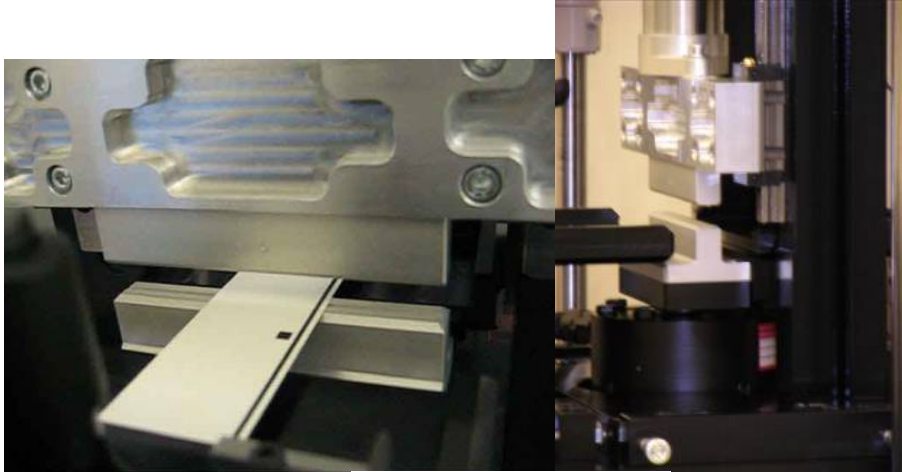


Figure 5.8 Topography with 30 lines cross the crease (left), plot of cross section with all lines (right)

## 5.2 First experimental part: straight creases

The first experimental part was on the straight creases and was done in the MTS 858 Table Top System.



*Figure 5.9 Straight creasing tool*

### 5.2.1 Parameters

Web tension:	1 kN/m, 1.5 kN/m, 2 kN/m
Displacement (thin paperboard):	0.0 mm, 0.05 mm, 0.1 mm
Displacement (thick paperboard):	0.0 mm, 0.08 mm, 0.16 mm
Paperboard (thin paperboard):	A1, B1
Paperboard (thick paperboard):	A2, B2
Creasing depth (thin paperboard):	0.15mm 0.20mm 0.25mm
Creasing depth (thick paperboard):	0.15mm 0.20mm 0.25mm
Creasing tools geometries:	Straight 1 (used with A1 and B1) Straight 2 (used with A2 and B2)

### 5.2.2 Laboratory creasing procedure

First, paper stripes with a width of 38 mm and a length of 100 mm were cut out from the paperboard with the MD parallel to the length. It was very important that all of the

## Experimental work

stripes had the same lengths and widths so it would be possible to compare the results. By using the earlier discussed method DOE, the tests were done in a specific order with specific parameters. The parameters that were used during the creasing tests are web tension, crease depth, displacement of the male die and paperboard stiffness. For each setup it was necessary to do 15 samples to be able to cover the need for samples during RCS testing, which is a destructive test method (the sample is destroyed during the test).

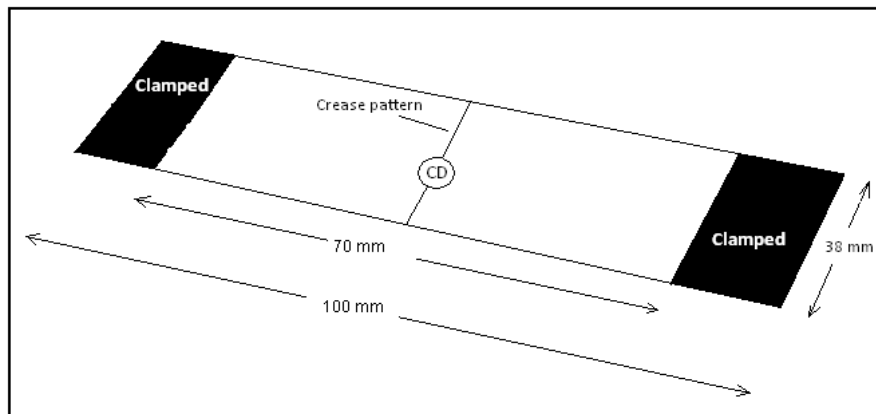


*Figure 5.10 Sample for straight creases*

The most difficult part during changing setup was to get a precise displacement of the male die. At first the male die were adjusted to a more or less random position and then checked by creasing a plastic film that was later studied and measured in a light microscope. From the result the male die could be tuned into the desired position. However, this method did not work very well since the creasing marks in the plastic film were too wide and not precise enough to get good measurements in the light microscope. The plastic film was switched into two component putty (a clay also used by dentists to make imprints of the teeth) since the imprint of the crease is very easy to measure in the microscope with its sharp edges.

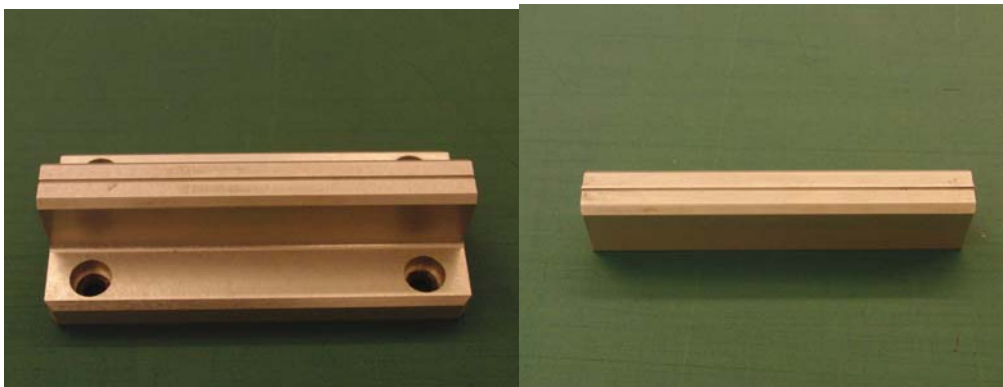


*Figure 5.11 Female die straight crease (left), male die straight crease (right)*



### 5.2.3 Creasability procedure

The five total RCS values from each setup were used to calculate a mean value that can be compared to the mean values from the other setups.

### 5.3 Second experimental part: bottom crease pattern

The second experimental part was also performed in the MTS 858 Table Top System. This time tests on the bottom crease pattern were investigated. The reason why tests on the bottom crease pattern are important is because samples from different directions can be measured. Also, the bottom crease pattern gives the result of several simultaneously engaged creases.

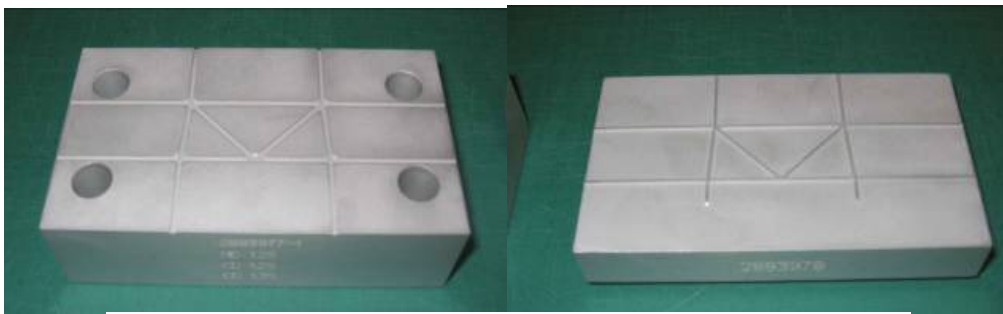


Figure 5.12 Female bottom crease pattern (left), male bottom crease pattern (right)

#### 5.3.1 Parameters

The parameters were similar to previous parameters. The difference was that only one web tension was applied for each thickness of paper. The reason why 1 kN/m was chosen for the thin paperboard was because it is the most similar to the web tension used in the production line. For thick paperboard 0.5kN/m was chosen, because when tests with 1kN/m web tension were applied, the load cells maximum limit was reached.

Web tension (thin paperboard):	1 kN/m
Web tension (thick paperboard):	0.5 kN/m
Displacement CD (thin paperboard):	0.0 mm, 0.05 mm, 0.1 mm
Displacement MD (thin paperboard):	0.0 mm, 0.05 mm, 0.1 mm
Displacement CD (thick paperboard):	0.0 mm, 0.08 mm, 0.16 mm
Displacement MD (thick paperboard):	0.0 mm, 0.08 mm, 0.16 mm
Paperboard (thin paperboard):	A1, B1
Paperboard (thick paperboard):	A2, B2

Crease tool geometry:	Bottom 1 (used with A1 and B1) Bottom 2 (used with A2 and B2)
Creasing depth:	As deep as possible without any initiation of cracks

### 5.3.2 Laboratory creasing procedure

To crease the whole pattern from the bottom tool it is necessary to use much wider paper samples. The size chosen to cover the whole pattern and fit into the MTS-machine was 110 x 100 mm with the length parallel to the MD. From the results obtained from the tests with straight creases it was determined that the web tension was not a significant factor. Since it was insignificant, the web tension was removed as a factor in order to reduce the number of tests. To obtain as much relevant information as possible from the fewer tests, a separate crease depth for each paperboard and each displacement was used. When tuning the bottom crease tool into a desired crease depth it was not as simple as for the straight creases since the crease depth changed every time, even though no parameters had been changed. As a result from the undesired changing in crease depth a tolerance had to be established. It was decided that any test that lay in the tolerance  $\pm 0.005$  mm of the desired crease depth was accepted. By creasing with the specific displacement, tests were made by creasing as deep as possible without letting any cracks occur. The deepest crease without any cracks from 10 tests in a row was chosen. It can be very difficult to determine if there is a crack or not when looking in a microscope. Therefore it is very important to be consistent so all of the samples are treated in the same way. For example, sometimes it is possible to see fibers from the paperboard spreading in different directions out of the paper, but it was decided that this phenomenon is not a crack. Only when the paper is separated in the plies is it rated as a cracked sample (*figure 4.11*).

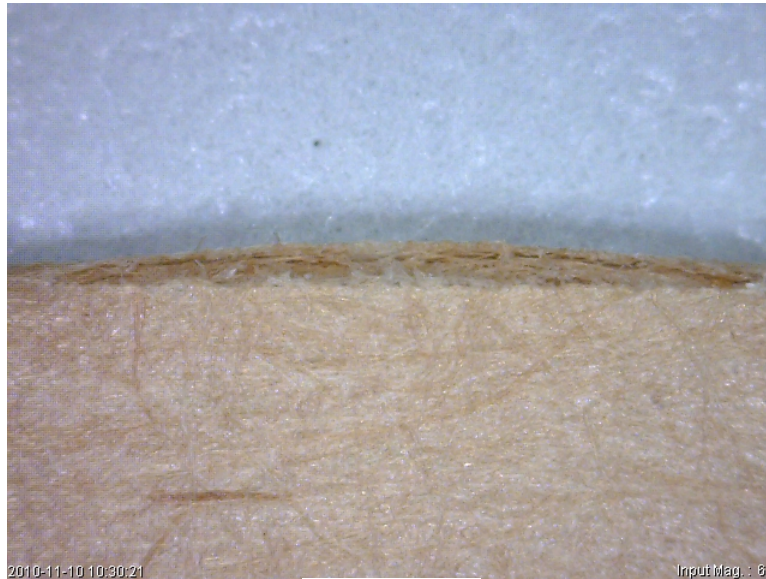


Figure 5.13 Crack

It is even more difficult to calibrate the setup for the bottom pattern than for the straight crease since the tool, when using the bottom crease pattern, can be dislocated both in the CD and the MD. To get a setup as accurate as possible, the same two component clay was used again. It was much harder to get an exact crease depth when using the bottom crease pattern. The depth changed a lot without changing the parameters on the computer. A tolerance was therefore introduced. This tolerance let the desired value to change  $\pm 0.005$  mm. Since it was possible to get 4 creases from one sample, only 5 creasing samples were made for each setup.

### 5.3.3 Creasability procedure

From the creased paper with the bottom pattern it is possible to get two creases in MD and two creases in CD from each sample. When the straight crease was used the samples had a width of 38 mm but, unfortunately, it was impossible to get the same width when creasing with the bottom pattern. The critical crease was the MD that could be only 15mm wide. Because of this, both of the directions were cut to a width of 15mm to make comparison possible. Besides the different widths, the creasability procedure was the same as for the straight creases.

## 5.4 Third experimental part: Pilot plant

The third experimental part was done in the Tetra Pak's pilot plant, where tests are made in full scale.

#### 5.4.1 Parameters

Web tension:	1kN/m
Displacement MD (thin paperboard):	0.0 mm, 0.05 mm, 0.1 mm
Displacement CD (thin paperboard):	0.0 mm
Displacement MD (thick paperboard):	0.0 mm, 0.08 mm, 0.16 mm
Displacement CD (thick paperboard):	0.0 mm
Paperboard (thin paperboard):	B1
Paperboard (thick paperboard):	B2
Creasing depth:	As deep as possible without any initiation of cracks
Creasing tool geometry:	Plate 1 (used with B1) Plate 2 (used with B2)

#### 5.4.2 Creasing procedure

The crease plates for the male and female die were mounted on large rotating cylinders (*Figure 4.10*). Two different kinds of paperboards were tested in the pilot plant, B1 and B2. Each paperboard has its own creasing pattern, i.e. one creasing pattern for B1 and another for B2. For B1 six plates were mounted on the cylinder and for B2 only four plates were mounted. The reason for the different number of plates was because it is the same size on the cylinders but a different size on the crease plates.

The procedure was the same as for the bottom creases in the MTS-machine. The maximum crease depth was investigated. The experiment started with centered crease plates and with the B1 paperboard. After the tests were performed, the plates were tuned a short distance. To be able to have a controlled displacement a dial indicator was fastened at the male crease plate's short end. The screws that holds the plate were loosened a bit to be able to move the plate with help of a hammer into the desired displacement. Since the dial indicator registers a thousand of a millimeter it was easy to tune the plate to a desired displacement. The same procedure was followed for the following displacement and for the other paperboard with its displacements.

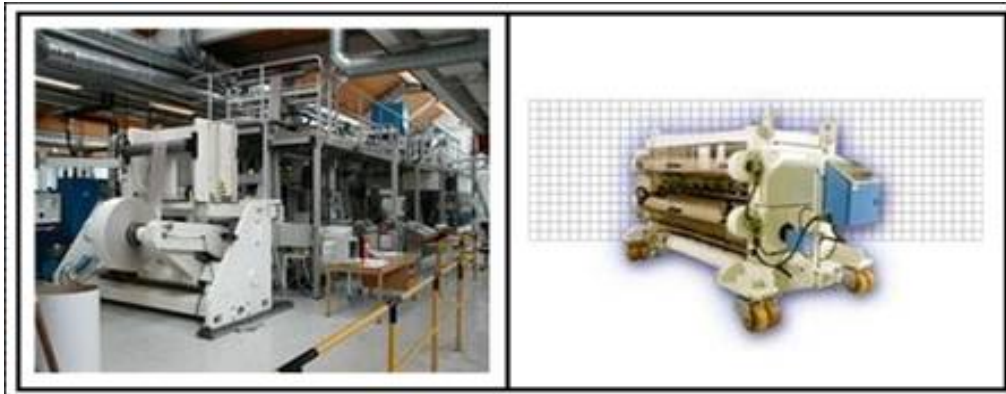


*Figure 5.14* Pilot plant (left), rotational cylinders (right)

### 5.4.3 Creasability procedure

From the pilot plant, the distortion and the crease height could be measured automatically by using the in-line RCSp-system. This made it easy to compare with the previous experimental procedures. The paper strips for the measurements in the creasability tester were cut out manually, four creases in each direction and for each plate (*Figure 4.11*). For paperboard B1, 24 creases in MD and CD were cut out and measured by an automatic creasability tester. For paperboard B2, 16 creases in each direction were cut out and measured. The automatic creasability tester works in almost the same way as the manual one, but it requires a specific size of the samples which was only possible to achieve when full scaling tests were made.

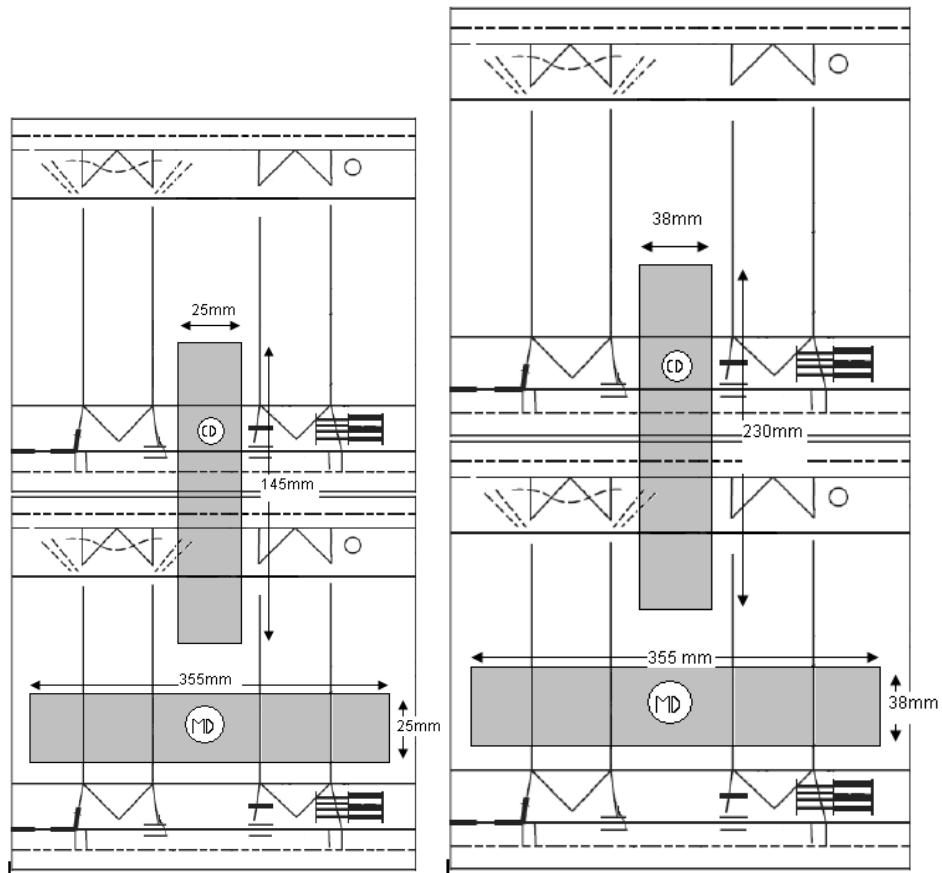


Figure 5.15 Crease pattern for B1 (left). Crease pattern for B2 (right)

## 6 Computer simulations

Computer simulation is important since it is of interest to compare it with the real tests that were made. The simulations make it easy to obtain graphs that can be compared with the different experimental parts. This chapter describes how the simulations were made.

### 6.1 ABAQUS

ABAQUS is graphical finite element analysis software which is used to solve both linear and nonlinear problems. The analysis comprises three different steps.

The first step is called preprocessing and is done in ABAQUS/CAE. The preprocessing is about modeling the problem in the program. It is possible to generate models in the program or import them from external CAD programs. Finally, boundary conditions and loads are applied to the model to create a problem as similar to reality as possible.

The second step is when the file created in the first step is sent to ABAQUS/Standard or ABAQUS/Explicit. In this step the numerical problem is solved and a file is created where all the data is stored. The ABAQUS/Standard is an implicit solver and ABAQUS/Explicit solves the problem explicitly.

The third and last step is called post-processing and is also done in ABAQUS/CAE. The post-processing shows the results obtained in the second step graphically. This can be shown as animations, color contour plots and X-Y plots [14].

### 6.2 Model

The whole model including paperboard, female die and male die were constructed as 2D models, but received an offset depth of 0.1 mm. The model was locked in the offset direction hence it could be resembled to a two dimensional model, but still have a width like a 3D model.

The model was based on a previous model [8], but modified to fit this kind of problem. Only straight creases were looked at. Two different models were used, one for thin paperboard, and one for thick paperboard. The greatest difference between the two models was the height of the paperboard. The thin paperboard was 0.28 mm thick and the thick paperboard was 0.4 mm thick.

The paperboard, regardless of type of paperboard, consisted of four different plies that were divided by three different interfaces. Two of these plies were so called chemical plies and the other two were mechanical plies. The material parameters can be seen in the *Appendix L*. The interfaces are made by cohesive elements and both the mechanical and chemical plies are continuum elements. There are only interface elements in the creasing area since the paperboard is expected to delaminate in this region. The total length of the model was 60 mm. The model consisted of 6 different parts; one female die, one male die and four plies. The reason why four different plies were used was because they all have different behavior, and therefore different parameters.

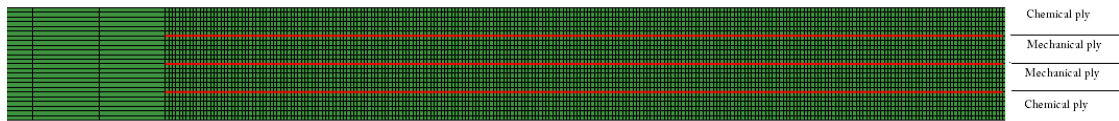


*Figure 6.1 Paperboard with its four plies and three interfaces (red)*

### 6.3 Boundary conditions

To obtain a model that is as close to reality as possible it is very important to choose the boundary conditions carefully. First of all, boundary conditions to prevent rigid body motion are created by locking the parts in all directions. In reality, the paperboard is exposed to web tension which is a factor that can not be ignored. To simulate web tension, the paperboard is stretched a short distance to obtain the tensile stress that the web tension generates. The required distance needed to generate the desired tensile stress can be calculated with Hooke's law  $\sigma = E \cdot \varepsilon$ .

When performing outside creasing (which is used in this master thesis), the male die presses the paper into the female die. To simulate this, the female die was locked in the same position during the simulation, while the male die translated towards the female die.

When paperboard is creased it delaminates in certain regions, which means that the different plies in the paperboard separate from each other. In a simulation this is not easy to do since, when choosing constraints, it is necessary to decide if the plies are bonded to each other or if they can slide. If the surfaces are bonded together no delamination can occur. The reality is therefore a combination between those two. To obtain a simulation model that was as close to reality as possible, a combination between those was generated. The idea was to have the plies bonded (like glued together) in the contact regions outside the creasing area to prevent sliding. In the creasing area the plies are free to glide so that delamination can occur.

### 6.4 Mesh

Generally speaking, a model gets better results (closer to reality) the more elements it contains. The negative side of using a lot of elements is that it requires much more computer power. To obtain good results without using too much computer power, it is possible to employ a finer mesh (smaller elements) in the regions that are expected to deform, and a coarser mesh (larger elements) in the areas where deformations are expected to be small or nonexistent. By using this way of thinking the model of the paperboard is divided into three parts; the left part, the creasing part and the right part. The right and left parts are not much affected by the creasing procedure. Therefore these parts comprise larger elements. The creasing part is where most of the deformation occurs, which is why it comprises many small elements.



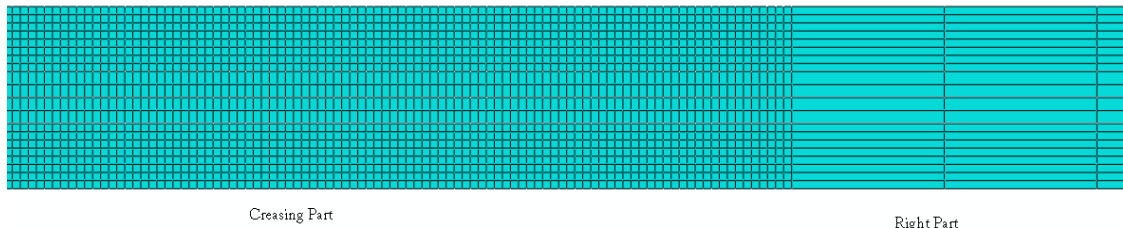


**Figure 6.2** Paperboard that shows the finer mesh (left) and coarser mesh (right)

### 6.5 Procedure

In a simulation everything has to be divided into steps to be sure that everything happens at the right moment. All the steps are so called ramped, which means that the distance moved goes from zero to maximum value in a linearly increasing speed. The creasing procedure contains four steps:

1. Apply web tension – First, the paperboard must be stretched until the desired web tension is reached. This is done by letting the right side of the paperboard be fixed in one position, and pulling the left side a specific distance. Only when the maximum value is reached can the procedure continue to the next step.

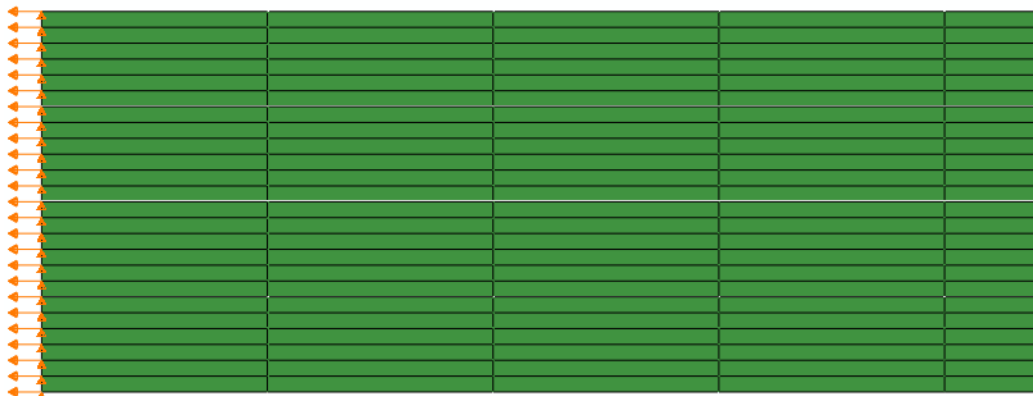


**Figure 6.3** The left side of the paperboard is stretched to obtain web tension

2. Male punch – When the desired web tension is reached the simulation continues to the step where the male die will move towards the female die to create a crease. The male die starts in a specific position and moves downwards into the female die. The distance the male die moves is determined by the desired crease depth. This step ends when the male die reaches the desired crease depth.

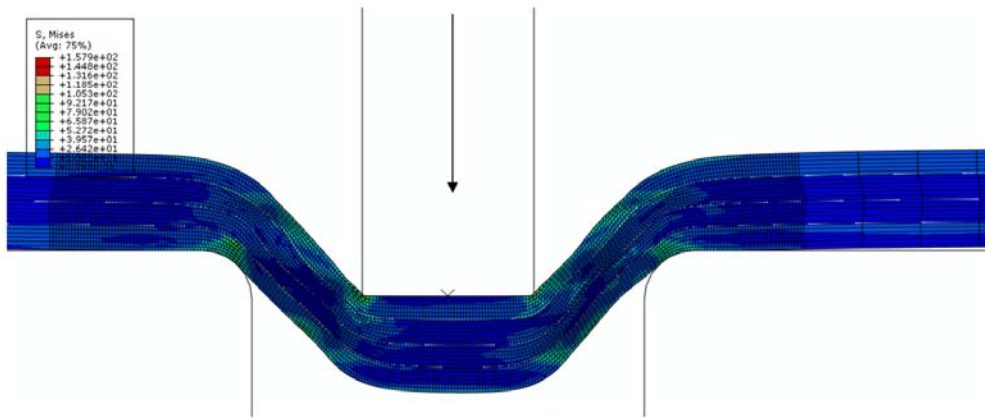


*Figure 6.4 The male die presses the paperboard into the female die*

3. Male – When the desired crease depth is reached, the male die has to go back to its original position. This step can not be ignored since the male die must not have any contact with the paperboard before the web tension is released.

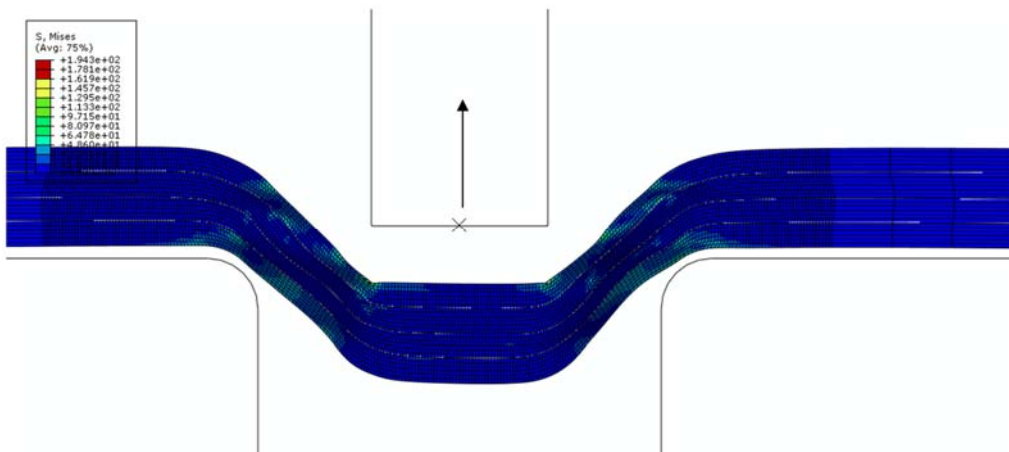


*Figure 6.5 The male die moves back to its original position*

4. Remove web tension – When the male die have reached its original position, the boundary conditions that holds the paperboard into place (including web tension) let go. When the paperboard is released from the tension, the plastic deformations still remain.

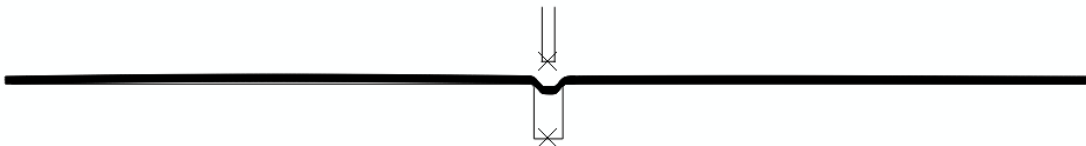


*Figure 5.6 Both ends of the paperboard are released*

## 7 Results

This chapter is divided into two main parts, the experimental part and the computer simulation part. Since the results from both parts contain a lot of numbers and diagrams, only some examples are included in this chapter while the main part is in the *Appendix L - O*.

### 7.1 Experimental part

The experimental part is, as mentioned in chapter 4, comprised of; straight creases, bottom crease pattern and pilot plant.

#### 7.1.1 Straight creases

The main goal with testing the straight creases was to get an understanding in how the different parameters affect the response. Therefore all the results in this sub chapter concern statistics evaluation.

The problem formulation was put into MODDE to achieve a worksheet that was to be followed during the tests. The worksheets, which consist of 20 tests, can be found in *Appendix A1* for thin paperboard and *Appendix A3* for thick paperboard. The numerical responses that were achieved during tests and put into MODDE can be found in *Appendix A2* for the thin paperboard and *Appendix A4* for the thick paperboard. When the responses were implemented in MODDE, it generates the summary of fit plot that can be used to evaluate how well the model fits the results.

The summary of fit plot for the thin paperboards can be seen in *Figure 6.1*. The first thing to observe is how good the bars goodness of fit ( $R^2$ ) and goodness of prediction ( $Q^2$ ) are, according to the states in chapter 2.2.1 Design of Experiments – DOE. As seen, in most cases it looks good with both bars high ( $R^2$  and  $Q^2$ ) and the difference between them being less than 0.2-0.3, as recommended. In some cases these bars do not show any satisfying results. In one case, the *Model validity* bar is even negative. These results show that the model is not good for these types of analyses. Even though some results have high bars and some have low it is good information for further analyses. Since the low-bar-factors are now known, this need not be investigated any further.

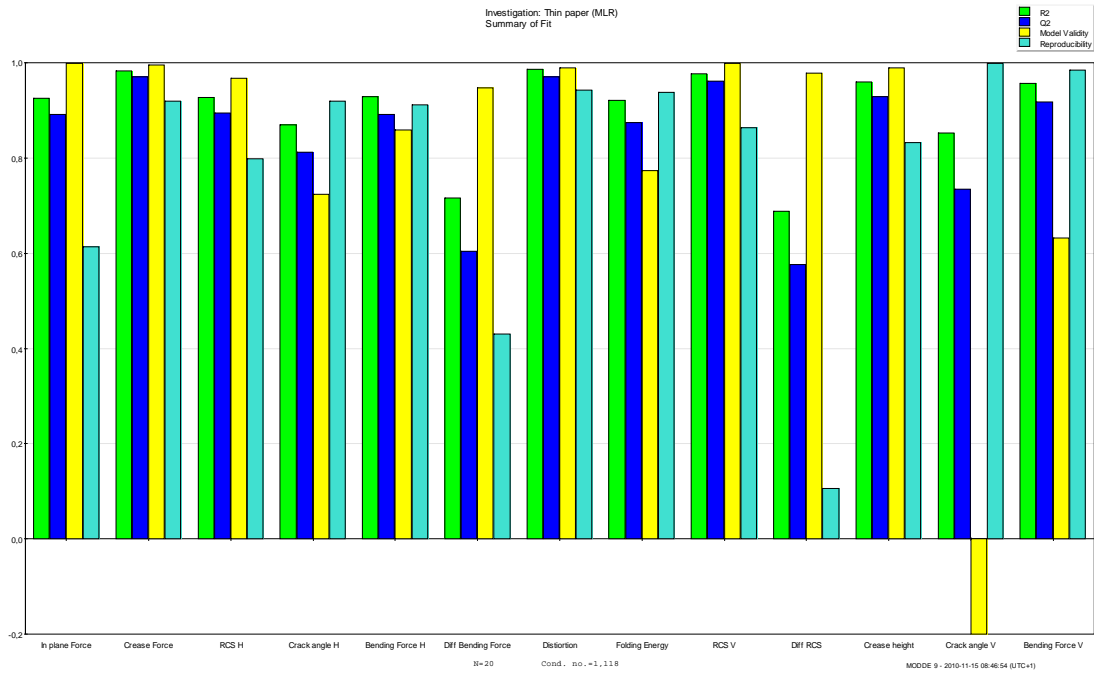


Figure 7.1 Summary of fit plot with the thin paperboard

As for the thick paperboard that can be seen in *Figure 6.2*, the main part of  $Q^2$  and  $R^2$  looks very good, but there are still some bad cases.

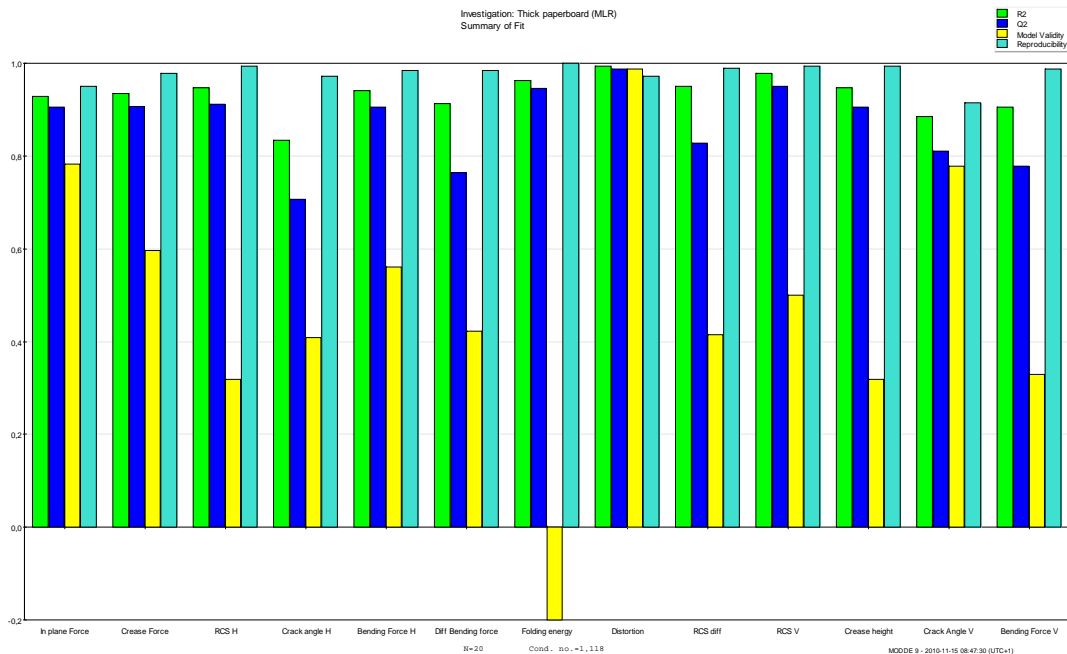
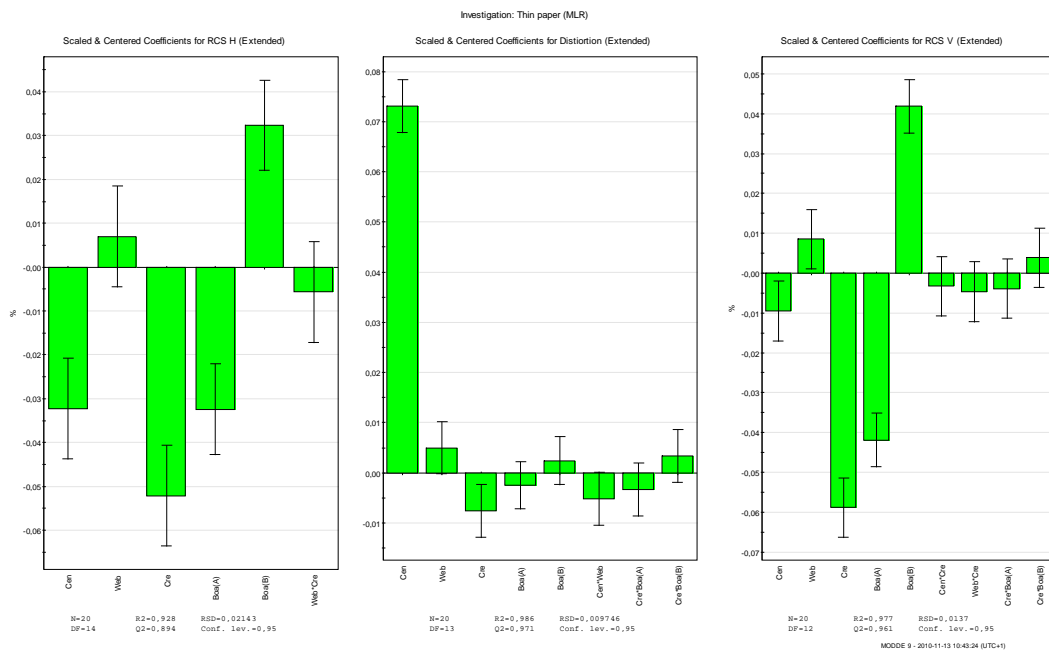


Figure 7.2 Summary of fit plot with the thick paperboard

The RCS value has already been discussed, but, as can be seen in the figures, there are two values, RCS H and RSC V. The difference between these two is that RCS H is the part of the crease that is on the same side that the male die has been displaced to. RCH V is thereby the side away from the displaced die. All of the coefficient plots that are established from the thin paperboards can be found in *Appendix B1* and the plots from the thick boards can be found in *Appendix B2*. It was chosen to have the three most relevant plots in this chapter since they are a commonly used means of measuring the creasing process. The three responses are; RCS H, RCS V and Distortion.

*Figure 6.3* below illustrates how the parameters affect the responses in a thin paperboard. The RCS H coefficient plot shows that crease depth (Depth) has the largest impact on this response, but displacement of the die (Cente) and the supplier of paperboard (Board) also affect the RSC H value. The other two factors can be ignored since they are not significant. The distortion coefficient plot shows very clearly that the displacement of the die is the main reason for changes of the distortion. The RCS V plot is similar to the RCS H plot, but it can be seen that the displacement of the die does not affect this response as much in RCS H.



**Figure 7.3** Coefficient plots for responses; RCS H, Distortion and RCS V for thin paperboards

The coefficient plots in *figure 6.4* bellow shows the same responses as earlier but with a thick paperboard. As can easily be seen, the plots with the thick paperboard look almost identical to the plots with thin paperboard. The reason why there is only one bar in the distortion plot is because the other factors were not significant and MODDE could establish a better model if these factors were ignored.

## Results

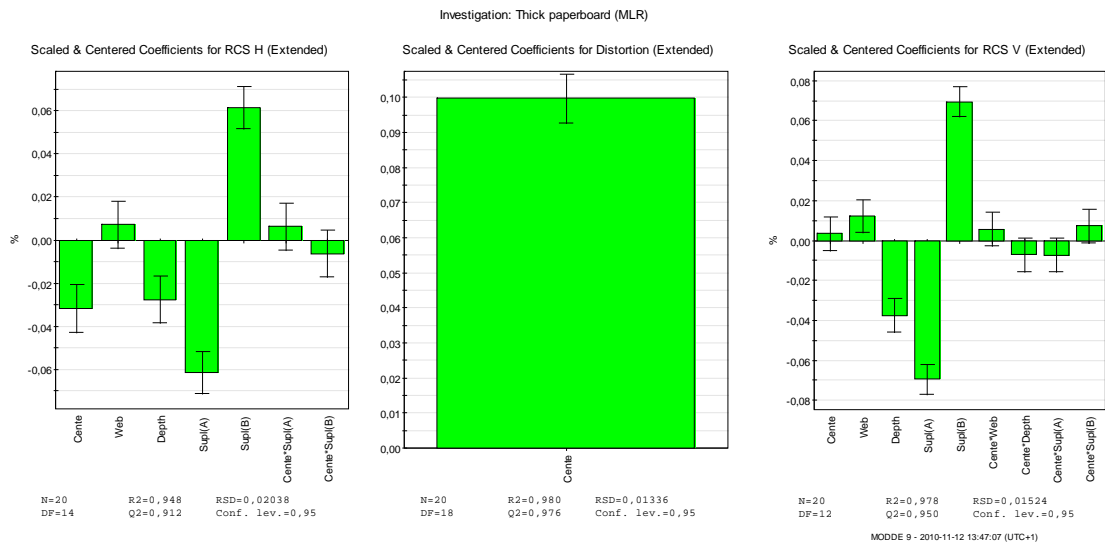


**Figure 7.4** Coefficient plots for responses; RCS H, Distortion and RCS V for thick paperboards

As can be seen in *Appendix B1* for thin paperboards, the only responses where displacement of the die is not significant are in Crack angle (R+V), Bending Force V, Folding energy and Crease height at a significant difference of 95%. For the thick paperboards it is only Folding energy, Crease height, Crack angle V, Bending Force V and RCS V where the displacement of the die is not significant at the same signification level, as can be seen in *Appendix B2* for thick paperboards.

It is possible to measure the crease's shape from the topography. In *Appendix C*, it is possible to see how the crease height and distortion changes with the different setups. It can be seen that the distortion mainly changes with the displacement of the die and the crease height mainly changes with the crease depth.

### 7.1.2 Bottom crease pattern

As mentioned earlier, the goal with the bottom crease pattern was to analyze how deep it is possible to crease without initiating any cracks. The table below shows the test plan and what it resulted in. The tests where cracks were initiated are marked in red for easier separation between good and bad results. RCS values were not measured for the tests with cracks since cracks are unwanted in the production line and are thus not relevant to the analysis.

Table 7.1 Results from tests with bottom crease pattern

Paperboard	Displacement CD/MD	Crease depth	RCS CD	RCS MD	Distortion CD	Distortion MD	Crease height CD	Crease height MD	Web tension	Crack
<i>Thin paperboard</i>										
A1	0	0.300	-	-	-	-	-	-	1	Yes
A1	0	0.275	0.562	0.440	-0.004	-0.011	0.103	0.121	1	No
B1	0	0.200	0.584	0.427	-0.001	-0.006	0.169	0.194	1	No
A1	0.05	0.300	-	-	-	-	-	-	1	Yes
A1	0.05	0.275	0.616	0.430	0.066	0.068	0.112	0.127	1	No
B1	0.05	0.300	-	-	-	-	-	-	1	Yes
B1	0.05	0.250	-	-	-	-	-	-	1	Yes
B1	0.05	0.225	-	-	-	-	-	-	1	Yes
B1	0.05	0.200	0.542	0.350	0.064	0.057	0.175	0.199	1	No
A1	0.1	0.200	-	-	-	-	-	-	1	Yes
A1	0.1	0.175	0.669	0.468	0.141	0.115	0.109	0.123	1	No
B1	0.1	0.200	-	-	-	-	-	-	1	Yes
B1	0.1	0.175	0.543	0.373	0.132	0.116	0.134	0.154	1	No
<i>Thick paperboard</i>										
A2	0	0.200	-	-	-	-	-	-	0.5	Yes
A2	0	0.150	-	-	-	-	-	-	0.5	Yes
A2	0	0.125	0.329	0.423	0.044	0.012	0.087	0.094	0.5	No
B2	0	0.150	-	-	-	-	-	-	0.5	Yes
B2	0	0.100	-	-	-	-	-	-	0.5	Yes
B2	0	0.075	0.483	0.606	0.044	0.007	0.151	0.155	0.5	No
A2	0.08	0.125	-	-	-	-	-	-	0.5	Yes
A2	0.08	0.100	0.354	0.403	0.090	0.083	0.065	0.070	0.5	No
B2	0.08	0.100	-	-	-	-	-	-	0.5	Yes
B2	0.08	0.075	0.465	0.598	0.104	0.097	0.098	0.109	0.5	No
A2	0.16	0.100	-	-	-	-	-	-	0.5	Yes
A2	0.16	0.050	-	-	-	-	-	-	0.5	Yes
A2	0.16	0.025	0.393	0.484	0.213	0.180	0.090	0.092	0.5	No
B2	0.16	0.050	-	-	-	-	-	-	0.5	Yes
B2	0.16	0.025	0.479	0.655	0.212	0.163	0.151	0.153	0.5	No

### Pilot plant

To optimize the use of time and the costs of buying paper, only one supplier's paperboard was analyzed during this test. As with the bottom crease pattern, the deepest crease possible without any initiation of cracks was to be determined, and the red marked values are samples where cracks were found.

## Results

*Table 7.2 Results from tests in pilot plant*

Paperboard	Displacement	Crease depth	RCS CD	RCS MD H	RCS MD V	Distortion	Crease height CD	Crease height MD	Crack
<i>Thin paperboard</i>									
B1	0	0.200	-	-	-	-	-	-	Yes
B1	0	0.175	-	-	-	-	-	-	Yes
B1	0	0.150	0.688	0.709	0.721	0.0073	0.0240	0.0446	No
B1	0.05	0.150	-	-	-	-	-	-	Yes
B1	0.05	0.125	0.710	0.680	0.765	0.0358	0.0248	0.0382	No
B1	0.1	0.150	-	-	-	-	-	-	Yes
B1	0.1	0.125	-	-	-	-	-	-	Yes
B1	0.1	0.100	0.733	0.693	0.792	0.0721	0.0217	0.0334	No
<i>Thick paperboard</i>									
B2	0	0.190	-	-	-	-	-	-	Yes
B2	0	0.140	0.588	0.543	0.578	0.0087	0.0613	0.0336	No
B2	0.08	0.140	-	-	-	-	-	-	Yes
B2	0.08	0.115	-	-	-	-	-	-	Yes
B2	0.08	0.09	0.614	0.558	0.606	0.0738	0.0586	0.0324	No
B2	0.16	0.09	-	-	-	-	-	-	Yes
B2	0.16	0.065	0.638	0.540	0.631	0.1054	0.0486	0.0278	No

It can be seen in the table that the distortion follows the displacement of the die very closely, both for the thin paperboard and for the thick paperboard. Another thing that can clearly be seen in the table is that the RCS H value for the MD crease is always lower than the RCS V-value which is exactly what MODDE predicted it to be in chapter 6.1.1 Straight creases.

## 7.2 Simulations

The computer simulations are divided into two parts, where the first part is about analyzing how the crease force changes with crease depth and displacement of the male die. These simulations are compared to the results obtained in the laboratory part for straight creases. The second part is about analyzing the appearance of the paperboard's plastic deformations.



### 7.2.1 Simulation vs. experiments

The results from the comparison between simulations and laboratory tests for straight creases can be found in *Appendix M*, where simulations are plotted against the experimental results for the same setup. The simulations are only compared for paperboard B2 since that is the paperboard also used in the pilot plant and the only multi layer paperboard. As can be seen, all of the figures look almost the same. The simulations look good in the beginning where the crease forces follow each other, but after a while the simulations loses crease force and miss the spike. The figure below is the best matching plot but there are still big differences.

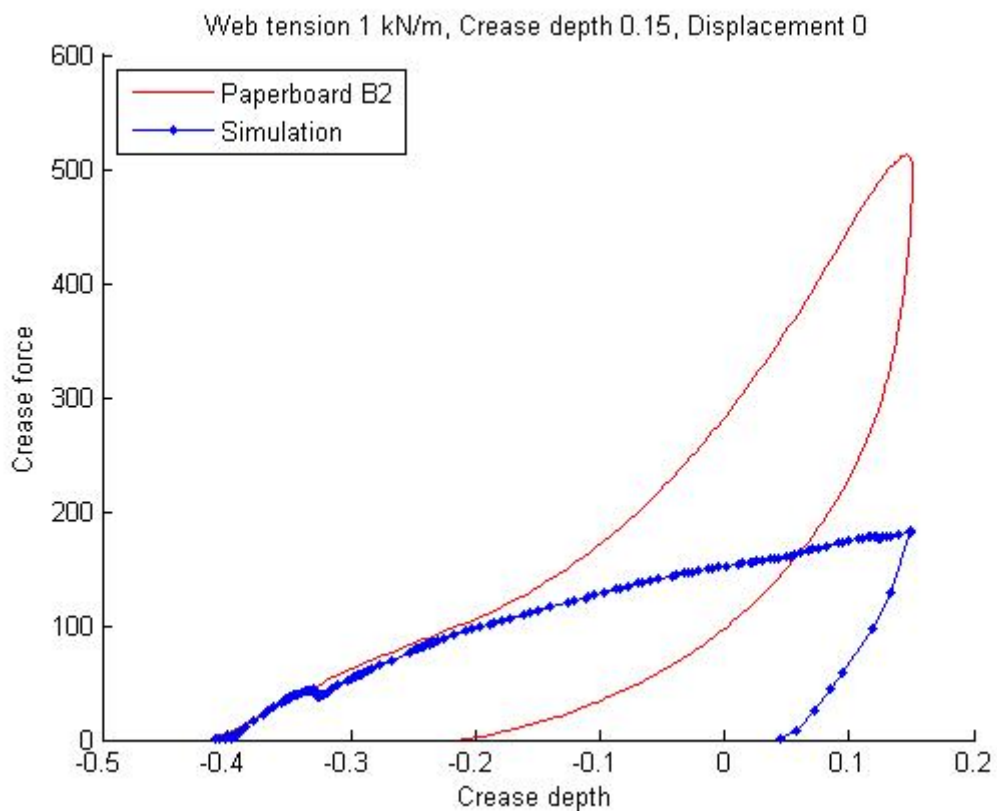


*Figure 7.7 comparing the simulation with experimental test*

The figure also shows that in the case of simulation, the male creasing die loses contact with the paperboard much earlier than in experiment which may indicate that the computer model is not as elastic as the real paperboard.

### 7.2.2 Plastic deformations

The results of the remaining deformations can be found in *Appendix O*. The figures show what the simulated paperboards look like after the creasing procedure. It can

## Results

easily be seen that when the male die displaces to the left, the paperboard get more squeezed and thereby more weakened on that side.

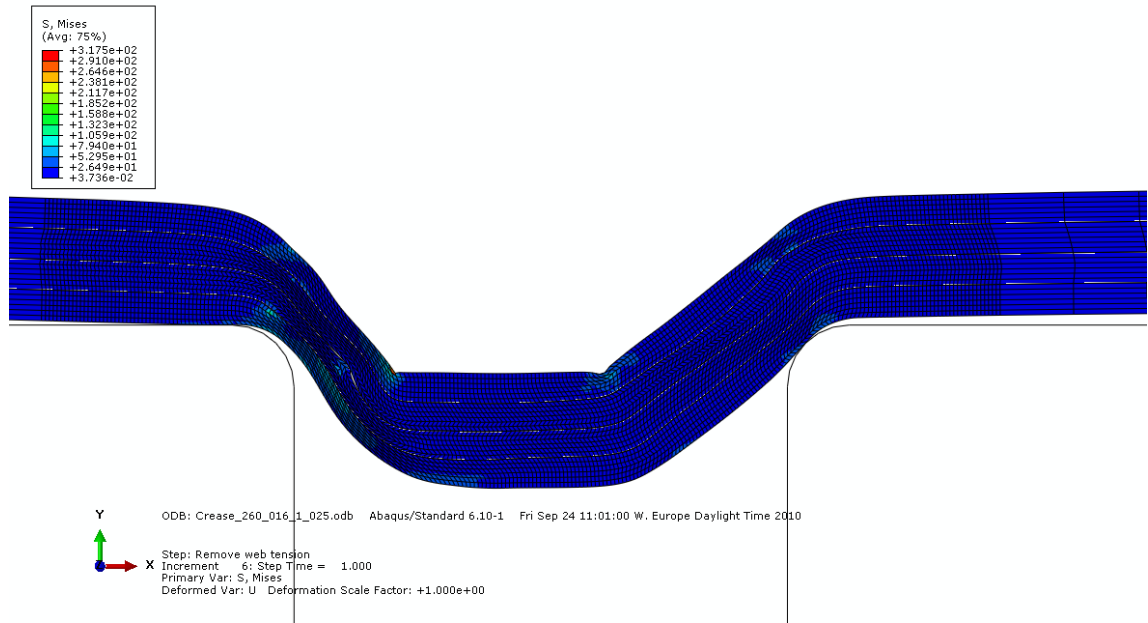


**Figure 7.8** Plastic deformations in the computer simulations

It can also be seen that the crease depth affects the appearance of the crease a lot. When creasing deeper, the paperboard has to stretch more, which makes it thinner in the side regions. The top of the crease almost seems to have the same thickness before and after the creasing, which can be seen by comparing the top of the crease with the thickness of the paperboard at the extreme right or left part in the figure.

## 8 Discussion

In this chapter the procedure are discussed.

### 8.1 Topography

In the topography results it was easy to observe that the tests made with the straight crease tool had considerably more clustered graphs (the graphs are closer to each other) than the tests made with the bottom crease pattern. Initially it was thought to be a lot harder to tune the bottom crease pattern to the desired displacement since it can be displaced both in MD and CD. But, on second thought, this may occur because of several creases are engaged at the same time.

When measuring the samples in the topography, graphs according to *Appendix C* were obtained. In the graph plots there is a built in coordinate system that is applied by the measuring program. When the crease height and the distortion had been calculated, the generated coordinate system was used. However, later tests made in the pilot plant showed that the generated coordinate system do not have its origin at the same place as it derived for the straight creases and the bottom crease pattern. When looking at the straight and bottom crease patterns, the origin was set to be in the bottom of the crease (which was desired), but when measuring the pilot plant tests, the origin was placed a lot higher in the y-direction (approximately half of the crease height). The reason why this phenomenon occurs is not really known, but tests were remeasured to clarify if measurements were made improperly, however, it still looked the same. A thought about why these tests do not look the same is that the paper used in the pilot plant was rolled onto big rolls and thereby had a concave appearance since the crease was on the inside of the roll. Having this bent shape, the sample does not adhere to the vacuum holder as desired and will thereby still retain the concave shape when it is about to be measured. Probably the measuring program chose to set the origin beside the crease where the paperboard was bent up a bit. This caused a problem when measuring the crease height since a smaller crease height was achieved when the origin was translated in the y-direction. A way of making the measuring more consistent is to measure the lowest value to the left and to the right of the crease, and then use the mean value of the two values as an origin.

It is possible to see that the crease height is higher for A1 and A2 than for B1 and B2. This also depends on the differences in paperboard structure. The kind of paperboard that company B produces, which consists of several plies, probably, has better properties in getting compressed than the type of paperboard that company A produces. An idea of why this happens is that a paperboard which comprising only one ply has the same density throughout the paperboard. On the other hand, a paperboard with several plies has less density in the middle and is thereby easier to compress, yet has surface plies that are denser to achieve greater strength. This theory indicates that a paperboard with only one ply has different properties in compression and the crease height is therefore larger for single ply.

During the tests in the pilot plant an opportunity to measure the crease's shape by a topography register was available. These automatic measures were later on compared

to the manual topography measures. It is easy to observe that both distortion and crease height varies a lot between these two methods. It does not seem to be any relationship between them. The reason why this occurs is because when doing the manual measurements very bad results are obtained since the paperboard has a rounded shape as earlier mentioned. The measure method that seems to give the best results is the automatic one. When using the automatic topography measurer the paper is stretched with web tension, which do not allow the paper to get a concave shape and thereby gives the most satisfying result.

## 8.2 MTS

Concerning the MTS-machine during the tests in the pilot plant, observations were made on cracks that were easy initiated in MD. This raised the question: why was the MTS not set to crease in MD to get a more realistic result? This was due to the web tension that had to be applied, and that it was more important to have a good CD crease than MD crease.

When starting to investigate the creases from the bottom crease pattern, it was very fast concluded that the paper had a tendency of wrinkle in the area where several creases join. This problem was solved by making the areas a bit larger, but the tool in the experiment was created before the change was made. Since the problem is already solved, it was decided to ignore this and just analyze the creases.

In the results for the bottom crease pattern it can be seen that when testing the bottom crease pattern on the thin paperboard, a web tension at 1 kN/m was used, but when creasing the thick paperboard only 0.5 kN/m web tension was used. The reason why the web tension had to be changed was because the load cell sometimes registered too high values and shut down. To be on the safe side, the web tension was reduced.

## 8.3 RCS

The crack angle is obtained during the folding process. When the sample is folded, the force required is measured and the maximum force below 30 degrees is called the crack angle. The reason why many of the crack angle values in *Appendix E* are 29.9 degrees is because the maximum bending force is above 30 degrees. The reason why the crack angle is above 30 degrees is because the low bending stiffness makes the sample to flex a bit and thereby obtain a higher angle.

In *Appendix F* it can be seen that the RCS-values for B1 is larger than A1, and B2 is larger than A2. This is because on the two paperboard suppliers do not use the same technique for manufacturing paperboard. A1 is a so called single ply and B1 is a so called multi ply, as described in chapter 4.2 *Paperboard*. The two different types of paperboard do not have the same material properties, which resulted in differences when measuring RCS-values. It is a kind of a trade-off when determining the perfect RCS-value; if it is too low it is easy to initiate cracks, and if it is too high the resistance when folding is higher and the risk off wrinkles are higher during package folding.

It was observed in *Appendix F.4* that the bending force was higher when folding the paperboard manufactured by A. By using the same reasoning as earlier, it was possible to explain why this happened. It may seem strange that a paperboard that has a lower RCS still has a higher bending force, since a low RCS indicates that the difference in bending force between a creased and an uncreased sample is big. This can be explained by paperboard A requiring a higher bending force both on the creased and uncreased sample than paperboard B.

When performing creasing in the ideal case, in theory, the RCS-value should be the same on both sides of the crease if the dies are centered. In reality, it is not the same since the plates are never exactly centered or equally worn on both sides of the rule. When a paperboard with exactly centered tools is creased, the distances from the male die's edges to the female die's edges will be the same on both sides. This implies that the paperboard is deformed and thereby weakened the same amount on both sides of the male die. However, if a displacement or a worn tool is involved, the distance on the right side of the male die will not be the same as for the left side. Since the distances are not equal on both sides, the paperboard will not be sheared the same amount on both sides. The side that is more compressed will thereby be more weakened than the side that is less compressed. This is why two different RCS-values are obtained.

When performing RCS-tests on the samples from the bottom crease pattern, thinner samples had to be used compared to the samples used with straight creases. This was because when creasing with the bottom crease plate, a pattern that could be compared to a grid was obtained. The creases in the middle of the grid could not be used for evaluation of RCS since they were too small to fit the analyzing machine and must not have more than one crease at the time involved in the folding process. To be able to measure RCS on the creases from the bottom plate it was necessary to cut samples from the creases that pointed away from the grid. The maximum width of these samples was 15 mm compared to the samples with straight creases that were 38 mm wide. The intention was however, not to compare the bottom pattern with the straight creases. The reason why the samples from the bottom patterns were so narrow was because it was only possible to use the part of the creases that were not involved in the grid.

## 8.4 Tuning

As mentioned in *4.2.2 Laboratory creasing procedure*, plastic film was used to determine the displacement of the male die. The distance that was measured was from the male die's right side to the female dies right side and vice versa for the left side. The lowest value was then subtrahend from the higher value, and the difference was divided by two to get the displacement distance. The problem that appeared was the marks where the male die's imprint was situated were too wide and not sharp enough to study under a light microscope. Furthermore, the edges changed position depending on how the plastic film was positioned and what kind of light setting was used. This was because the light changed direction in the plastic film. This type of measuring method was excluded since it was not as accurate as required. Worth

mentioning was that this method worked fine if a rough evaluation of the male die's displacement was wanted. To get the required strict accuracy, putty (which is two-component clay) was used to make imprints of the crease tools when creasing. A thin cross section slice was cut out from the creased putty and measured under a light microscope to get the displacement. Would it not be better to use the putty in the production line as well? During the tests in the pilot plant, measurements with putty were attempted, but gave no good results since the crease plates were mounted on big cylinders and it was very difficult to determine when the putty was exactly in the middle between the cylinders, i.e. when the putty was squeezed together the most. By these means, putty is probably never going to be used in the production line, but works perfectly well in the MTS-machine.

### 8.5 Pilot plant

The tuning of centering and displacement in the pilot plant could not be performed with the same accuracy as in the MTS. The creasing plates had to be tuned into the right position with plastic film, as mentioned previously, since the method of using putty did not work in this case. The critical part was to get a displacement as close to zero as possible without using any putty. Plastic film was used several times and studied under magnifying glass and a microscope in order to be able to decide if the creasing plates were centered. Of course there is a risk that the plates were not exactly centered, but they were centered as close as the method allowed. As mentioned before the settings in the pilot plant is not perfect since if the plates were not perfectly centered in the beginning, this error last through all of the displacements.

The crease height changes with crease depth (including wear of the plates) and the distortion changes with the displacement of the dies. The test that was performed in the pilot plant was worst case scenario, which means that the deepest crease possible with a given displacement was achieved. By using a plot of the crease height and distortion measured in the pilot plant, it is possible to check if the current settings will result in crack initiation (*figure 6.5 and 6.6*), e.g. an operator is running the pilot plant and wants to know if the creases are going to be free from cracks. He reads the distortion and crease height values and uses them as coordinates in the plot. If the coordinates describe a point under the line in the figure, the settings are good.

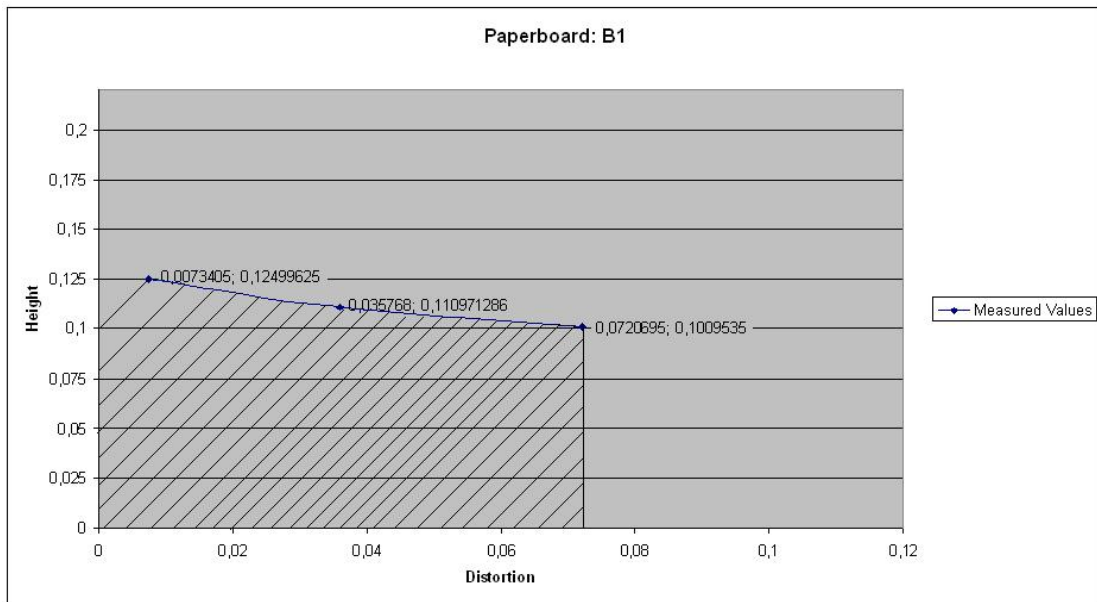


**Figure 8.5** If distortion and crease height is used as coordinates, the marked area indicates that no cracks are initiated (for thin paperboard B1)

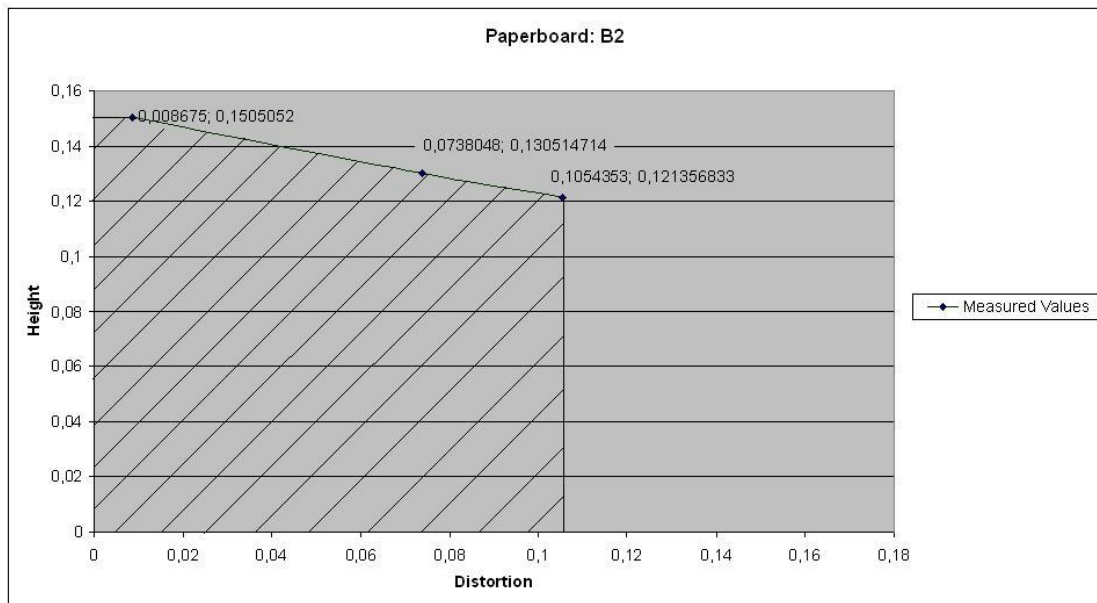


**Figure 8.6** If distortion and crease height is used as coordinates, the marked area indicates that no cracks are initiated (for thin paperboard B1)

From the preformed tests it is achieved that crease depth and displacement are the factors that regardless supplier, affect the weakening in the paperboard the most. The difference between these two is that the displacement is an unwanted factor and the crease depth is desired and easily tuned.

## Discussion

By looking at the different RCS-values when the displacement changes it was easy to see in a plot (figure 6.5 and 6.6) that the difference between the different sides increases when the displacement grew. It can also be seen were the displacement is significant and not significant by looking were the plotted line crosses each other (displacement 0.22mm). This means that on the left side off this point the displacement is insignificant and on the right side it is significant.

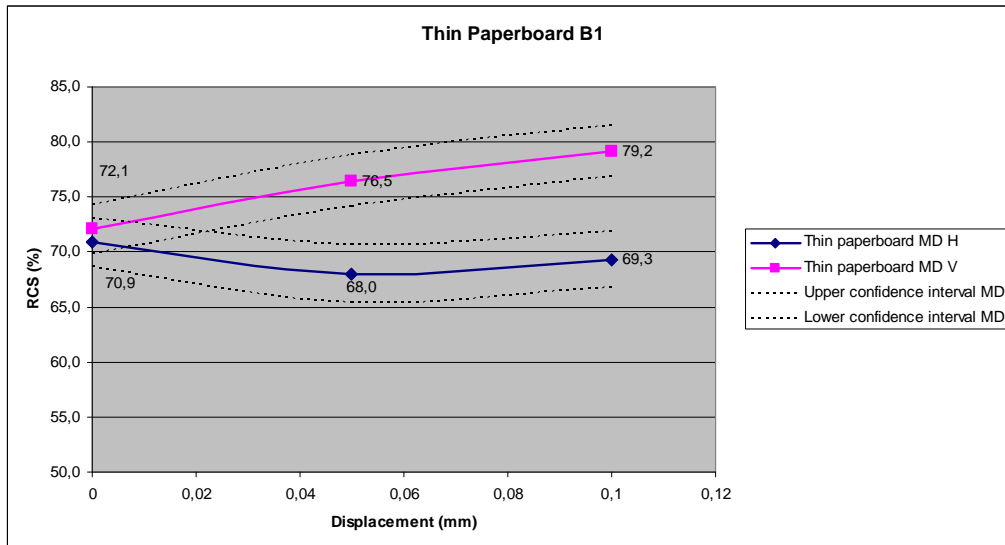


Figure 8.7 The different RCS-values plotted against the displacement for the thin paperboard.

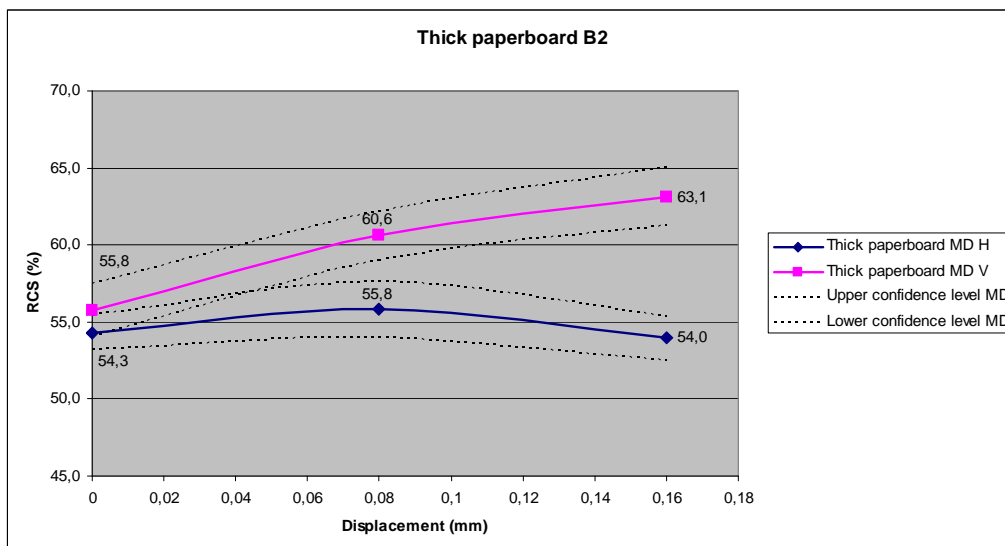


Figure 8.8 The different RCS-values plotted against the displacement for the thin paperboard.



## 8.6 Computer simulations

The intention was to have two different models, one for the thick paperboard and one for the thin paperboard. Unfortunately, the simulation did not work on the thin paperboard. For some reason the model did not converge. The strange part is that convergence problems occurred before the male die caused any deformations in the model. Several people working with simulations have been trying to solve the problem without any success. This is why simulations on only the thick paperboard were preformed.

The results from the simulations have been compared to the test results, mainly by analyzing how the crease force changes during the crease process. As can be seen in *Appendix M*, the plots do look alike in the beginning of the procedure, but already after a tenth of a millimeter the simulation model loses crease force. However, the greatest difference is that the simulation model misses the large crease force peak. This phenomenon has been observed in other studies that involve simulation of a creasing process. The reason why the simulation misses the peak is probably because the simulation do not simulate that the friction between the plies rises when pressure is added. Due to the lower friction the plies in the simulation slides and the higher creasing force is thereby missed out. Another aspect where the simulation did not behave as the tests was when observing the maximum crease force and changing crease depth, web tension and/or displacement. In the tests, the maximum force changes remarkably when one or several of these parameters changes, whereas in the simulation it does not seem to have any impact at all.



## 9 Conclusion

- It is determined that it is possible to crease different depths depending on what type of paperboard supplier is used. This also affects the displacement of the die since it is possible to crease less deep if the dies are displaced.
- Crease depth and displacement are the two factors that affect the initiation of cracks in the paperboard the most.
- The distortion does not completely change with displaced dies.
- When creasing with displaced dies two RCS-values are achieved. One of them is lower than the other and is less resistant to cracks.
- The topography in pilot plant can be used together with the *figure 8.5 and 8.6* to be able to foresee if the risk for initiating cracks is high or low.
- The RCS value for a single ply paperboard is always lower than for the multi ply paperboard.
- The L&W creasability tester often misses the peak since the maximum bending force is above 30° for the thin paperboard.
- Cracks initiate easier on the side with the lower RCS-value.



## 10 Recommendations and further investigations

It would be interesting to investigate how the friction changes due to different coatings on the creasing plates, and how the friction affects the creasing process.

It would also be interesting to do some more tests in the Pilot plant to study how the RCS-values changes with centered tool but with various crease depths. This is to get a register of how the RCS-values changes due to various crease depths. By doing this it is possible to make a form that tells what RCS-value is achieved, when knowing the specific distortion and crease height.

The simulation was not as close to reality as desired. Since the thin paperboard model did not work, it would be interesting to see if it gives any better results than the thick paperboard model. Another thing in the simulation that can be added is to change the behavior of the model to get the crease force peak. Also it would be good to add a folding process to investigate if it is possible to achieve a RCS-value that is similar to the tests.



# 11 References

## Internal information

- 1 Creasing investigation in pilot scale with MTS machine and L&W RCS machine, v 1.1, information brochure
- 2 Johan Tryding, Magnus Just, (2008), *Memo*, Tetra Pak Packaging Solutions – Base Materials
- 3 Mikael Nygårds, (2008), *Creasing of Paperboard*, STFI-Packforsk Report No.:395
- 4 Mikael Nygårds, Magnus Just, Johan Tryding, (2009), *Experimental and numerical studies of creasing of paperboard*, Elsevier
- 5 Mikael Nygårds, (2009), *Modelling and simulation of paperboard damage and deformation – Executive summary of the Liquid Paperboard Cluster*, Innventia Report No.:45

## External information

- 6 Christer Engman, Christer Fellers, Myat Htun, Ragnar Lundberg, Alf de Ruvo, (1978), *Kartong – Grundläggande samband mellan råvaror och mekaniska egenskaper hos skiktade ark*, Svenska Träforskningsinstitutet
- 7 Eriksson, L., Johansson, E., Kennaneh-Wold, N., Wikström, C. & Wold, S., (2008), *Design of Experiments – Principles and Applications*, 3<sup>rd</sup> ed., Umetrics
- 8 Huang H, Nygårds M. (2010). "A simplified material model for finite element analysis of paperboard creasing", *Nordic Pulp and Paper Research Journal* (in press)
- 9 Niels Ottosen, Hans Petersson, (1992), *Introduction to the finite element method*, University of Lund, Sweden
- 10 Niels Saabye Ottosen, Matti Ristinmaa, (2005), *The Mechanics of Constitutive Modeling*, Elsevier
- 11 Prof. Dr. Ing. Wolfgang Grebe, (2002), *Creasing, creasing techniques and their particular importance for the folding carton and its applications*, Heilbronn

## Internet

- 12 Iggesund Paperboard (2010), Vad är kartong? (Elektronisk), Information från Iggesunds hemsida om hur deras kartonger tillverkas, <http://www.iggesund.com/Main.aspx?ID=a2d5fbb8-4624-4783-b909-ebf890db818e>, 2010-10-30
- 13 Tetra Pak, (2010), Historia (Elektronisk), Tetra Paks historia från start till idag, [http://www.tetrapak.com/se/about\\_tetra\\_pak/the\\_company/history/Pages/default.aspx](http://www.tetrapak.com/se/about_tetra_pak/the_company/history/Pages/default.aspx), 2010-11-05

#### **Manuals**

- 14 ABAQUS v 6.10, (2010), ABAQUS/CAE User's Manual, Simulia
- 15 MODDE v 9.0, (2010), *User's guide*, Umetrics

#### **Interviews**

- 16 Johan Nilsson, Systems Engineer, Tetra Pak Technical Dev, Product Dev & Engineering, June 30<sup>th</sup> and November 1<sup>st</sup>
- 17 Johan Tryding, Senior Specialist, Tetra Pak Base Material, Technical Dev, Product Dev & Engineering, June 22<sup>nd</sup> December 1<sup>st</sup>
- 18 Mattias Månsson, Systems Engineer, Tetra Pak Technical Dev, Product Dev & Engineering, September 23<sup>rd</sup>, October 14<sup>th</sup>

#### **Master thesis**

- 19 Jennie Lillienberg, Emma Lörd, (2009), *Outside vs. Inside Creasing – A Parameter Study*, Div. of Packaging Logistics, Div. of Solid Mechanics, Lund University, Sweden
- 20 Kent Persson, (1991), *Material Model for Paper – Experimental and theoretical aspects*, Div. Solid Mechanics, Lund University. Sweden



## **List of Appendices**

<b>Appendix A</b>	<b>Straight creases: Tables</b>
<b>Appendix B</b>	<b>Straight ceases: MODDE Coefficient plots</b>
<b>Appendix C</b>	<b>Straight creases: Topography</b>
<b>Appendix E</b>	<b>Straight creases: RCS</b>
<b>Appendix F</b>	<b>Bottom crease pattern: Tables</b>
<b>Appendix I</b>	<b>Bottom crease pattern: Plots</b>
<b>Appendix J</b>	<b>Pilot plant: Tables</b>
<b>Appendix K</b>	<b>Confirmation of MODDE statements</b>
<b>Appendix L</b>	<b>Computer simulation: Material parameters</b>
<b>Appendix M</b>	<b>Simulation vs. test</b>
<b>Appendix O</b>	<b>Simulations: Plastic deformation</b>

## Appendix A *Straight creases: Tables*

*Table A.1 MODDE worksheet, thin paperboard*

Run order	Board	Displacement CD	Web tension	Crease depth
[Nr]		[mm]	[kN/m]	[mm]
1	A1	0.05	1.5	0.20
2	B1	0.05	1.5	0.20
3	A1	0	1	0.15
4	A1	0	2	0.15
5	B1	0	1	0.15
6	B1	0	2	0.15
7	A1	0	1	0.25
8	A1	0	2	0.25
9	B1	0	1	0.25
10	B1	0	2	0.25
11	A1	0.10	1	0.15
12	A1	0.10	2	0.15
13	B1	0.10	1	0.15
14	B1	0.10	2	0.15
15	A1	0.10	1	0.25
16	A1	0.10	2	0.25
17	B1	0.10	1	0.25
18	B1	0.10	2	0.25
19	A1	0.05	1.5	0.20
20	B1	0.05	1.5	0.20

Table A.2 Numerical values of thin paperboard

Run order	Creasing		Topography		Folding right				Folding left			
	Crease force	In plane force	Crease Height	Distortion	Bending force	Crack angle	Folding energy	RCS	Bending force	Crack angle	Folding energy	RCS
	[N]	[N]	[mm]	[mm]	[N]	[deg]	[J]	[%]	[N]	[deg]	[J]	[%]
1	491.80	207.8	0,133	0.0461	820.3	29.9	74106	42.7	891.9	29.9	75659	47.8
2	466.16	226.1	0,086	0.0688	806.7	28.3	68181	52.6	857.4	29.9	69711	56.8
3	377.95	168.0	0,086	-0.0085	1015.8	23.9	84127	52.7	958.5	28.3	82188	52.5
4	409.82	196.1	0,075	0.0013	1071.7	22.3	85145	56.4	1043.7	22.5	85052	55.0
5	335.09	161.8	0,065	-0.0192	953.4	25.6	77698	60.8	955.5	25.4	78433	60.1
6	379.73	200.3	0,051	0.0166	979.5	22.7	78395	61.7	988.7	23.9	80668	63.5
7	563.84	230.4	0,137	-0.0335	834.9	29.9	73238	44.0	815.3	29.9	72564	42.3
8	592.84	243.9	0,133	-0.0171	861.1	29.9	75165	43.9	832.0	29.9	73123	42.4
9	510.43	228.8	0,112	-0.0196	807.3	29.9	67623	50.8	782.3	29.9	66231	50.8
10	507.64	224.9	0,082	-0.0006	816.9	29.9	67692	51.5	771.6	29.9	64568	51.1
11	462.77	203.5	0,091	0.1509	921.9	26.6	84410	47.6	987.9	29.7	82412	52.6
12	501.33	225.6	0,079	0.1449	964.2	23.9	87162	50.1	1018.8	23.8	82385	54.2
13	397.61	188.4	0,067	0.1475	844.9	26.8	75534	52.7	941.4	29.7	76431	58.2
14	444.39	230.6	0,056	0.1313	874.9	24.1	78275	55.8	961.5	24.1	76989	61.2
15	638.87	261.9	0,144	0.1245	737.2	29.9	71709	38.2	747.9	29.9	69373	39.1
16	646.43	278.4	0,145	0.1271	729.2	29.9	70126	37.9	762.2	29.9	68475	40.2
17	573.96	259.7	0,115	0.1219	686.6	29.9	62195	43.6	766.6	29.9	66177	47.8
18	597.84	286.0	0,093	0.1409	710.9	29.9	63604	44.4	789.6	29.9	67245	49.4
19	539.44	244.2	0,112	0.0781	836.8	29.9	75573	42.0	868.4	29.9	74252	43.1
20	448.19	206.4	0,074	0.0751	745.6	29.9	64793	46.5	864.0	29.7	70125	54.2

*Table A.3 Worksheet, thick paperboard*

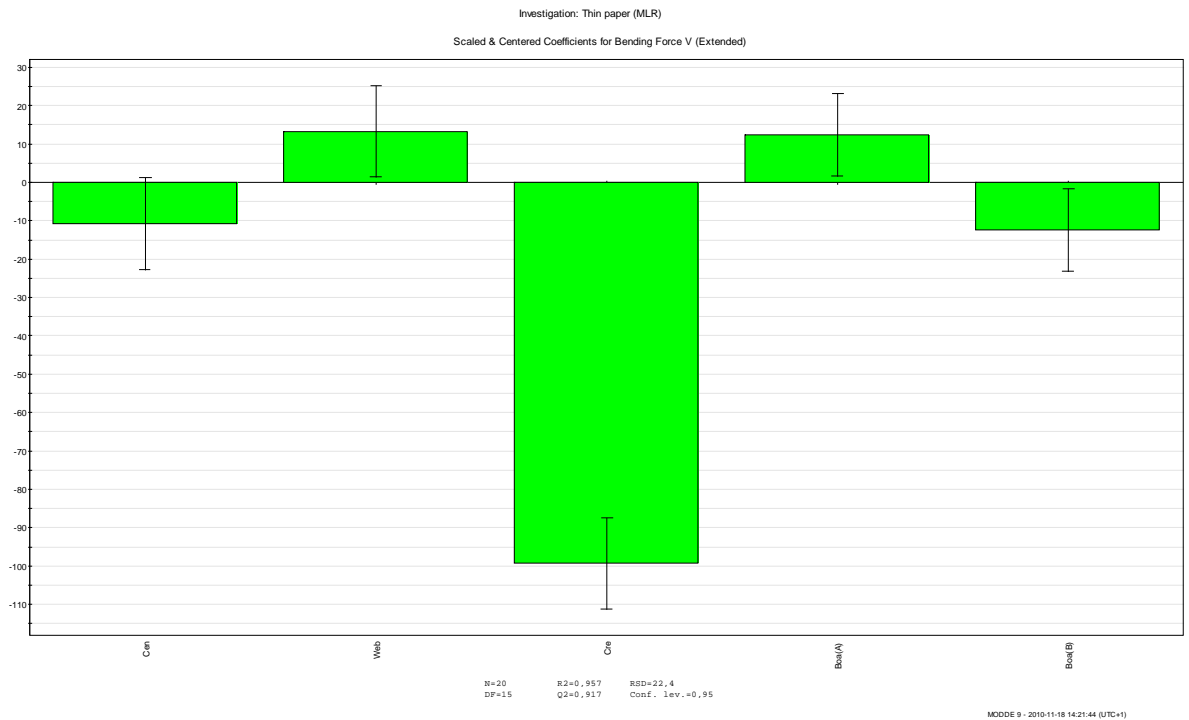
Run order	Board	Displacement CD	Web tension	Crease depth
[Nr]		[mm]	[kN/m]	[mm]
1	A2	0.08	1.5	0.20
2	B2	0.08	1.5	0.20
3	A2	0	1	0.15
4	A2	0	2	0.15
5	B2	0	1	0.15
6	B2	0	2	0.15
7	A2	0	1	0.25
8	A2	0	2	0.25
9	B2	0	1	0.25
10	B2	0	2	0.25
11	A2	0.16	1	0.15
12	A2	0.16	2	0.15
13	B2	0.16	1	0.15
14	B2	0.16	2	0.15
15	A2	0.16	1	0.25
16	A2	0.16	2	0.25
17	B2	0.16	1	0.25
18	B2	0.16	2	0.25
19	A2	0.08	1.5	0.20
20	B2	0.08	1.5	0.20

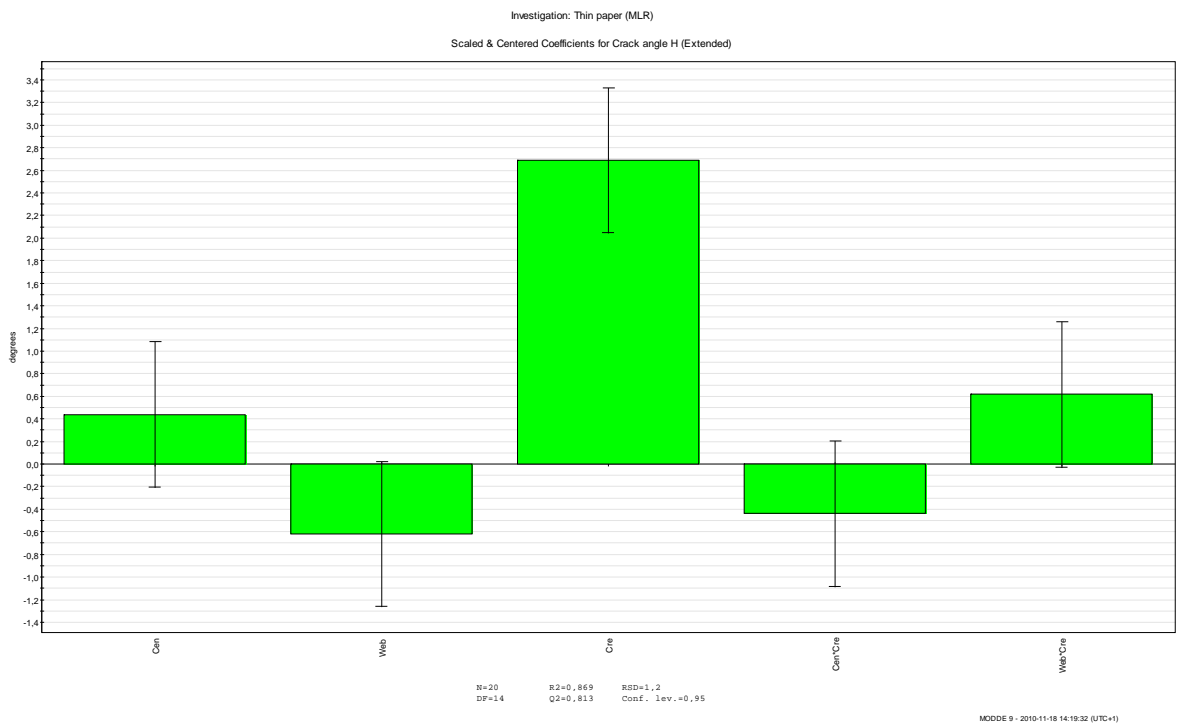
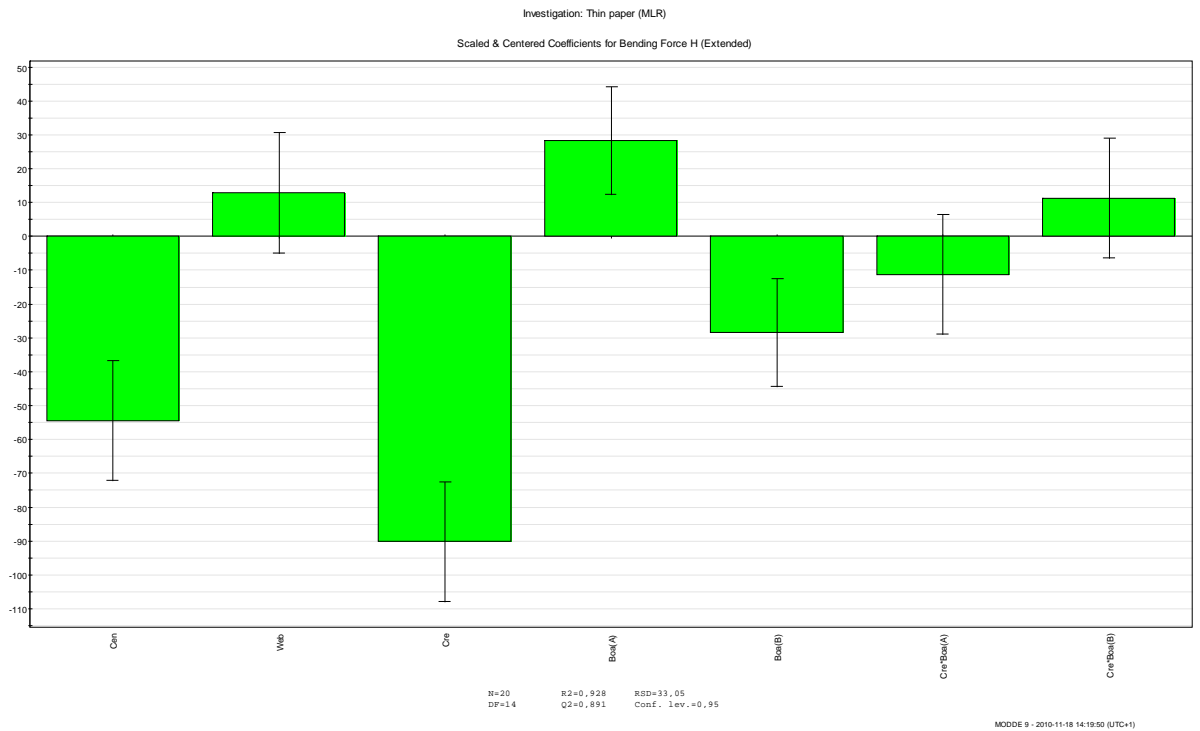
Table A.4 Numerical values of thick paperboard

Run order	Creasing		Topography		Folding right				Folding left			
	Crease force	In plane force	Crease Height	Distortion	Bending force	Crack angle	Folding energy	RCS	Bending force	Crack angle	Folding energy	RCS
	[N]	[N]	[mm]	[mm]	[N]	[deg]	[J]	[%]	[N]	[deg]	[J]	[%]
1	692.67	327.6	0.118	0.1025	1763.6	22.7	170042	42.0	1868.5	25.4	161076	43.1
2	601.85	322.9	0.081	0.0982	1553.8	22.3	140512	54.4	1653.3	22.7	133324	56.5
3	571.23	273.3	0.108	0.0246	1933.4	22.5	170522	43.3	1869.8	22.7	167053	43.1
4	654.76	320.1	0.108	0.0066	1919.2	21.1	172747	44.0	1911.8	21.1	170771	45.0
5	512.77	276.0	0.081	0.0290	1647.1	22.5	138398	56.7	1563.1	22.5	134005	56.4
6	561.37	317.8	0.069	0.0251	1746.5	19.6	150250	60.3	1628.0	21.1	137985	57.8
7	838.90	362.1	0.165	0.0219	1723.0	28.4	156086	39.3	1646.0	29.7	149320	38.2
8	883.33	393.2	0.138	-0.0034	1741.9	26.8	160178	38.6	1682.8	29.7	151016	38.8
9	729.91	359.2	0.103	0.0238	1453.0	26.8	123930	49.6	1434.2	28.3	126405	49.9
10	779.32	388.5	0.091	0.0346	1493.1	23.9	127748	52.2	1463.4	25.4	127393	51.2
11	658.87	311.7	0.124	0.2298	1658.6	23.9	170092	38.2	1878.8	25.6	162902	43.5
12	700.16	337.7	0.107	0.2275	1740.0	22.5	176291	39.7	1969.5	23.9	164980	45.9
13	547.04	294.5	0.077	0.2171	1319.9	26.8	133843	48.0	1628.0	23.9	127280	58.3
14	601.93	332.1	0.070	0.2444	1484.9	21.1	144385	50.5	1807.6	21.2	136318	63.1
15	874.95	371.6	0.175	0.2041	1478.9	29.9	152137	32.7	1457.8	29.9	131636	33.3
16	922.42	395.0	0.153	0.2077	1520.9	29.7	156742	34.3	1718.0	28.3	151677	39.3
17	780.59	380.5	0.108	0.2048	1268.6	29.7	124957	45.1	1431.4	29.7	117244	50.6
18	824.70	410.7	0.095	0.2227	1282.1	26.8	126048	44.8	1486.4	26.8	122240	51.8
19	704.13	343.0	0.117	0.1218	1810.3	22.5	170262	42.0	1904.8	23.9	165770	43.9
20	567.42	313.7	0.077	0.1228	1570.2	21.2	140353	55.5	1636.9	23.8	134343	57.5

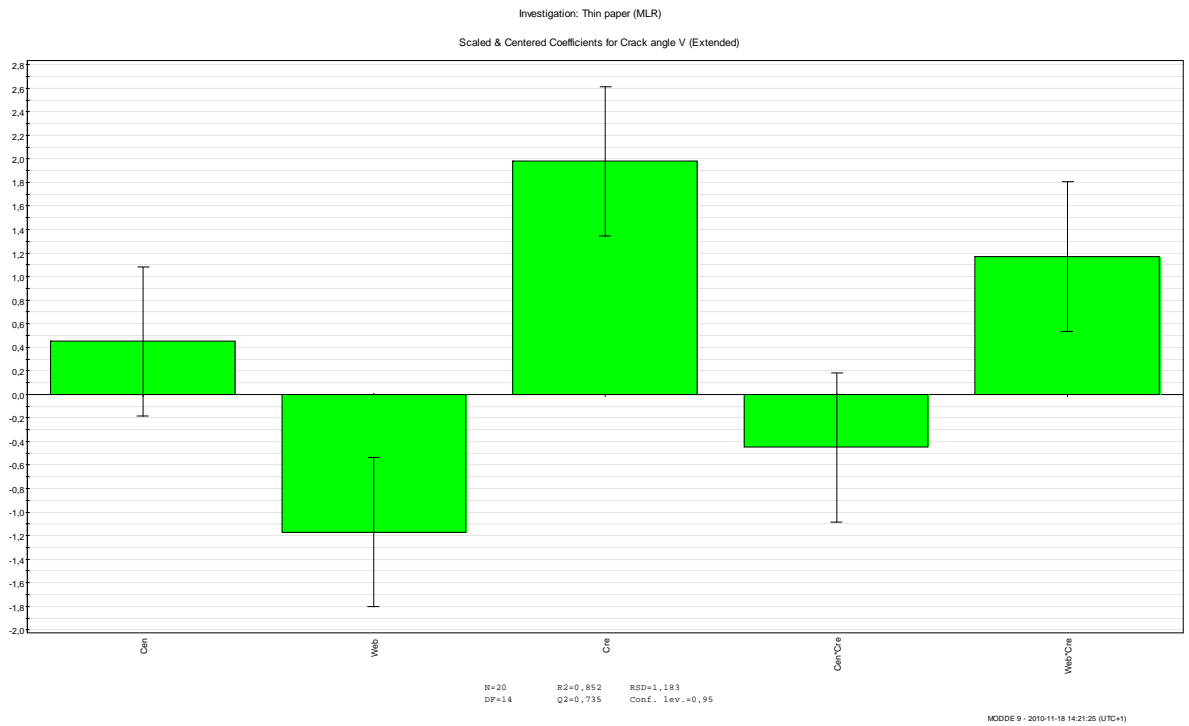
## Appendix B *Straight creases: MODDE* Coefficient plots

### B.1 Coefficient plots, thin paperboard

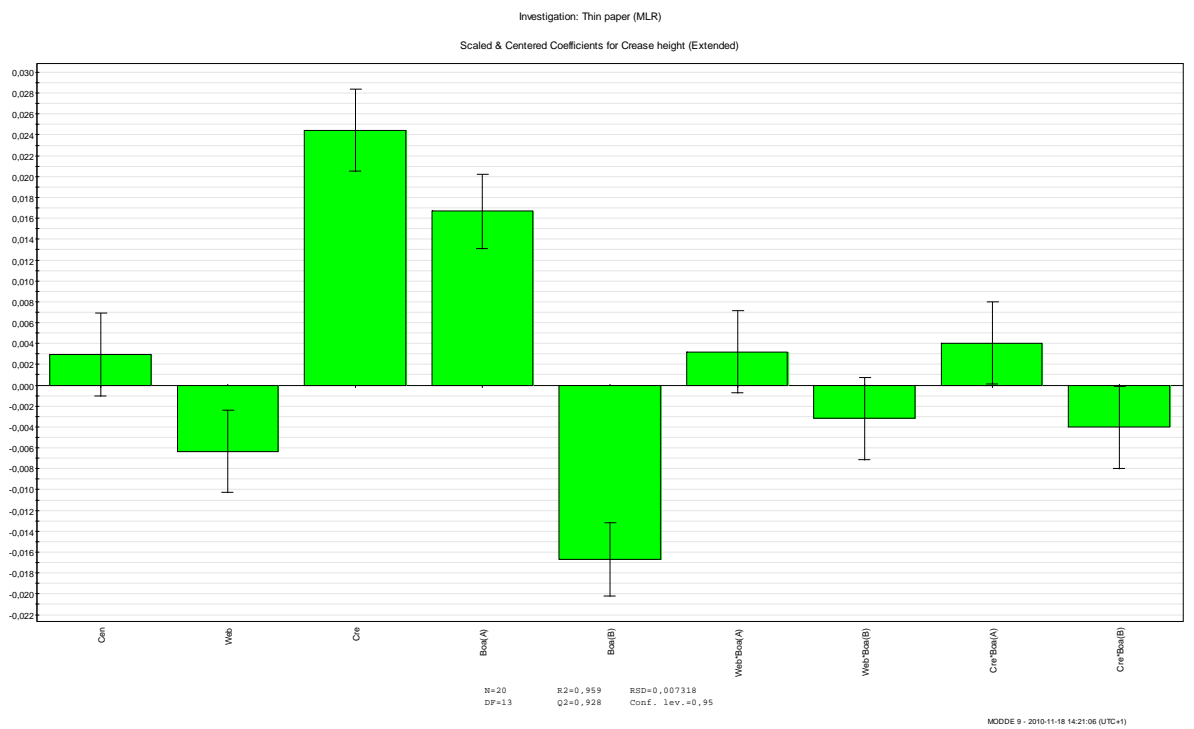
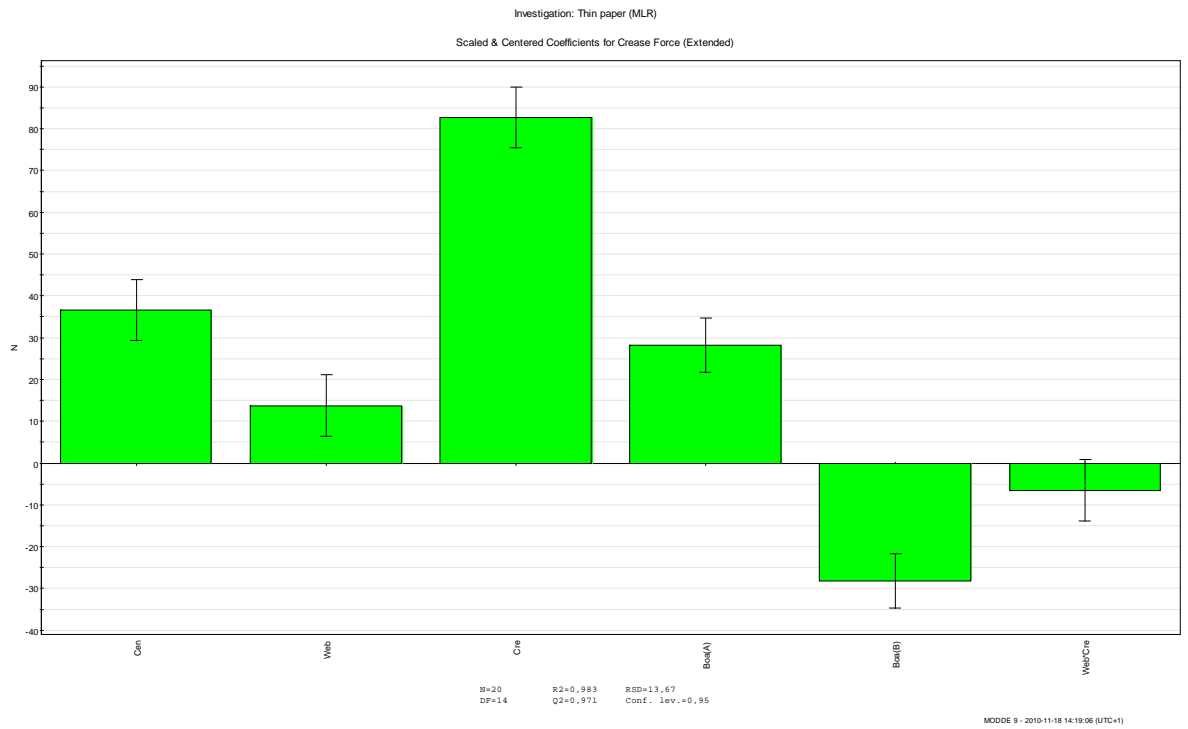




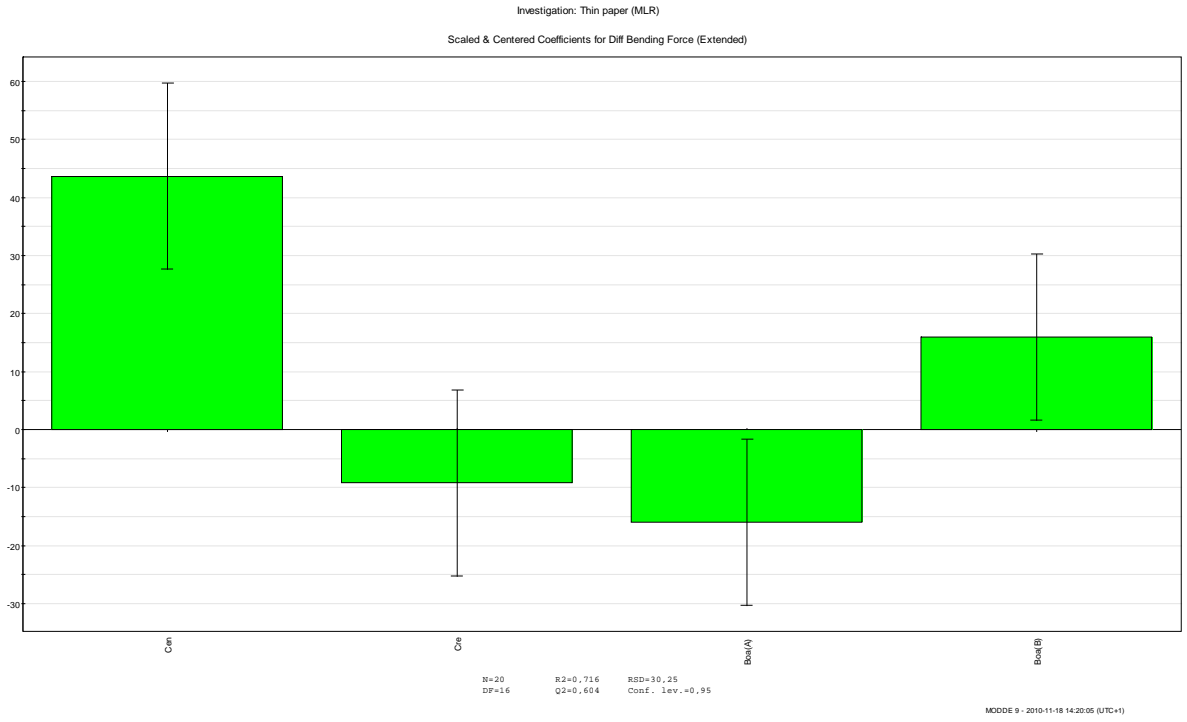
# Appendix

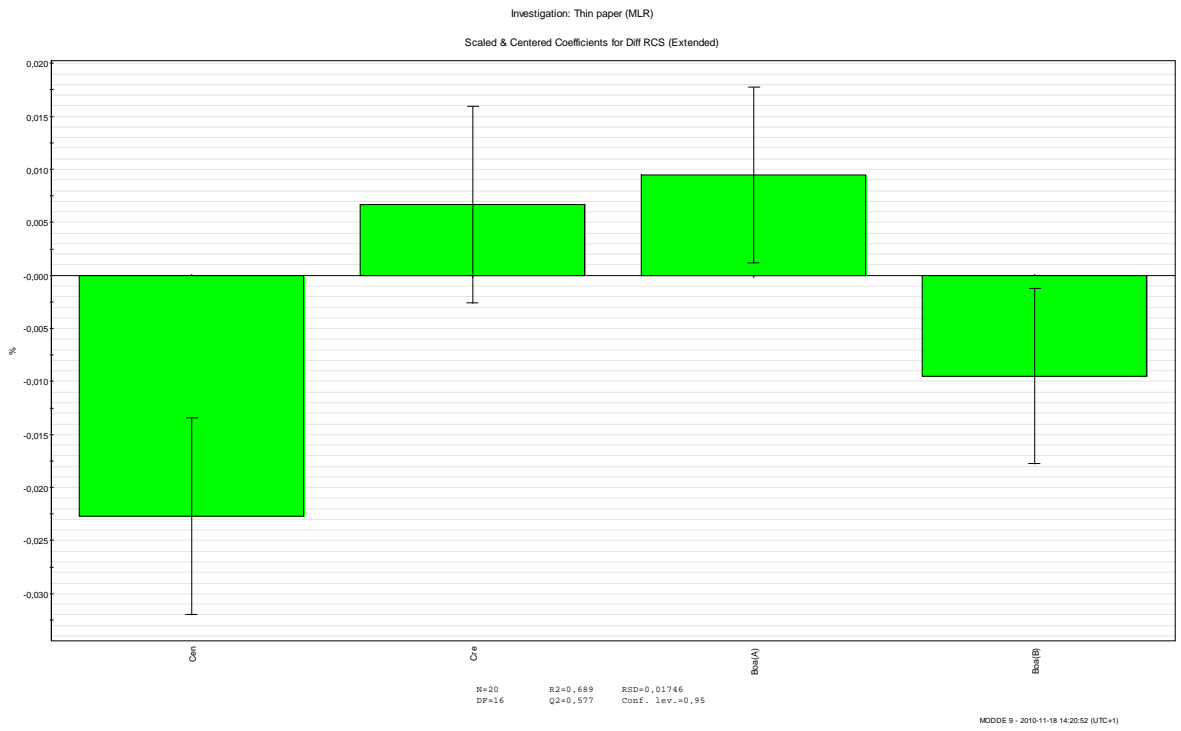




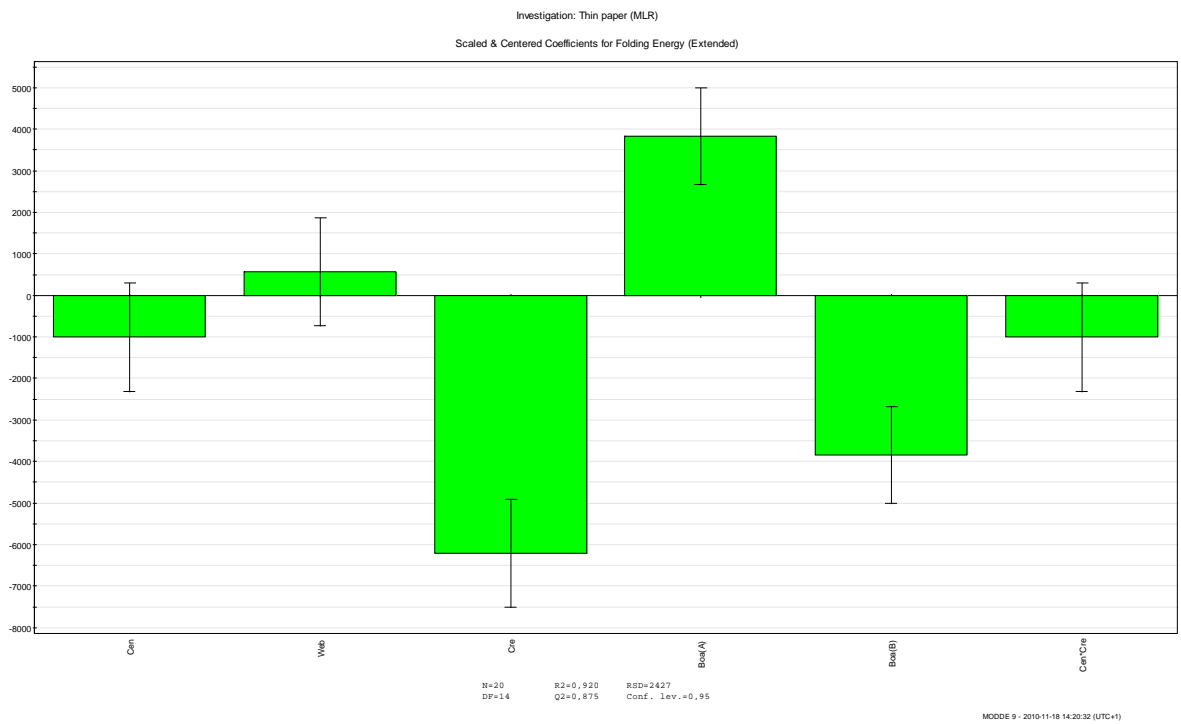
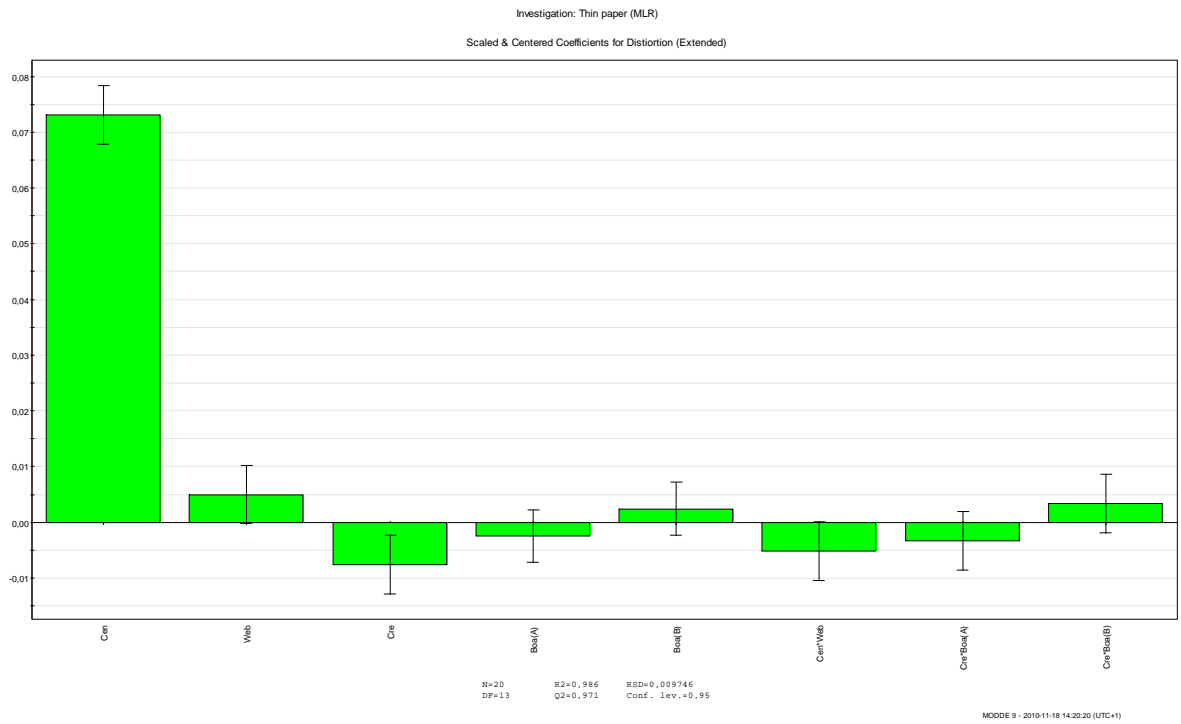


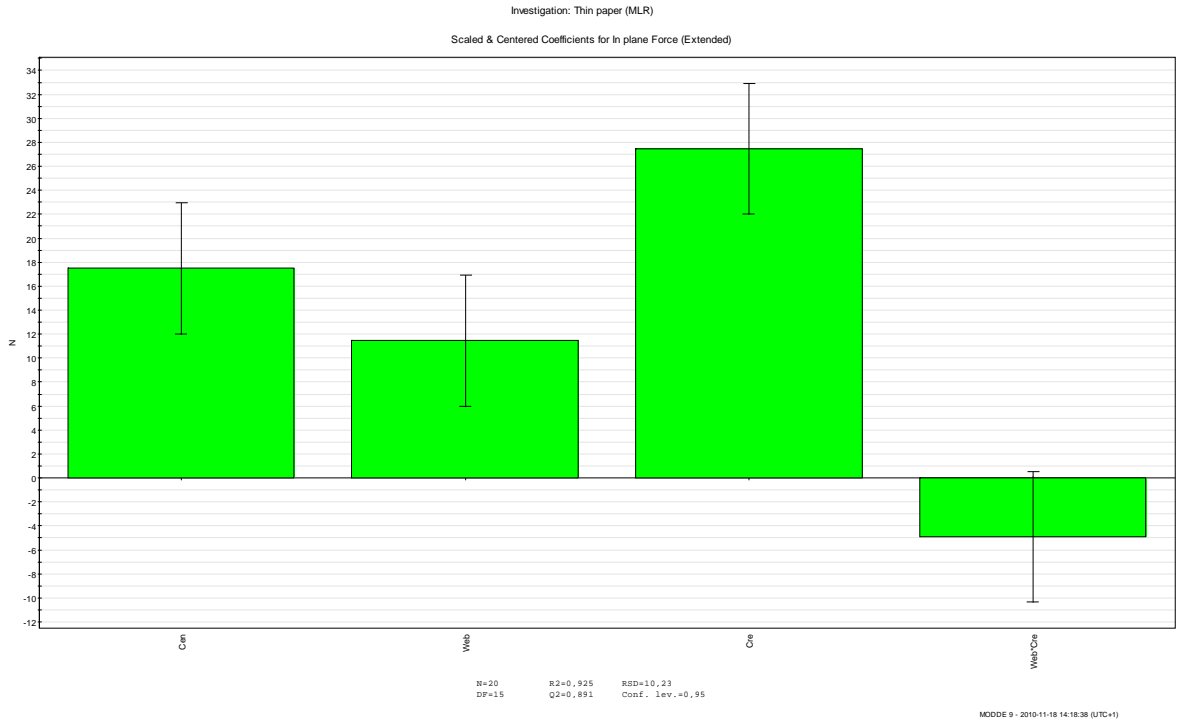
# Appendix



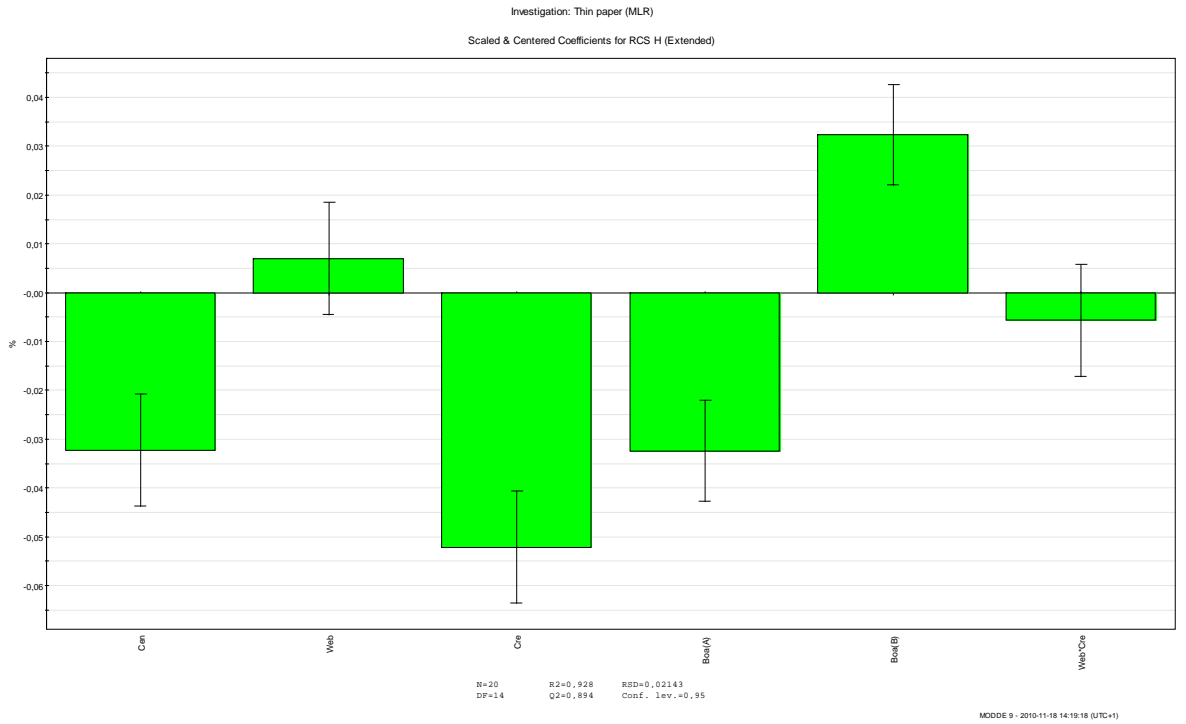


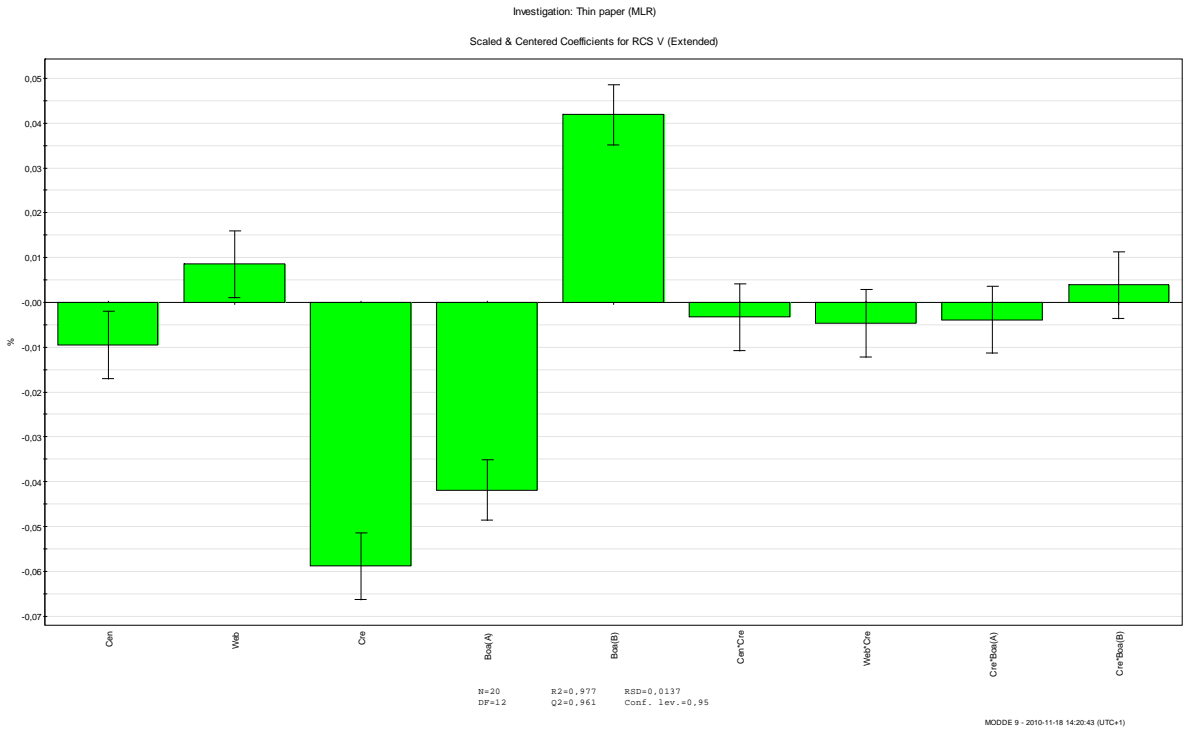
# Appendix



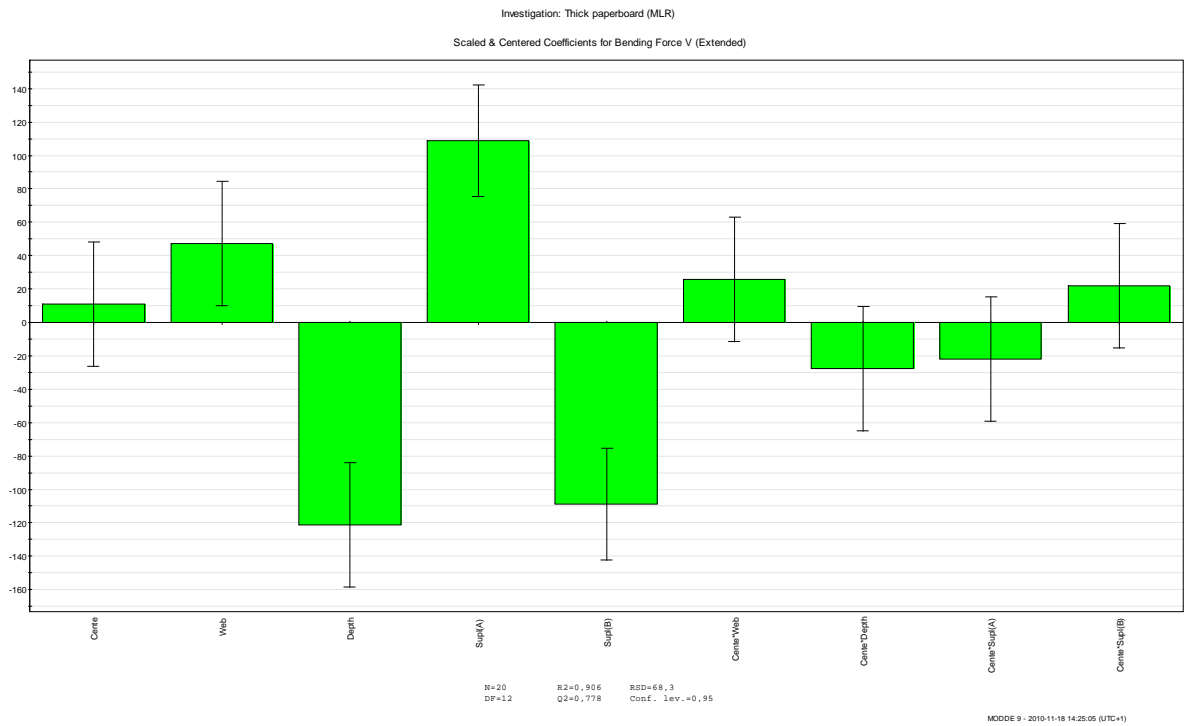
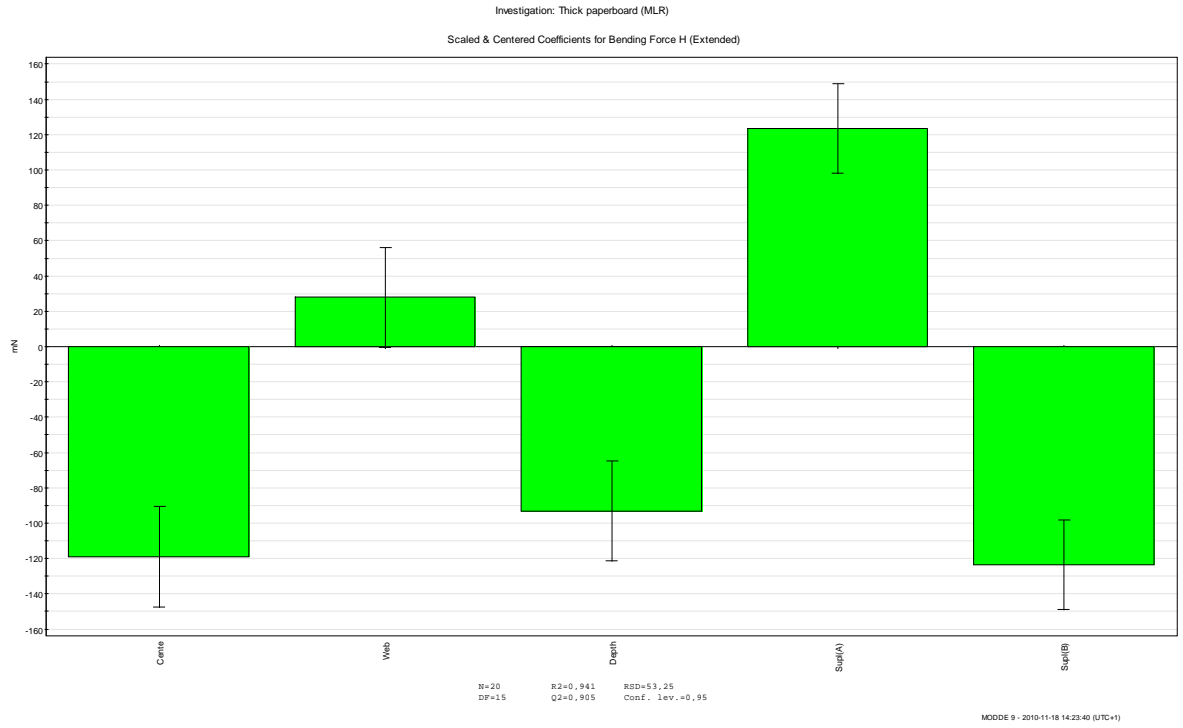


# Appendix

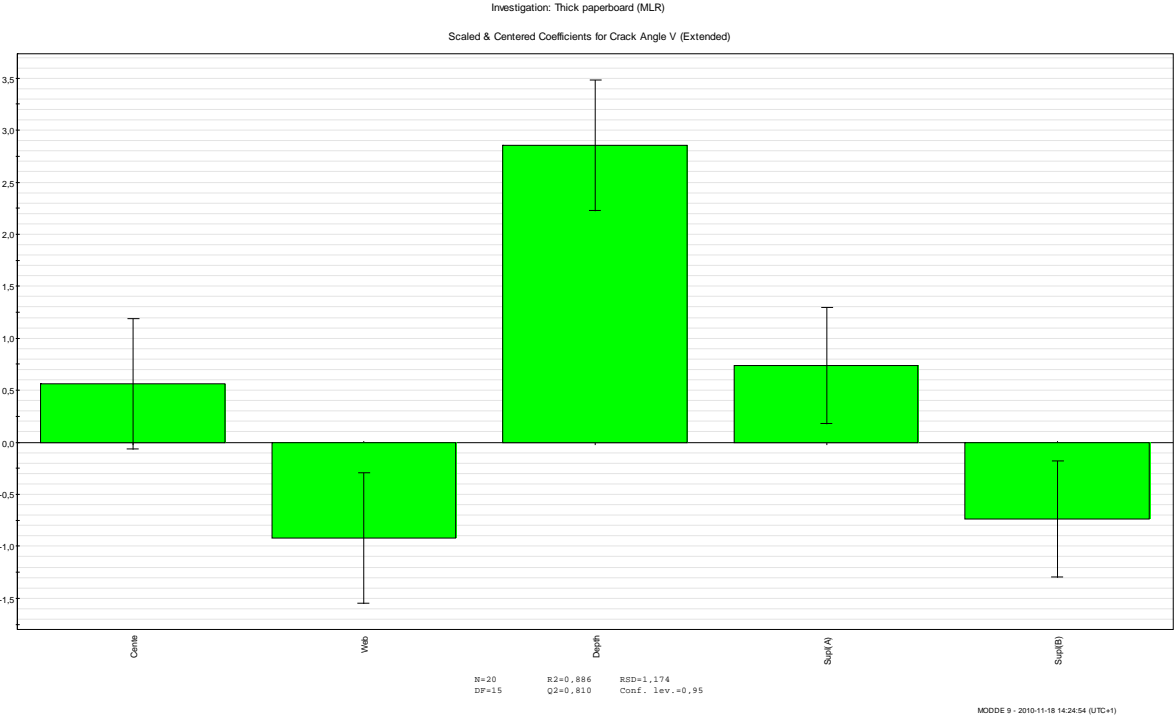
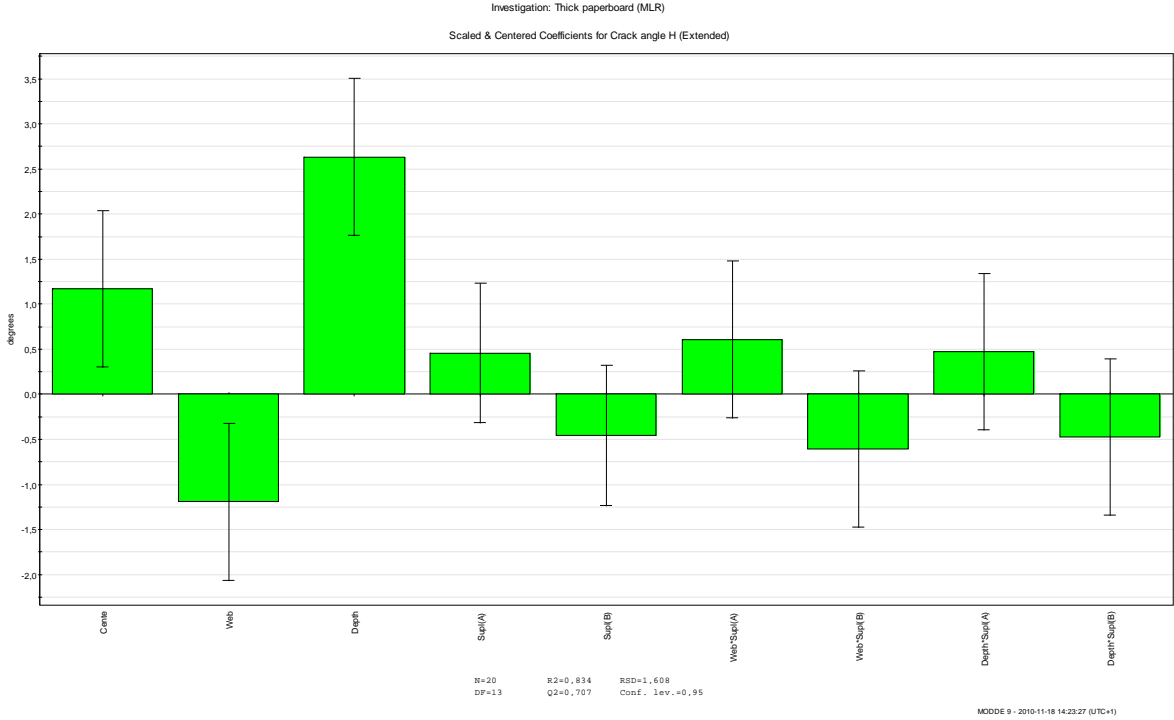




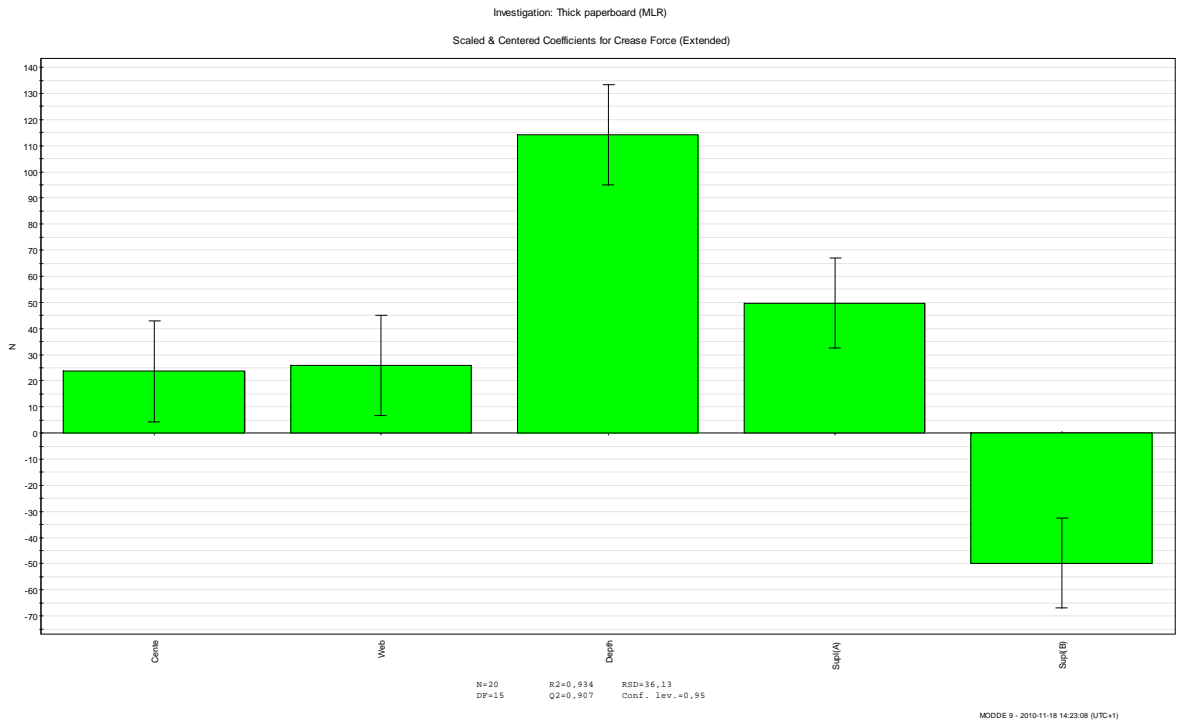
## B.2 Coefficient plots, thick paperboard

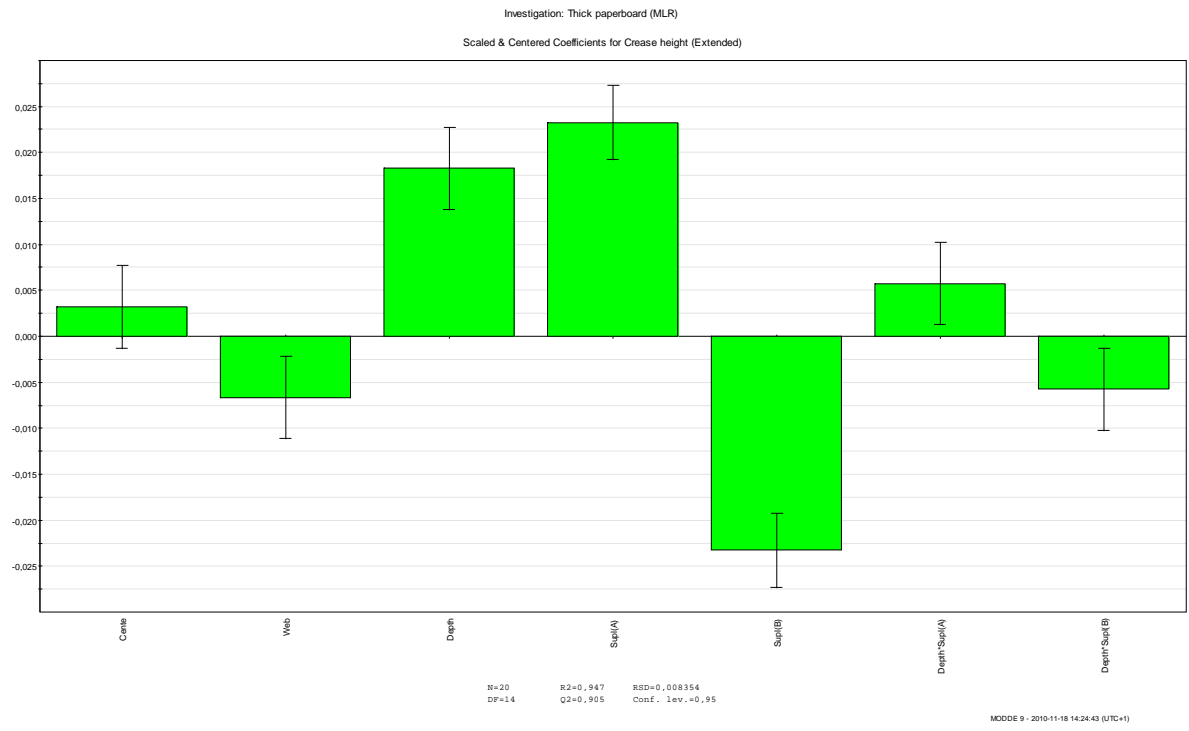




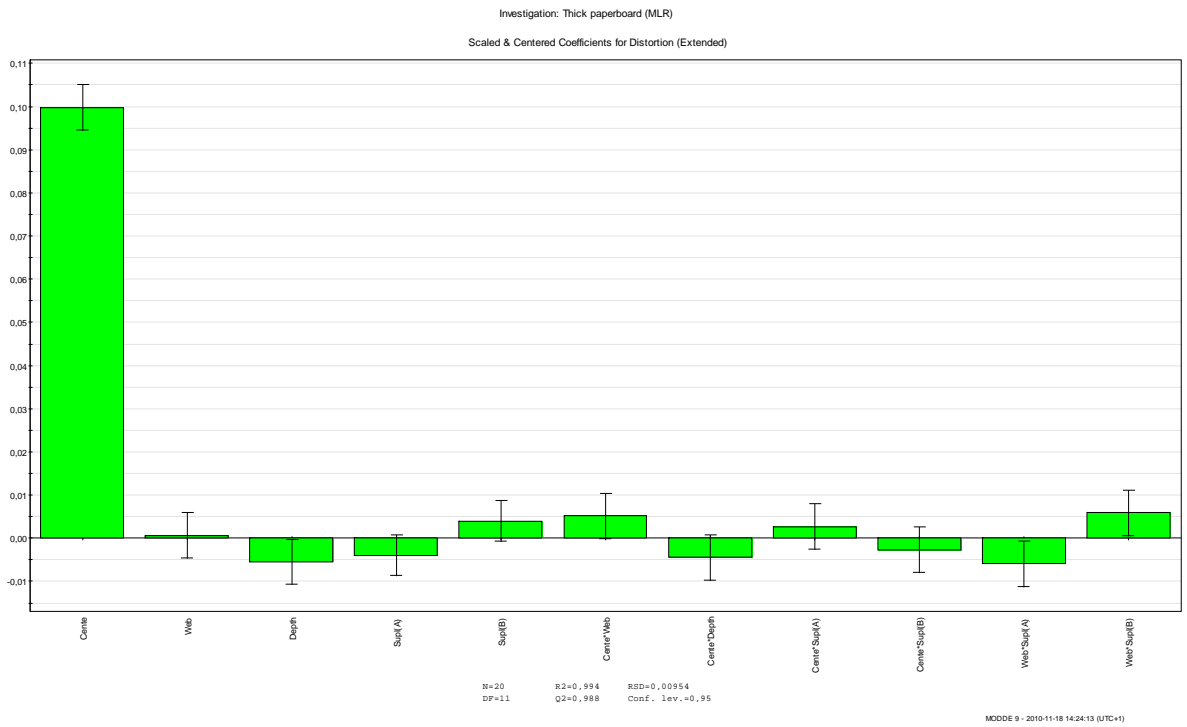
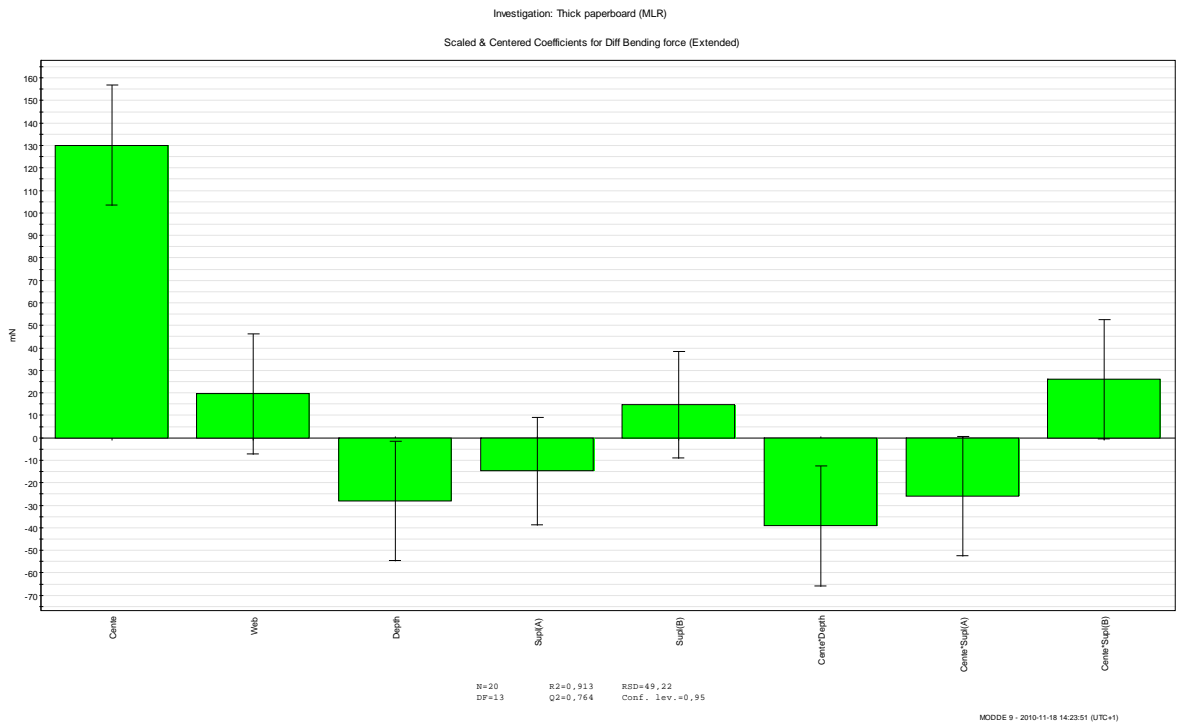


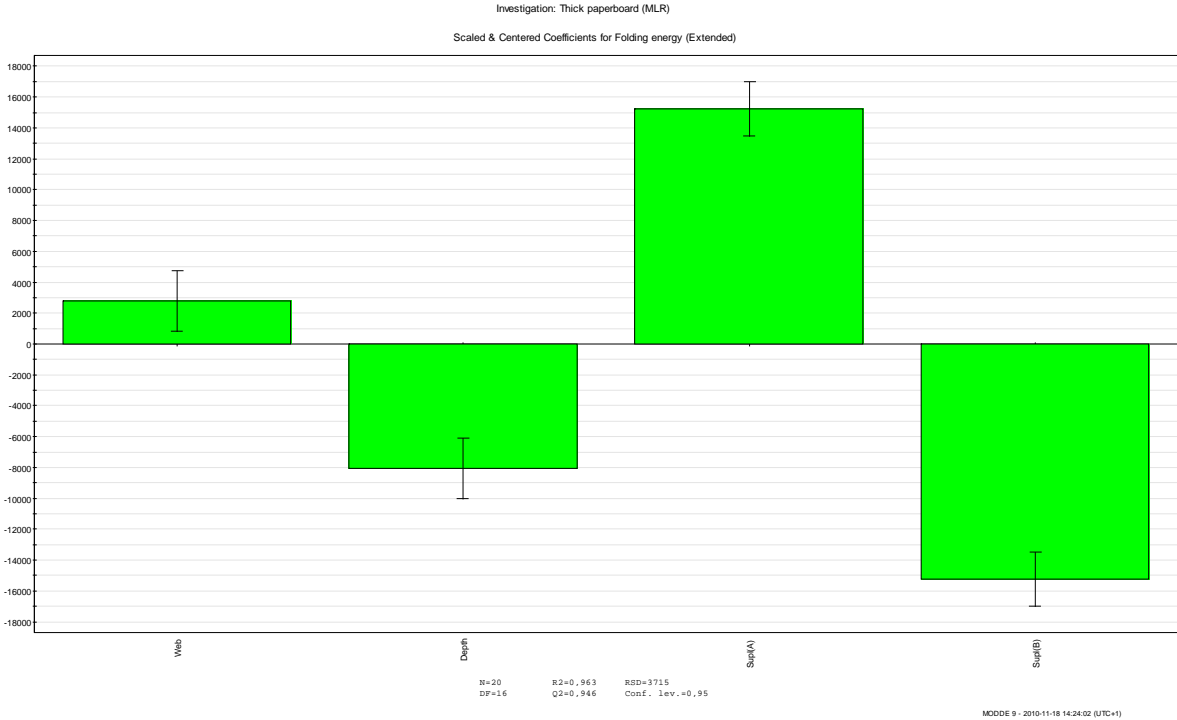
# Appendix



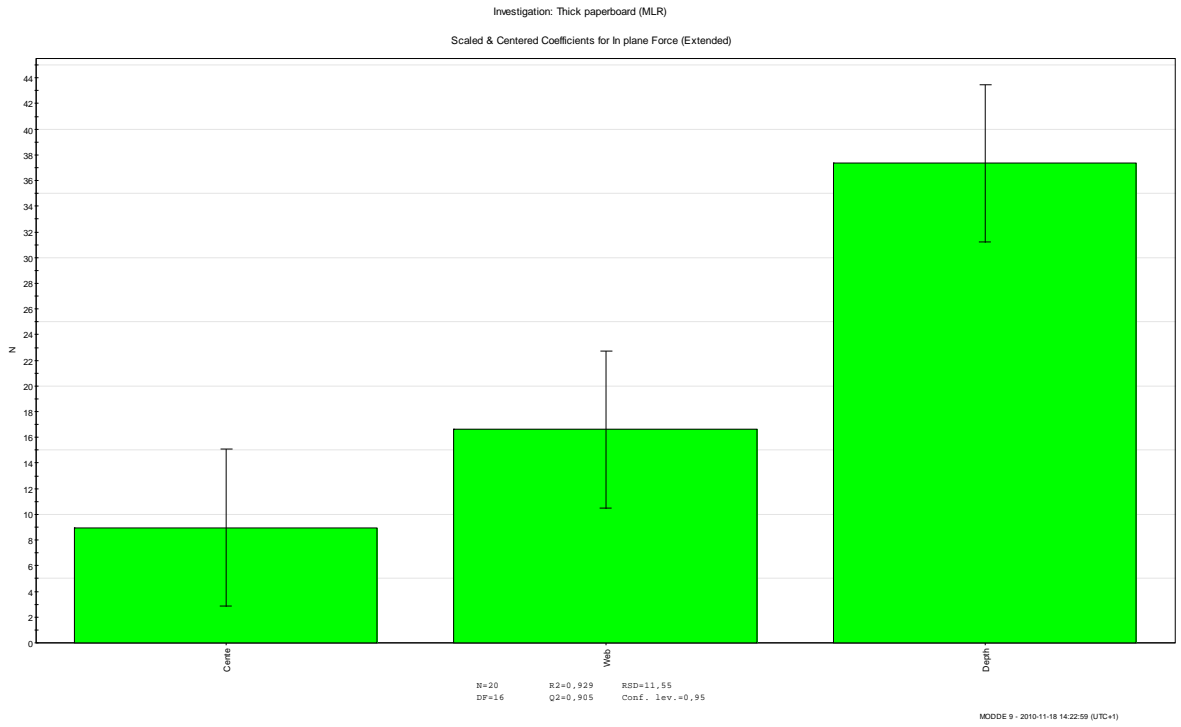


# Appendix

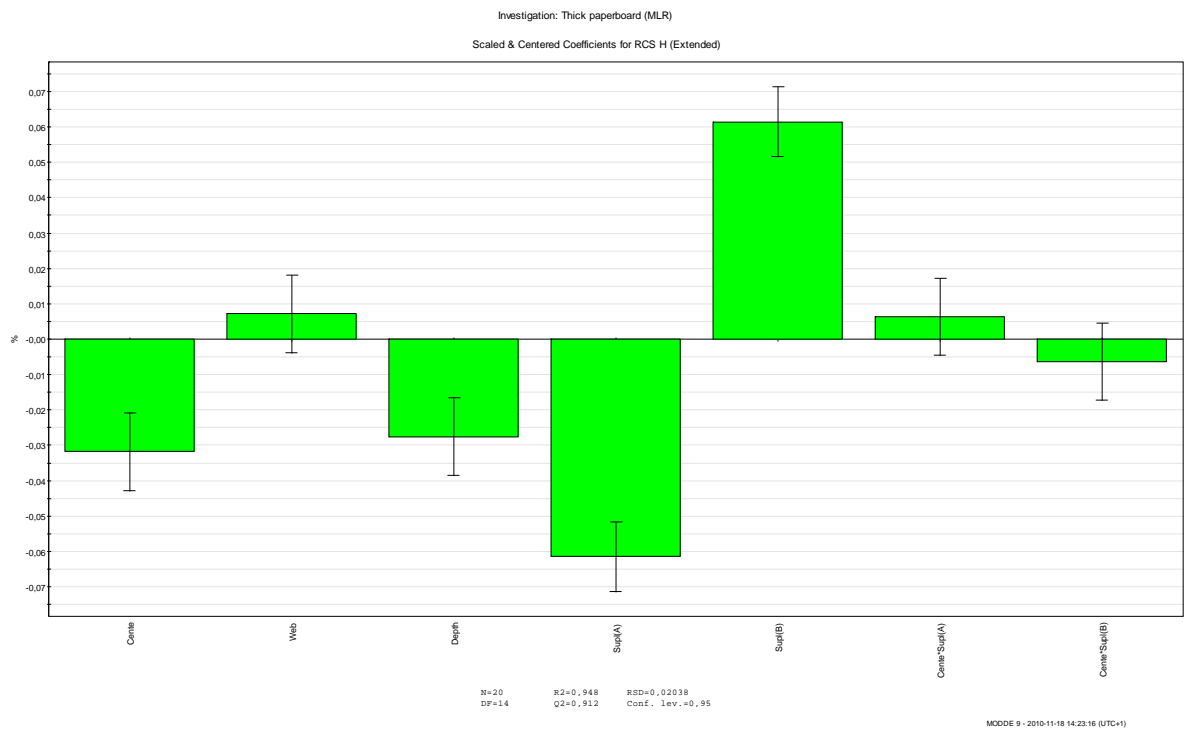
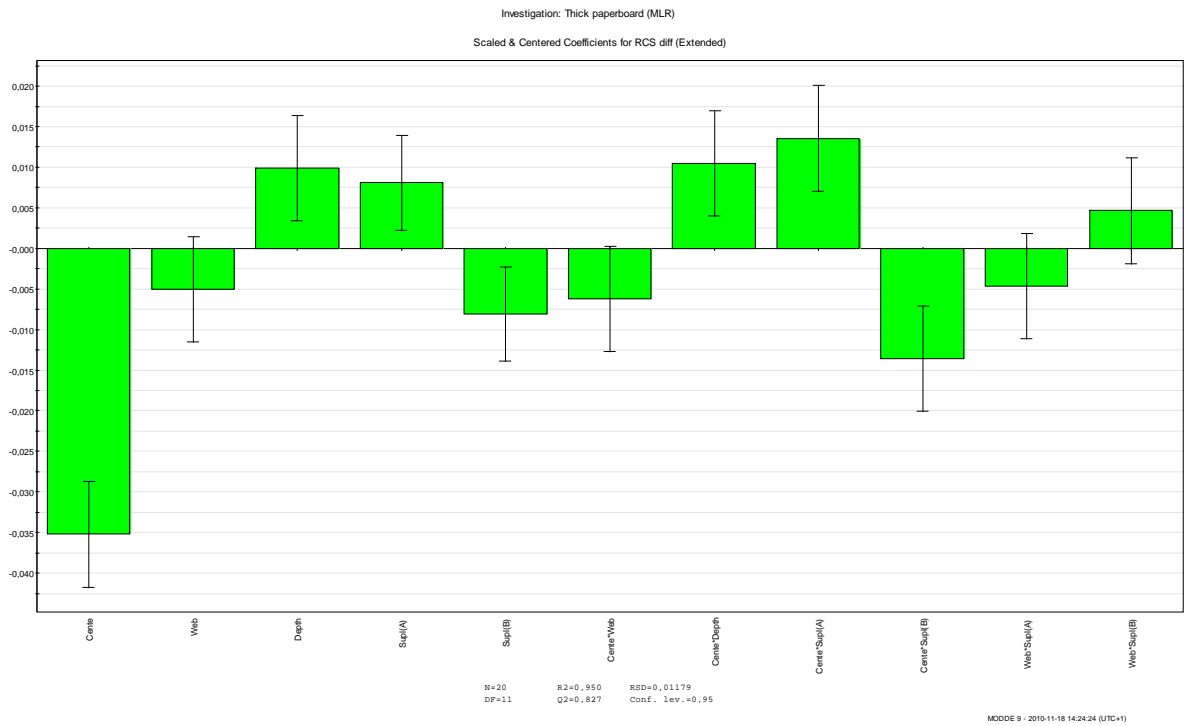




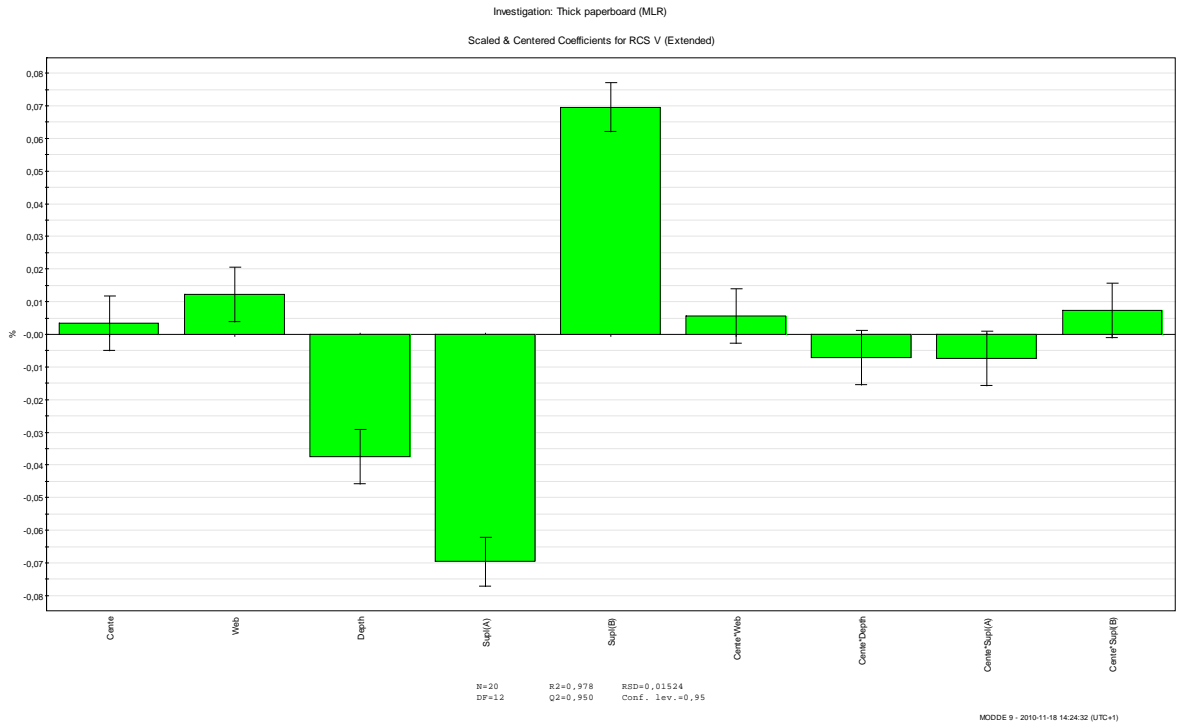
# Appendix



# Appendix



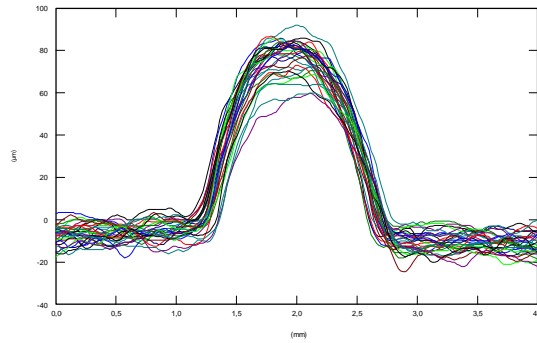
# Appendix



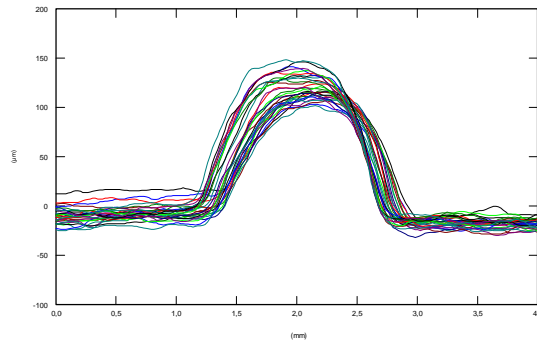


## Appendix C *Straight creases: Topography*

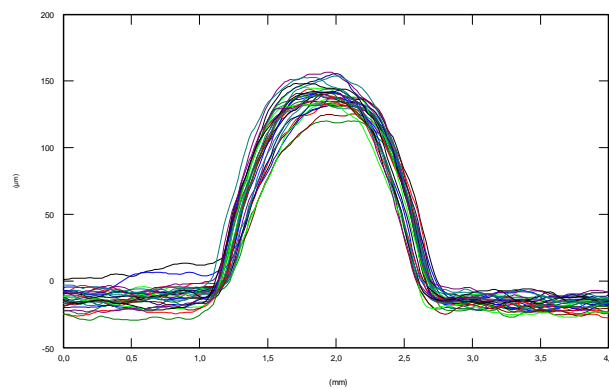
### C.1 Various crease depth from thin paperboard A1



Line 1

*Setting nr 3*

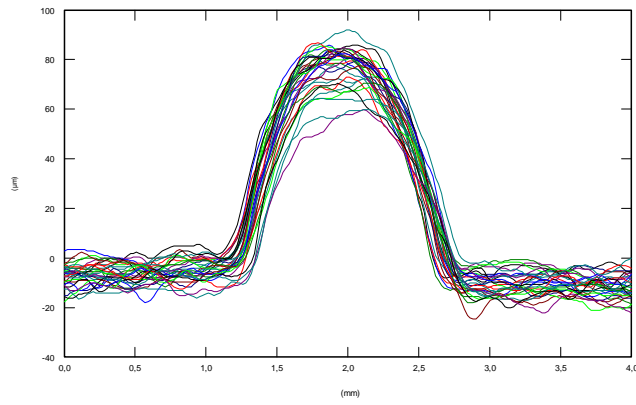
Line 1

*Setting nr 1*

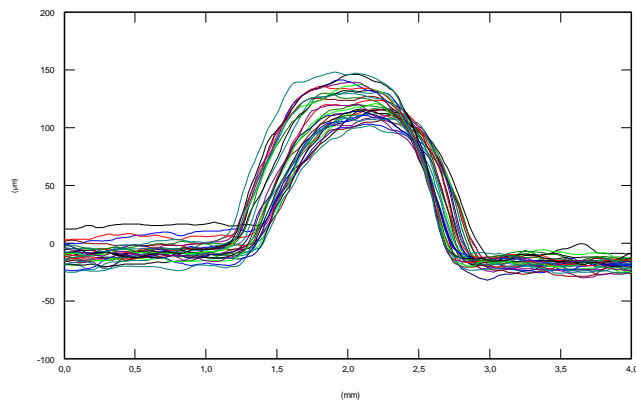
Line 1

*Setting nr 7*

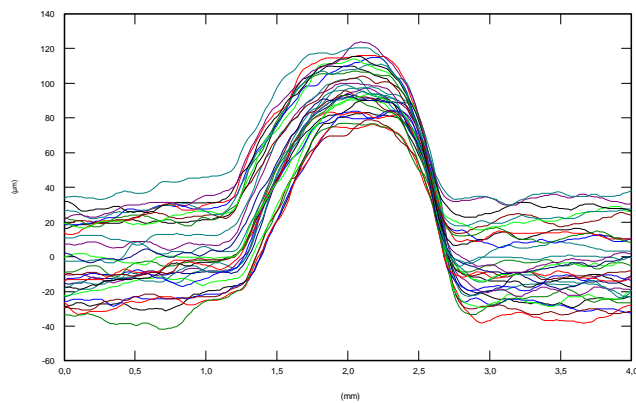
### C.2 Various displacements from thin paperboard A1



*Setting nr 3*

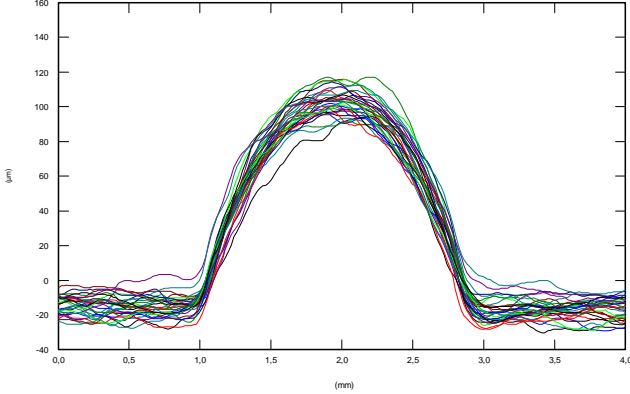


*Setting nr 1*

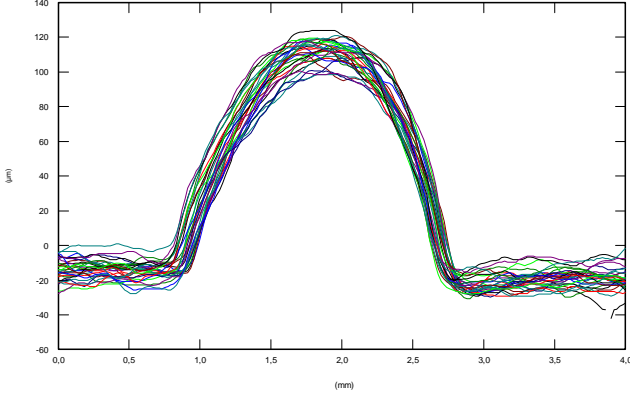


*Setting nr 11*

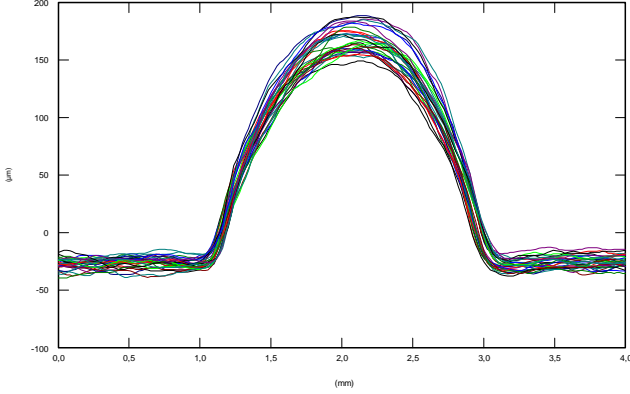
C.3 Various crease depth from thick paperboard A2



Setting nr 3

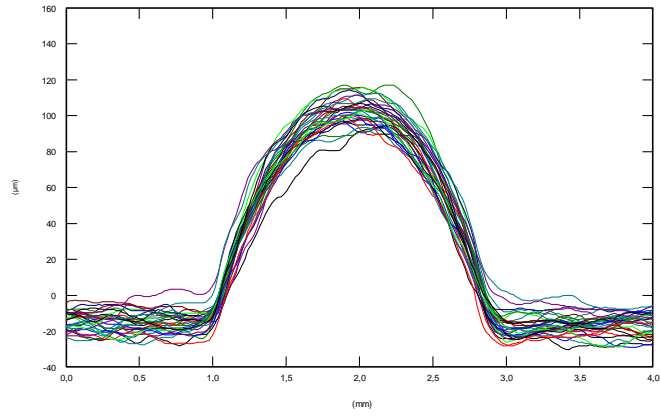


Setting nr 1



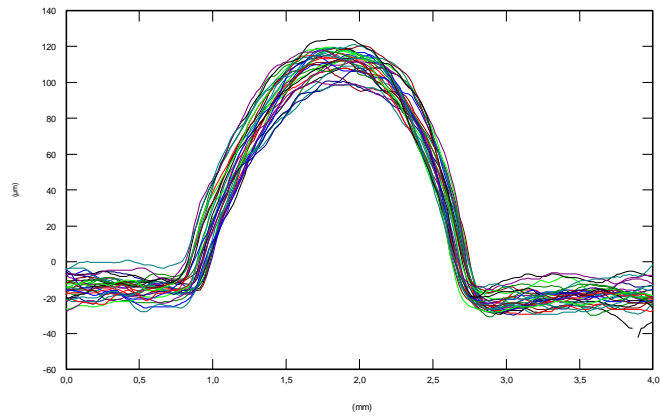
Setting nr 7

### C.4 Various displacements from thick paperboard A2



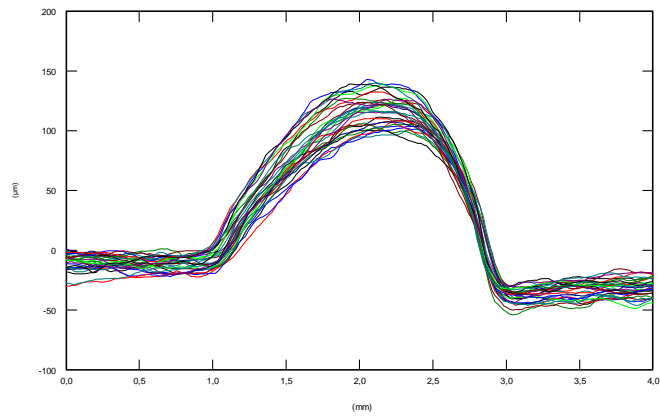
Line 1

*Setting nr 3*



Line 1

*Setting nr 1*



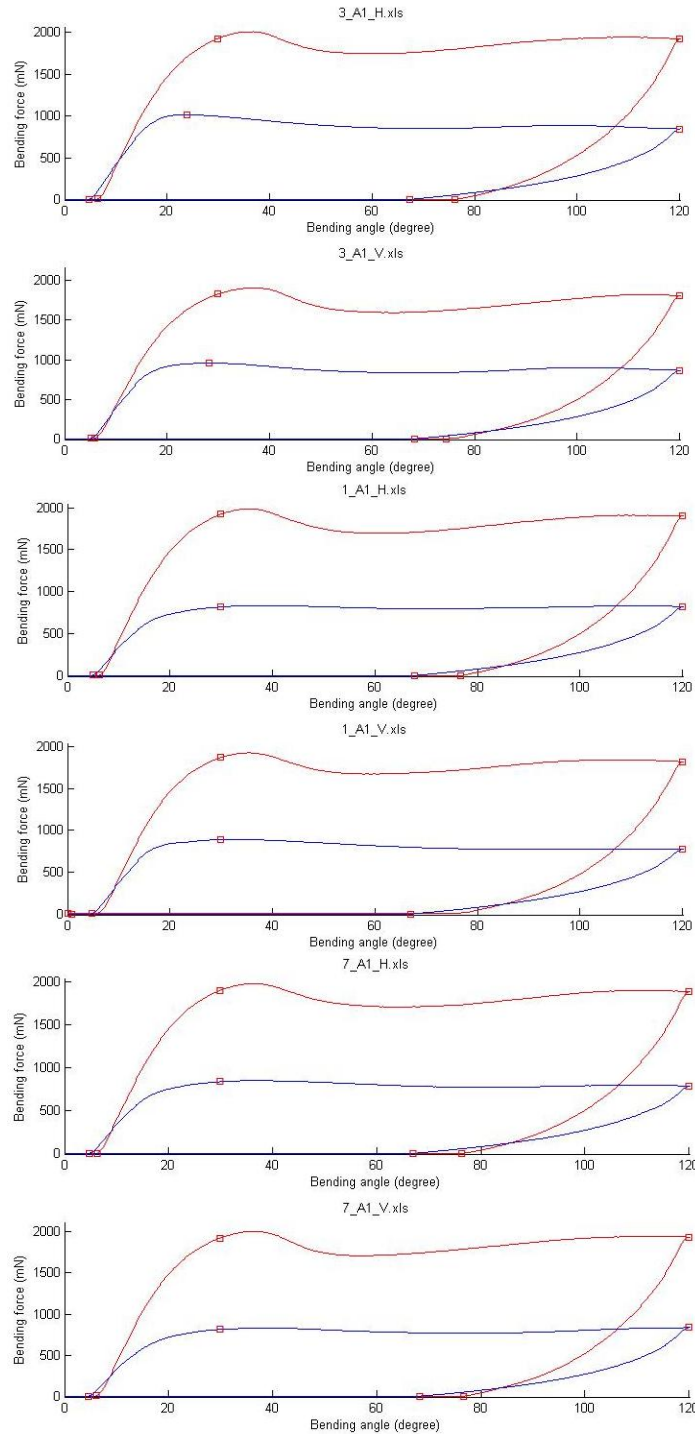
Line 1

*Setting nr 11*

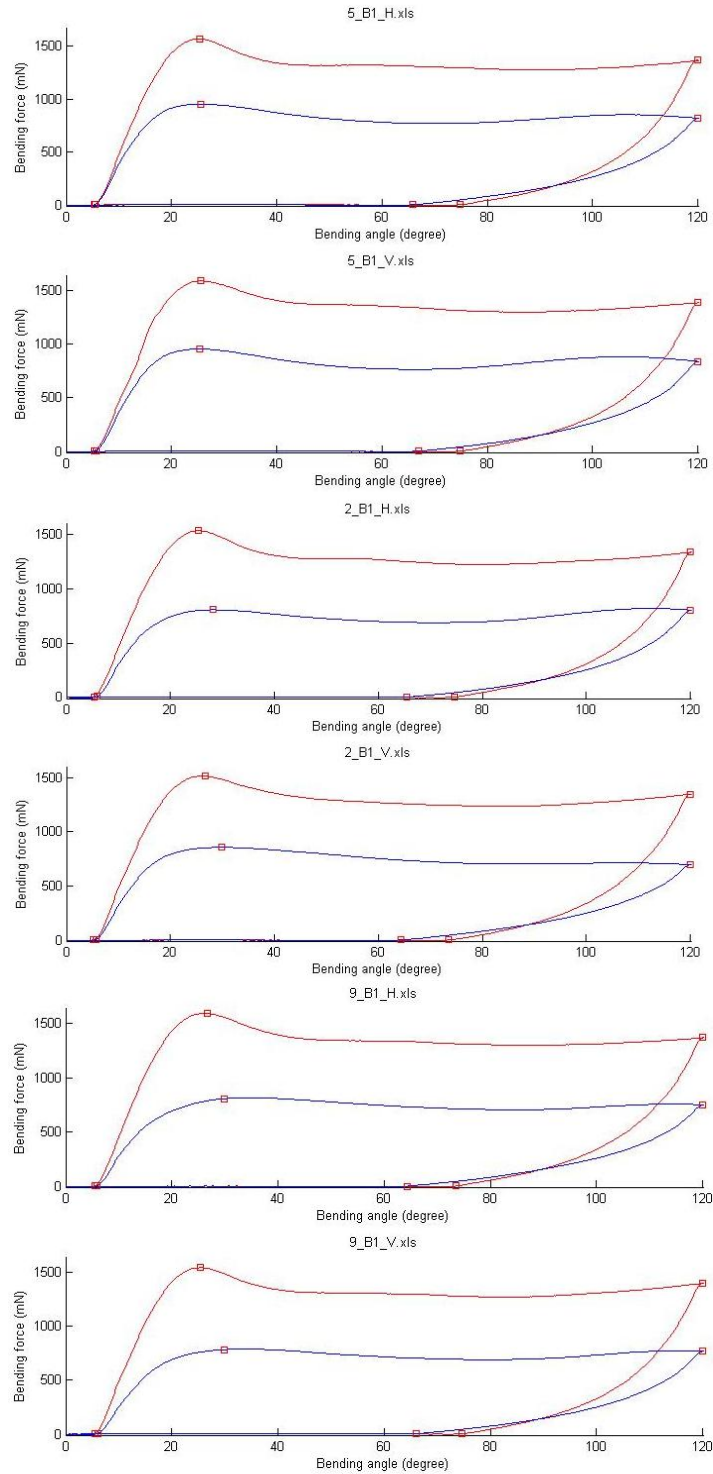
## Appendix E Straight creases: RCS

The name at the top of the figures indicates the run order in *Appendix A, table A.1.*

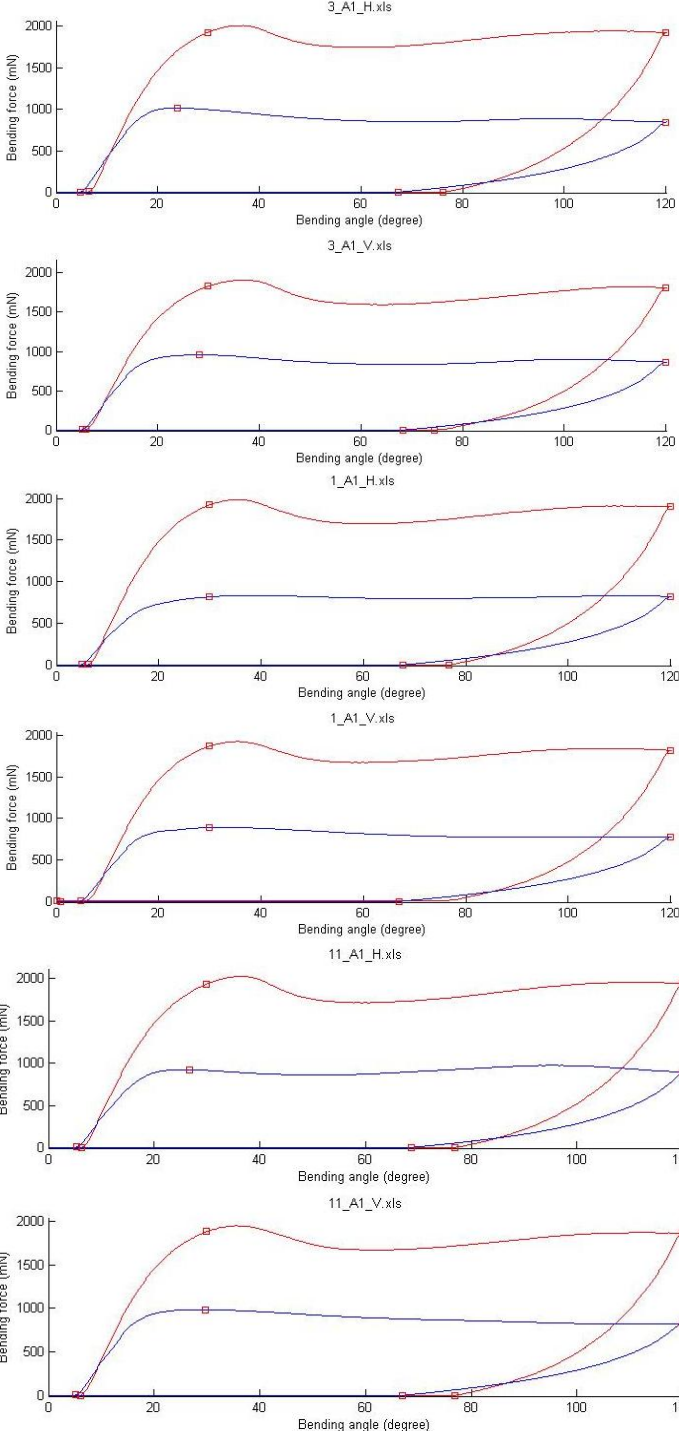
### E.1 Various crease depth from thin paperboard A1



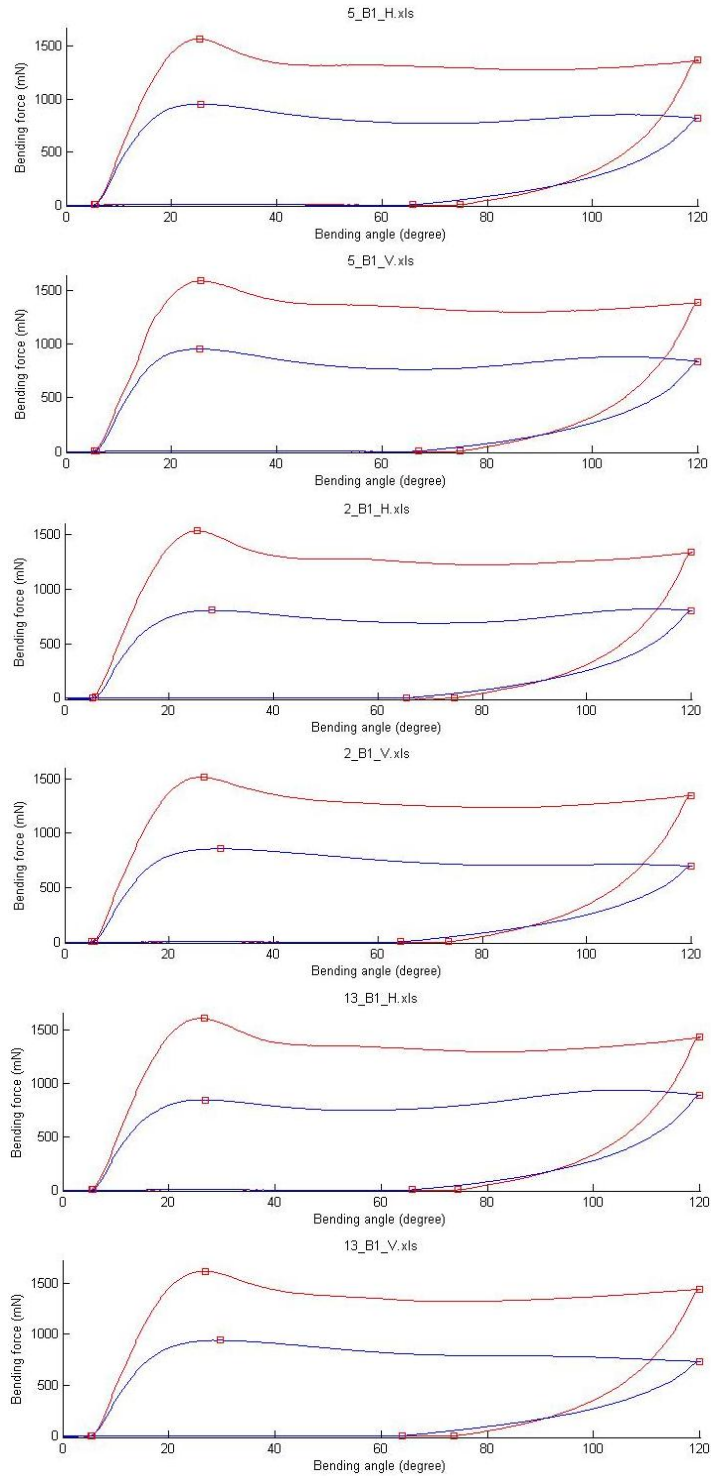
## E.2 Various crease depth from thin paperboard B1



### E.3 Various displacements from thin paperboard A1

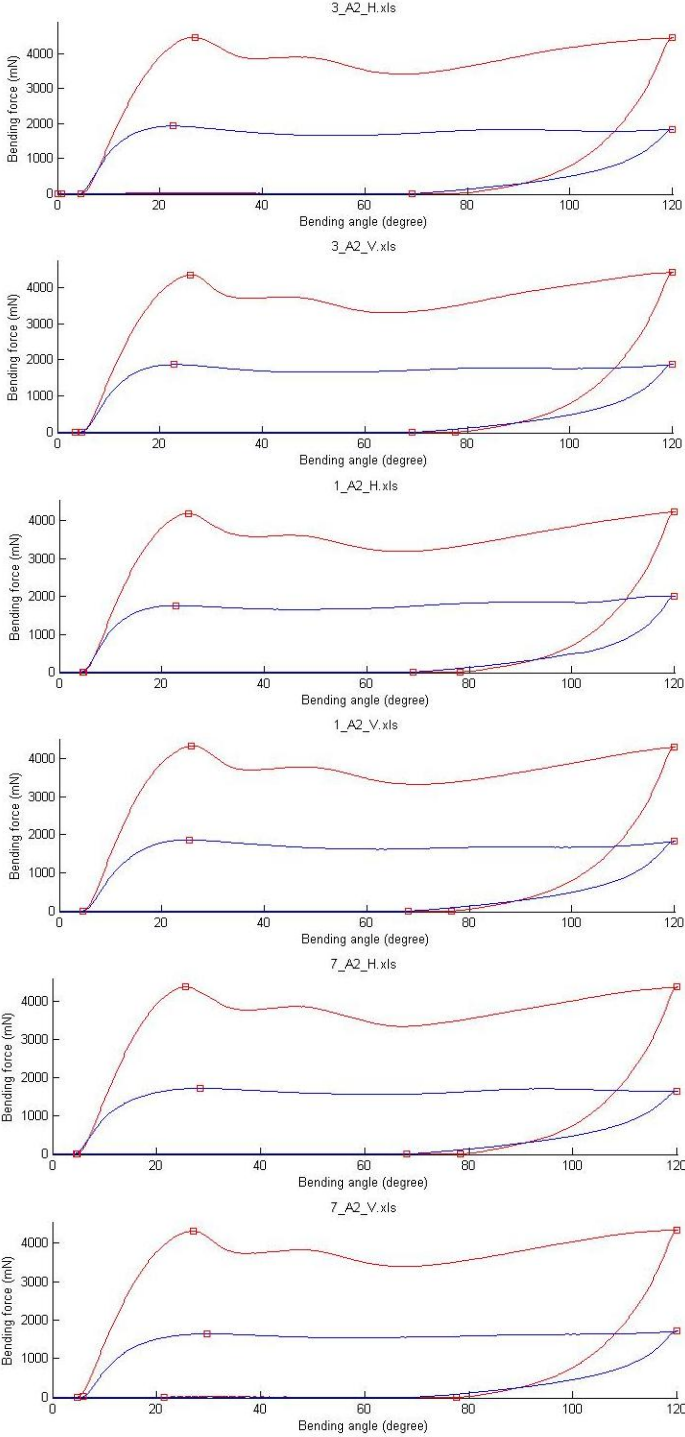


### E.4 Various displacements from thin paperboard B1

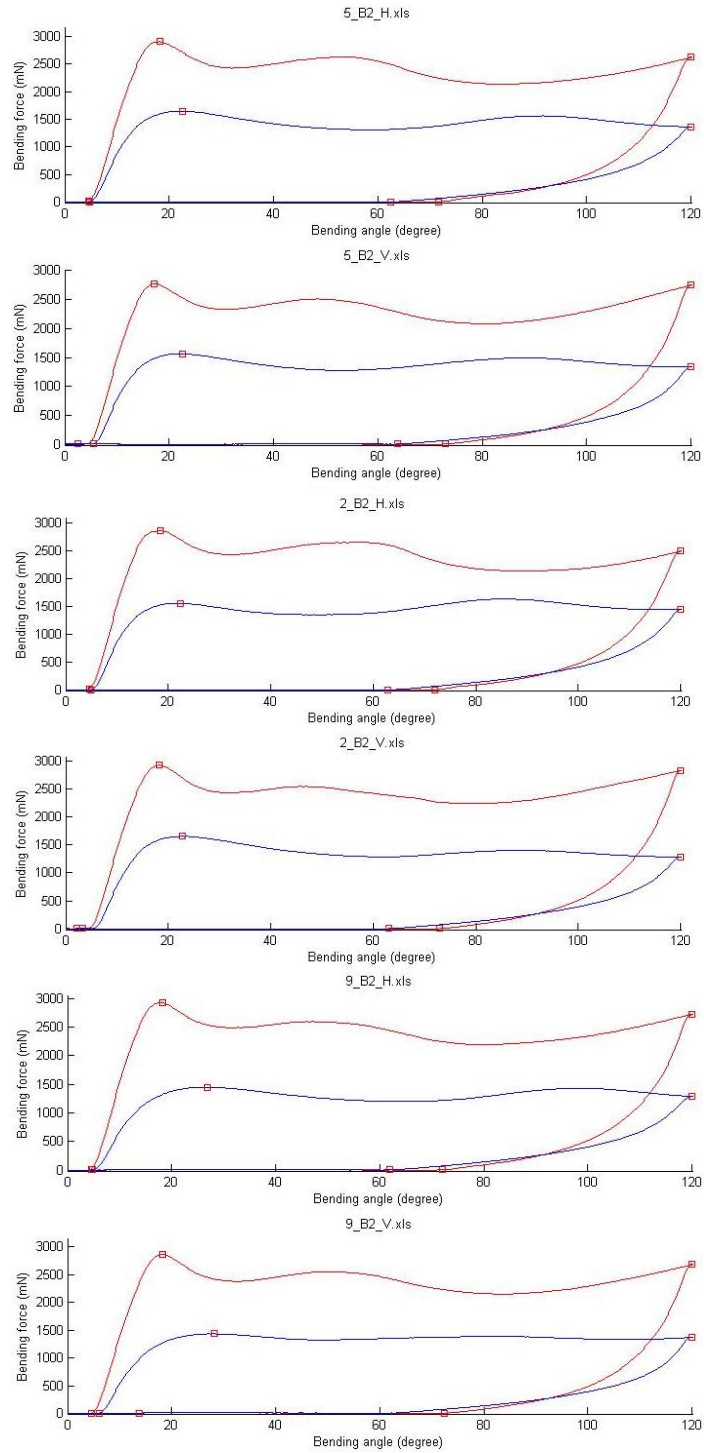




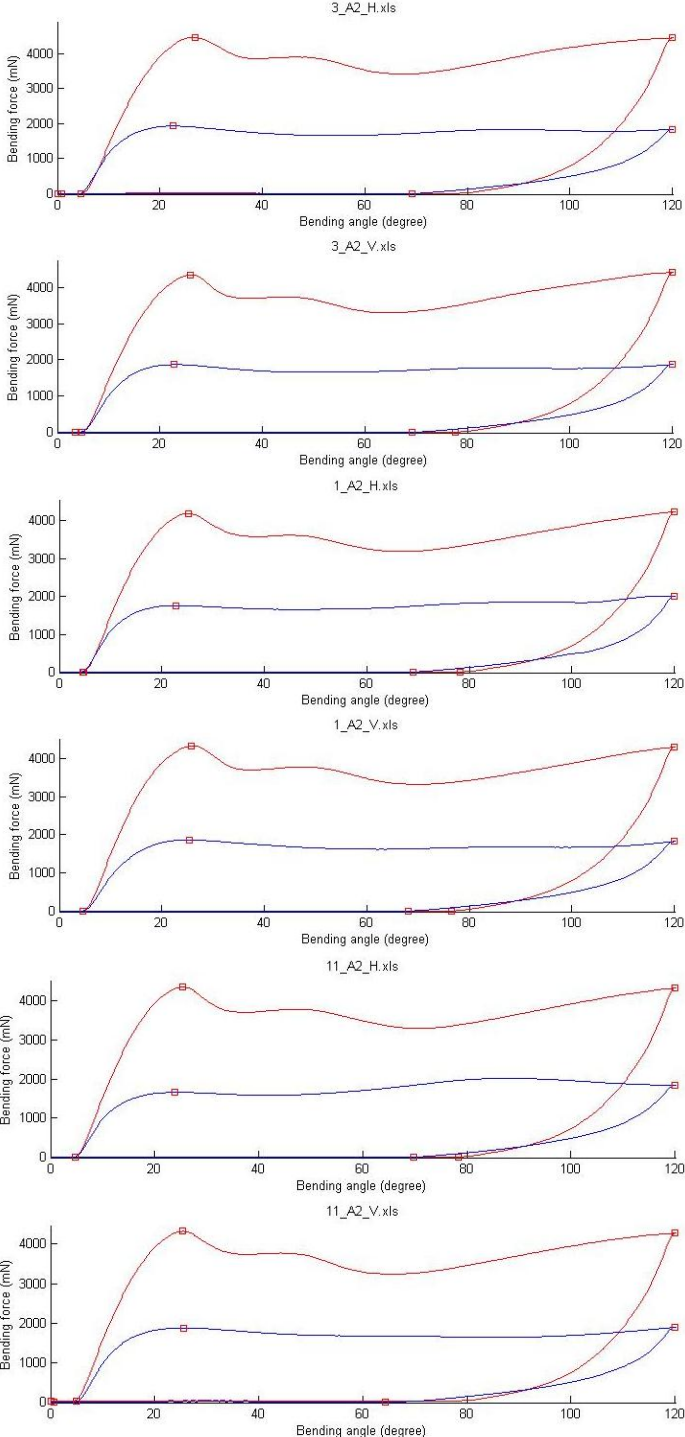
E.5 Various crease depth from thick paperboard A2



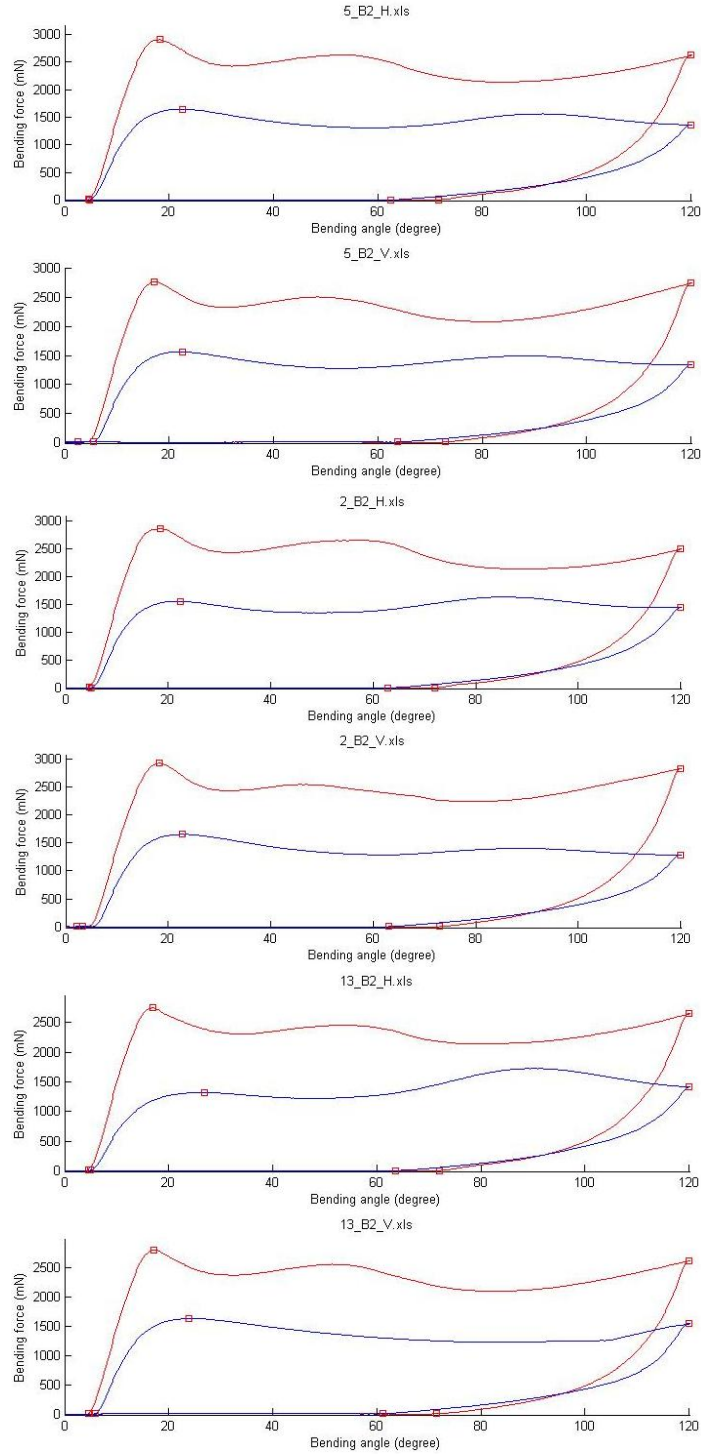
### E.6 Various crease depth from thick paperboard B2



E.7 Various displacements from thick paperboard A2



**E.8 Various displacements from thick paperboard B2**



## Appendix F *Bottom crease pattern: Tables*

Table F.1 Worksheet, thin paperboard

Run order	Board	Displacement MD	Displacement CD	Web tension	Crease depth
[Nr]		[mm]	[mm]	[kN/m]	[mm]
1	B1	0.10	0.10	1	0.175
2	A1	0.10	0.10	1	0.175
3	B1	0.05	0.05	1	0.200
4	A1	0.05	0.05	1	0.275
5	B1	0	0	1	0.200
6	A1	0	0	1	0.275

Table F.2 MD-values of thin paperboard

Run order	Creasing		Topography		Folding right			
	Crease force	In plane force	Crease Height	Distortion	Bending force	Crack angle	Folding energy	RCS
	[N]	[N]	[mm]	[mm]	[N]	[deg]	[J]	[%]
1	4630.4	355.9	0.1228	0.1160	149.86	29.9	15521	37.3
2	5707.4	438.0	0.1541	0.1147	154.16	29.9	17179	46.8
3	4233.6	436.1	0.1266	0.0571	163.62	29.9	16494	35.0
4	6409.9	485.9	0.1995	0.0681	143.10	29.9	16297	43.0
5	4386.4	425.0	0.1213	-0.0006	167.08	29.9	15879	42.7
6	6242.6	439.6	0.1942	-0.0108	143.88	29.9	16009	44.0

Table F.3 CD-values of thin paperboard

Run order	Creasing		Topography		Folding right			
	Crease force	In plane force	Crease Height	Distortion	Bending force	Crack angle	Folding energy	RCS
	[N]	[N]	[mm]	[mm]	[N]	[deg]	[J]	[%]
1	4630.4	355.9	0.1093	0.1321	245.16	29.9	23311	54.3
2	5707.4	438.0	0.1337	0.1414	266.40	29.9	26194	66.9
3	4233.6	436.1	0.1115	0.0638	239.82	29.9	22501	54.2
4	6409.9	485.9	0.1749	0.0665	226.86	29.9	22833	61.6
5	4386.4	425.0	0.1033	-0.0057	229.04	29.9	20112	58.4
6	6242.6	439.6	0.1688	-0.0040	230.50	29.9	23510	56.2



*Table F.4 Worksheet, thick paperboard*

Run order	Board	Displacement MD	Displacement CD	Web tension	Crease depth
[Nr]		[mm]	[mm]	[kN/m]	[mm]
1	B2	0	0	0.5	0.075
2	A2	0	0	0.5	0.125
3	B2	0.08	0.08	0.5	0.075
4	A2	0.08	0.08	0.5	0.100
5	B2	0.16	0.16	0.5	0.025
6	A2	0.16	0.16	0.5	0.025

*Table F.5 MD-values of thick paperboard*

Run order	Creasing		Topography		Folding right			
	Crease force	In plane force	Crease Height	Distortion	Bending force	Crack angle	Folding energy	RCS
	[N]	[N]	[mm]	[mm]	[N]	[deg]	[J]	[%]
1	4593.9	458.1	0.0940	0.0069	348.20	22.7	35948	60.6
2	6619.2	456.4	0.1550	0.0122	318.56	26.8	35161	42.3
3	4489.0	416.0	0.0923	0.0968	320.88	22.7	31808	59.8
4	6075.2	396.9	0.1526	0.0832	320.34	29.9	34442	40.3
5	4126.9	389.4	0.0696	0.1626	376.04	21.2	36067	65.5
6	5217.5	367.5	0.1088	0.1798	374.08	21.2	40546	48.4

*Table F.6 CD-values of thick paperboard*

Run order	Creasing		Topography		Folding right			
	Crease force	In plane force	Crease Height	Distortion	Bending force	Crack angle	Folding energy	RCS
	[N]	[N]	[mm]	[mm]	[N]	[deg]	[J]	[%]
1	4593.9	458.1	0.0867	0.0441	415.78	20.0	39620	48.3
2	6619.2	456.4	0.1514	0.0442	420.80	29.9	44427	32.9
3	4489.0	416.0	0.0904	0.1037	411.14	21.4	40417	46.5
4	6075.2	396.9	0.1509	0.0904	428.12	29.9	42251	35.4
5	4126.9	389.4	0.0651	0.2115	424.04	16.9	43488	47.9
6	5217.5	367.5	0.0984	0.2131	483.12	22.9	50143	39.3

## Appendix I Bottom crease pattern: Plots

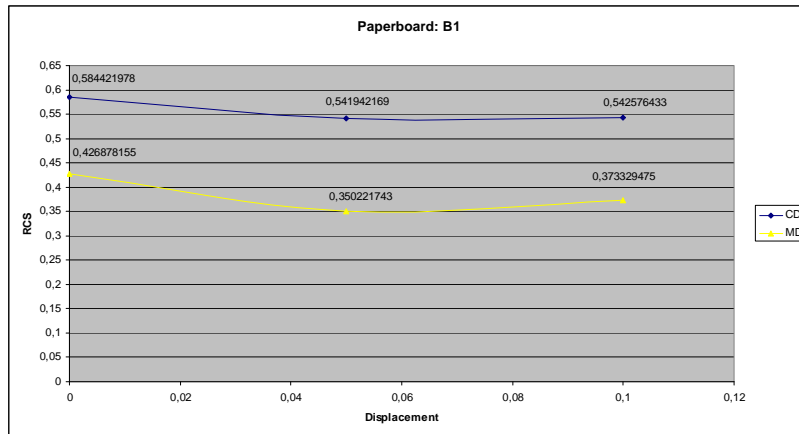


Figure I.1 Shows how RCS changes with displacement

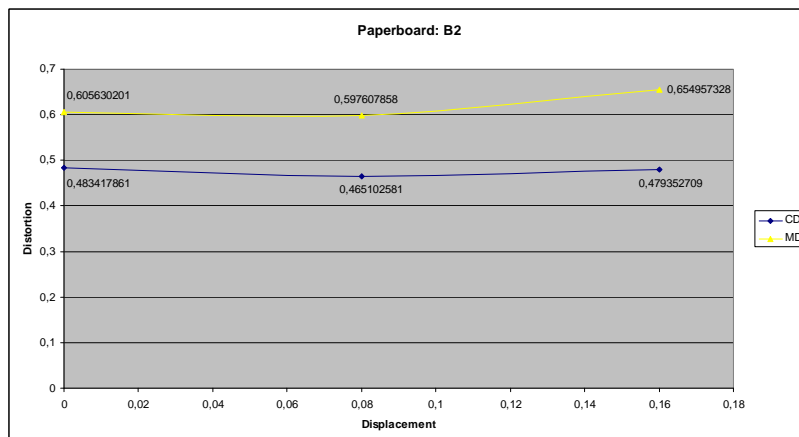


Figure I.2 Shows how distortion changes with displacement



## Appendix J Pilot Plant: Tables

Table J.1 Worksheet, thin paperboard

Run order	Board	Displacement MD	Displacement CD	Web tension	Crease depth
[Nr]		[mm]	[mm]	[kN/m]	[mm]
1	B1	0	0	1	0.150
2	B1	0.05	0	1	0.125
3	B1	0.10	0	1	0.100

Table J.2 MD-values of thin paperboard

Run order	Topography pilot plant		Topography		Folding right	Folding left
	Distortion	Crease height	Distortion	Crease height	RCS	RCS
	[mm]	[mm]	[mm]	[mm]	[%]	[%]
1	0.0073	0.1250	0.0083	0.0446	70.9	72.1
2	0.0358	0.1110	0.0297	0.0382	68.0	76.5
3	0.0721	0.1010	0.1203	0.0334	69.3	79.2

Table J.3 CD-values of thin paperboard

Run order	Topography		Folding
	Distortion	Crease height	RCS
	[mm]	[mm]	[%]
1	-0.0471	0.0613	68.8
2	0.0535	0.0586	71.0
3	0.0288	0.0486	73.3

*Table J.4 Worksheet, thick paperboard*

Run order	Board	Displacement MD	Displacement CD	Web tension	Crease depth
[Nr]		[mm]	[mm]	[kN/m]	[mm]
1	B2	0	0	1	0.140
2	B2	0.08	0	1	0.090
3	B2	0.16	0	1	0.065

*Table J.5 MD-values of thick paperboard*

Run order	Topography pilot plant		Topography		Folding right	Folding left
	Distortion	Crease height	Distortion	Crease height	RCS	RCS
	[mm]	[mm]	[mm]	[mm]	[%]	[%]
1	0.0087	0.1505	0.0742	0.0336	54.3	55.8
2	0.0738	0.1305	-0.0173	0.0324	55.8	60.6
3	0.1054	0.1214	0.0231	0.0278	54.0	63.1

*Table J.6 CD-values of thick paperboard*

Run order	Topography		Folding
	Distortion	Crease height	RCS
	[mm]	[mm]	[%]
1	-0.0156	0.0613	58.8
2	-0.1063	0.0586	61.4
3	-0.1595	0.0486	63.8

## Appendix K Conformation of MODDE statement

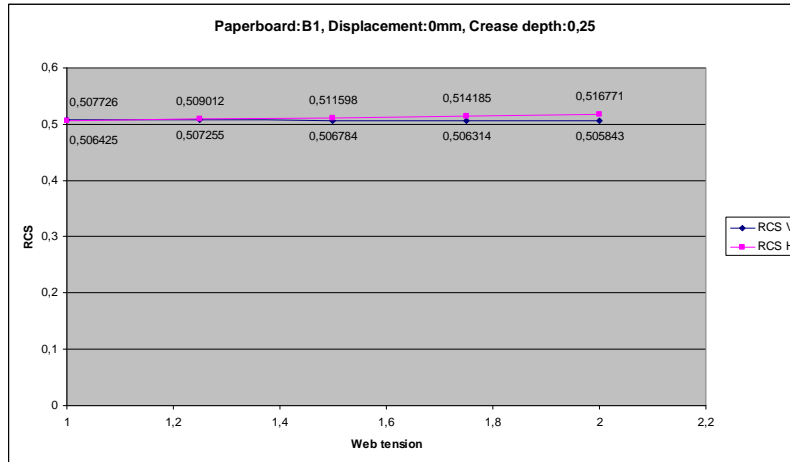


Figure K.1 Shows that web tension do not affect much

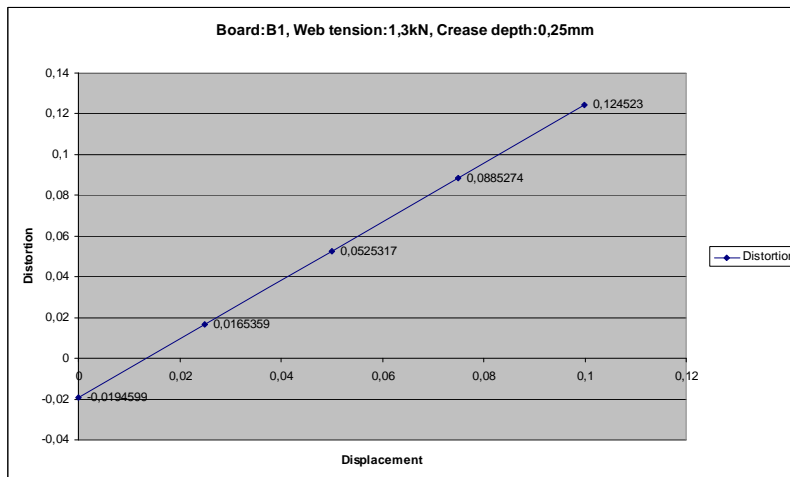
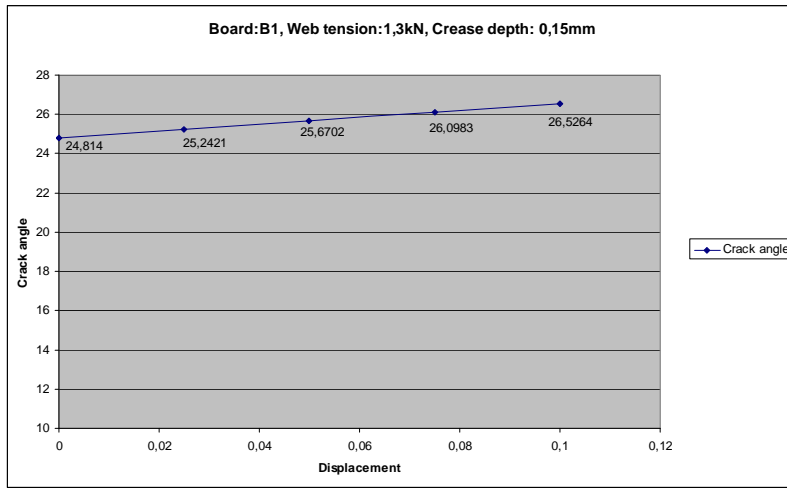


Figure K.2 Shows that distortion changes a lot with displacement

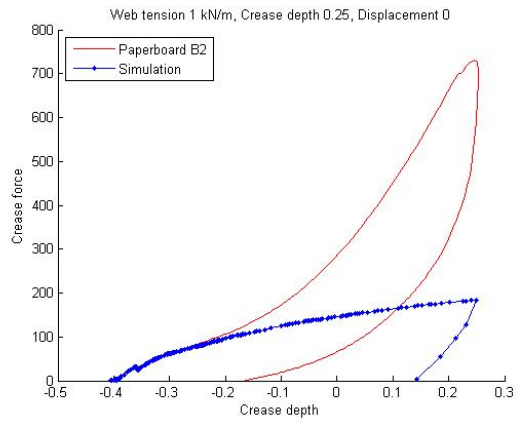
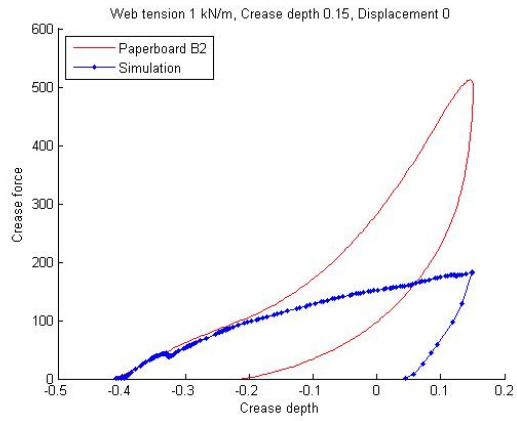


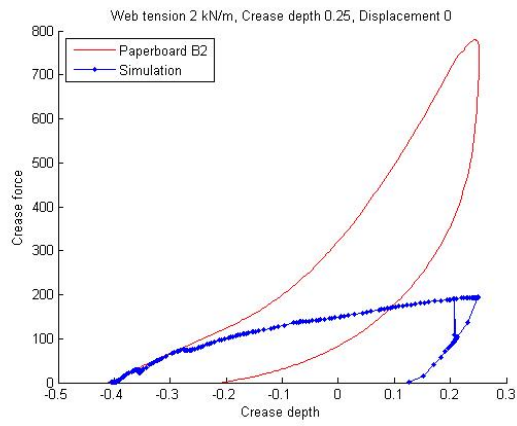
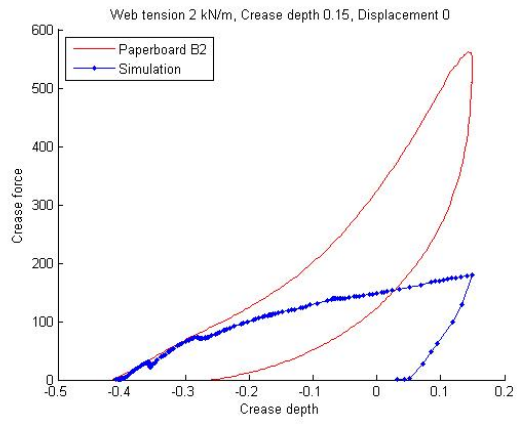
*Figure K.3 Shows that crack angle change a little bit with displacement*

## **Appendix L    Computer simulation: Material parameters**

Classified

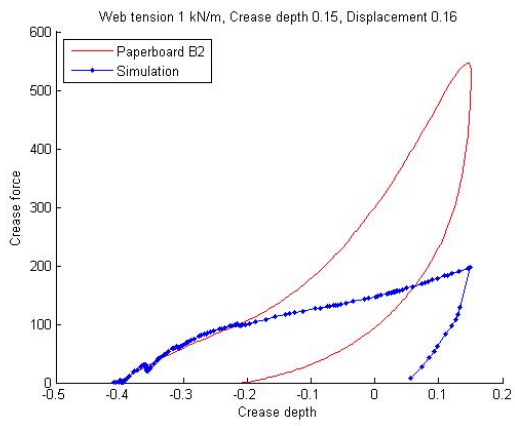
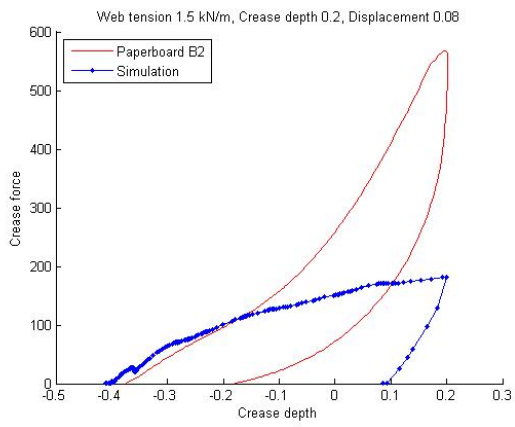
## Appendix M *Simulations vs. tests*



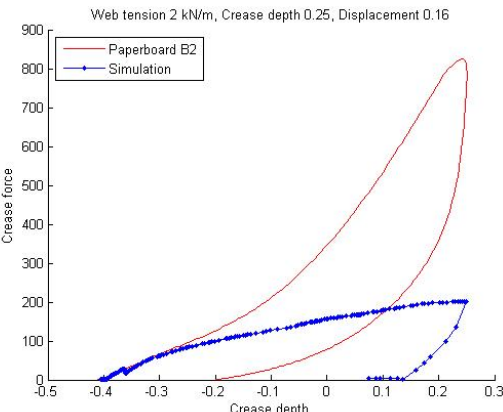
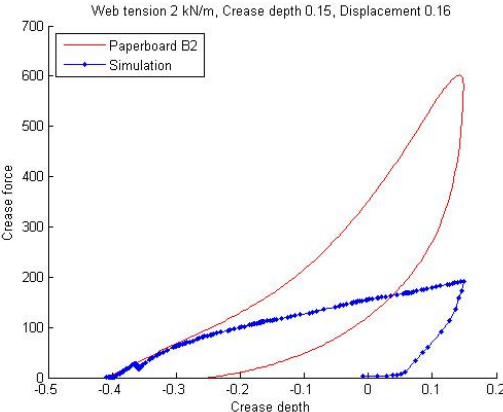
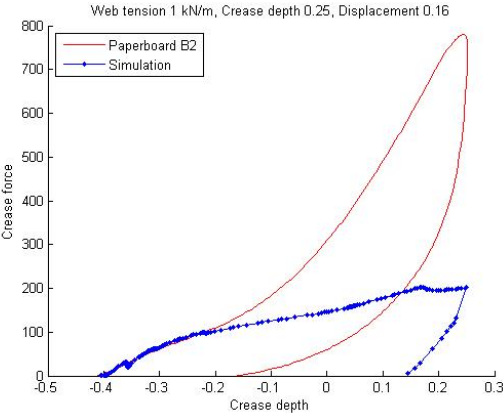


## Appendix

---

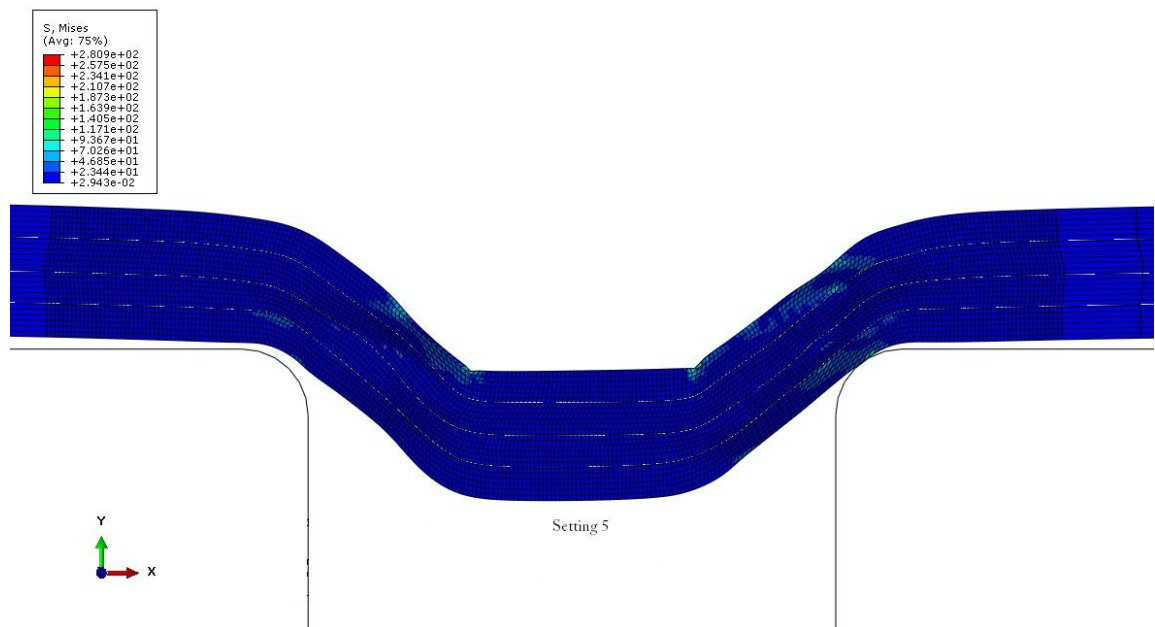
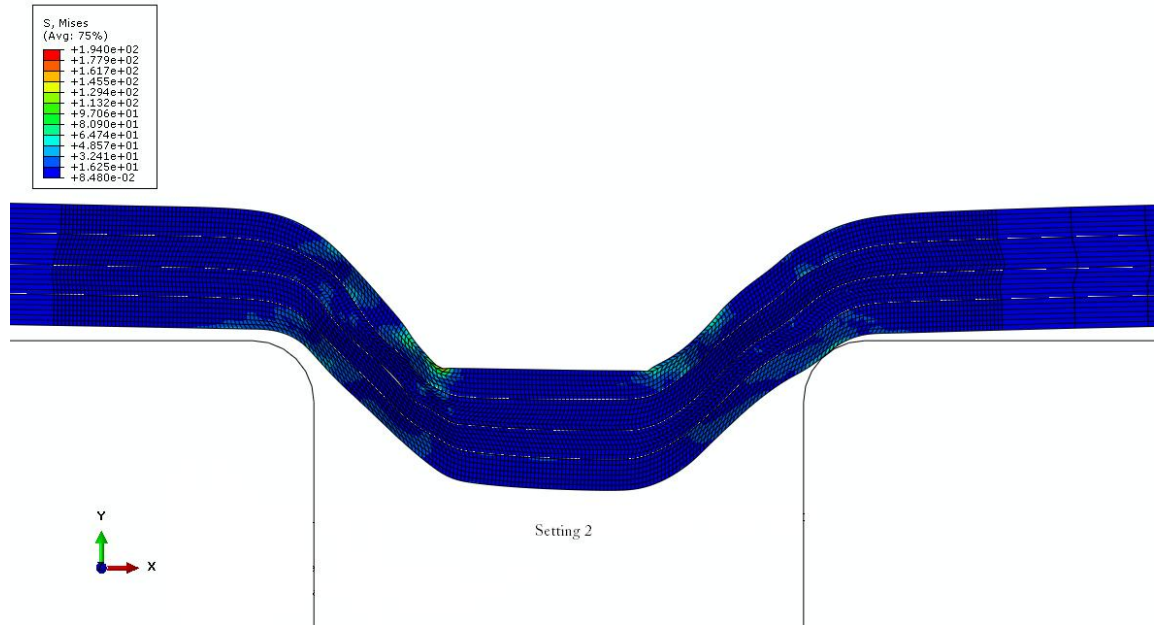


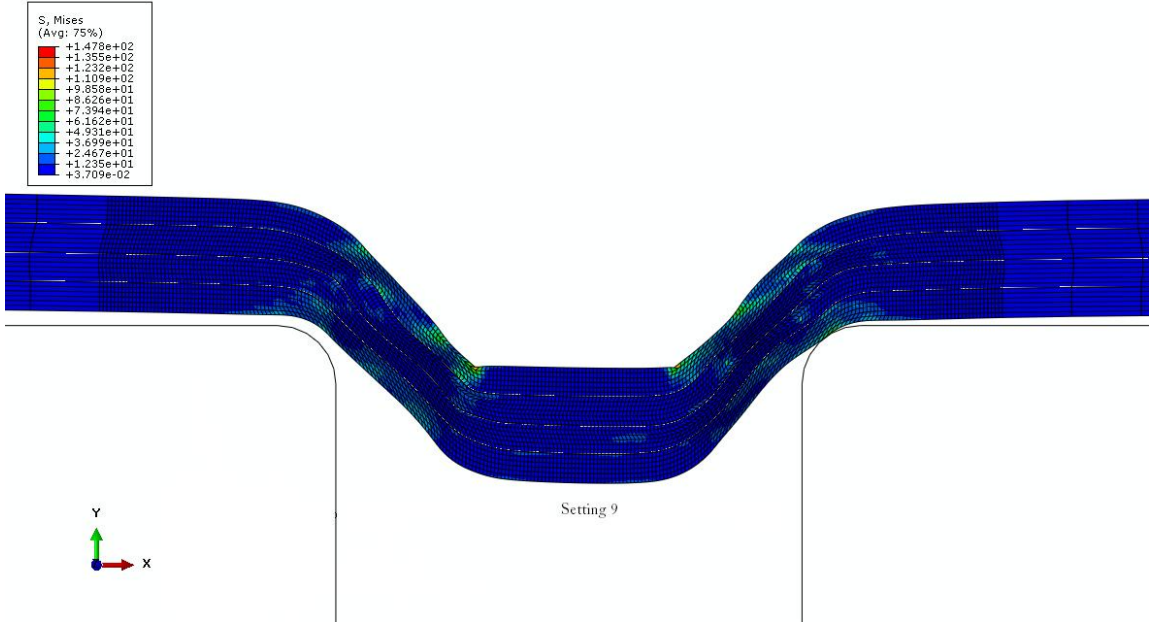
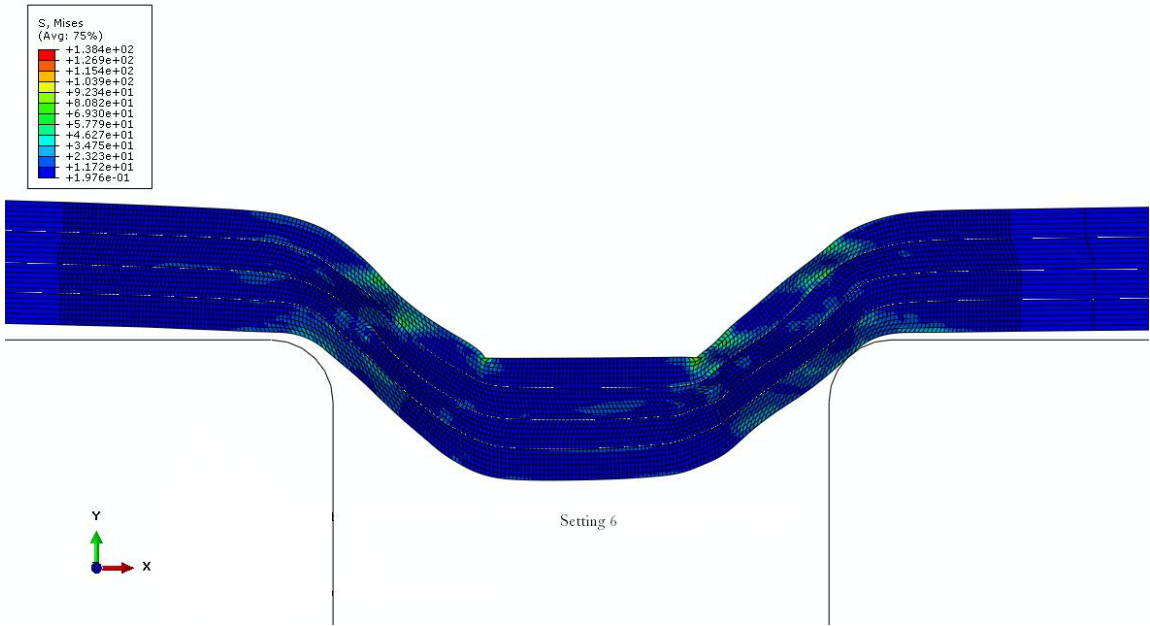




## Appendix O Simulations: Plastic deformation

The setting number in the figures indicates the run order in Appendix A, table A.3.





# Appendix

